ABSTRACT

Title of Dissertation: SONAR BEAM DIRECTION AND FLIGHT CONTROL IN AN ECHOLOCATING BAT

Kaushik Ghose, Doctor of Philosophy, 2006

Dissertation directed by: Professors Cynthia F. Moss and Timothy K. Horiuchi
Neuroscience and Cognitive Science Program

Echolocating insectivorous bats are nocturnal mammals that capture fast, erratically moving insects in flight. Bats emit short ultrasonic pulses that form beams of sound and use the returning echoes to guide behavior. The frequency, duration and timing of the sonar pulses, along with the spatial direction of the sonar beam restrict the information returning to the bat, and can be considered a component of the *acoustic gaze* of bats. A great deal is known about the time-frequency structure of bat echolocation calls and their relationship to the stages of foraging flight in bats. It is however not known how bats direct their sonar beam in flight or how beam direction is related to flight control.

This is the first study of the sonar beam direction in freely flying bats as they chase and capture insects. An apparatus and method to measure the sonar beam pattern of echolocating bats (*Eptesicus fuscus*, big brown bats) as they fly in a laboratory flight

room is described. It is shown that the bat locks its sonar beam tightly onto a target during pursuit (Chapter 2). The flying bat's sonar beam consists of two lobes directed apart in the vertical plane (Chapter 3). There is a coupling between acoustic gaze (sonar beam axis) direction and flight turn rate that can be expressed as a delayed linear control law. The gain of this law (steepness of the relationship) varies with the bat's behavioral state (Chapter 4). The bat, when pursuing erratically flying insects, adopts a strategy that keeps the absolute direction to the target a constant. This strategy is shown, under some assumptions, to minimize time-to-intercept of erratically maneuvering targets and is similar to parallel navigation implemented in guided missiles (Chapter 5). The bat is not helpless against ultrasound-triggered evasive dives evolved by some hearing insects. The bat adopts flight strategies to counter such dives (Chapter 6).

This work allows us to compare spatial behaviors well studied in visual animals, with similar behaviors in an animal that is guided by hearing and make inferences about common computational strategies employed by nervous systems.

SONAR BEAM DIRECTION AND FLIGHT CONTROL IN AN ECHOLOCATING BAT

by

Kaushik Ghose

Dissertation submitted to the Faculty of the Graduate School of the
University of Maryland, College Park in partial fulfillment
of the requirements for the degree of
Doctor of Philosophy
2006

Advisory Committee:

Professors Cynthia F. Moss and Timothy K. Horiuchi, Chairs
Professor Robert Dooling
Professor P.S. Krishnaprasad
Professor Jonathan Simon

DEDICATION

To Dr. Mom and Dr. Dad

With love and admiration.

ACKNOWLEDGMENTS

I thank Cindy for her enthusiasm, support, kindness and encouragement. Cindy is my first mentor in science and has led me to realize that I love biology and that I would like to keep doing science. She has nurtured a warm, friendly, cooperative and innovative environment for doing research. She has, by example, instilled in me the ideals that graduate students are to be respected and given independence, credit must be given where credit is due, information must be shared, not hoarded, people must be polite to one another, e-mails must always be responded to, if a student needs a piece of equipment for research, it will be arranged for, if a student wishes to attend a conference, it will be arranged for, diverse expertise makes for exhilarating science, good science is the most important thing in the world, except for the wellbeing of family. I believe these ideals to be essential for a good community and a productive life, and I intend to follow them.

Cindy introduced me to many researchers in different places, four of whom eventually joined my committee. I have benefited greatly from having this amazing core of enthusiasm, expertize and encouragement to draw from. I thank Timmer for being a model for an engineer-biologist. He let me discover that I liked building things and watching them work. I thank Dr. Krishnaprasad for letting me rediscover the joy of mathematics, undoing years of damage inflicted by formal high-school education. I thank Bob for help with statistics and for encouraging me in my work. I thank Jonathan for all his support, especially during the year Cindy was in Germany.

I thank everyone in the batlab - Aaron, Amaya (I'll do batcare this weekend, by the way), Amy (party on, girl!), Ben (Buzzel no function, texture guy!), Chen (We need more Christmas parties during the year), Ed (This thesis was pure therapy, dude), Gordon (Finally, we can do the 'Five Guys' trip!), Genni (Mommy, what's an ecologist?), Hannah (Where on earth is Hannah Gilkenson?), Kari(Bohn), Kisi (So, how does a liberal Californian survive in Red Texas?), Mohit, Murat (Now you be careful

with them balloons, ya hear?), Nachum (Don't touch no purple instruments now), Shiva, Tameeka (CSI rocks!) and Wei (hey Sam!) - for everything. It was great to have such a diverse and lively group that would discuss things from biology to mid-east politics to food with equal passion. Thank you for taking such an interest in my work and taking time to give comments and support. I thank Ben,Tameeka and Chen for beta testing d3, sunshine and moonbeam. I thank Ann, Wasim and Kari(Titcher) for help with digitizing the video data (The next version of d3 will have an integrated *minesweeper* game, a *sudoku* generator, and of course an *InstantMessenger*). The more you clicked the more I could type. I thank Lavanya and Christina for soldering parts for the vertical array together. The more you soldered, the more I could type.

I thank the crazy bunch over at CSSL - Roc, Matt (hope this thesis lets me peel tape, man) and Hisham - for keeping me in touch with my academic ancestry.

I thank Jeff, Melinda and Dr. Yager for a fun collaboration with the bats and mantises.

Thanks go to Sandy (P.S. Do I still have your Harry Potter?) for being a wonderful friend and for being the Official Dragon Mistress and taking care of feeding the University's pet Bureaucratic Dragon at regular intervals, as demanded by the ancient rituals of academia and the NACS bylaws.

I thank my colleagues in the NACS community for taking an interest in my work and often giving left-field suggestions that always stimulated me to break out of my thinking box.

Mikki, some say, after that long march out of Africa our tribes split up. Some went north, some went south. (Some people have more complicated schemes, but that's basically the gist). Who would have thought that four millennia later one of their daughters and one of their sons would travel far west, and meet up again? Thank you for all your support and care and understanding and love. I am singularly blessed to find in one person a colleague, a friend and some one to face life's adventures together with.

I am now sure of what I want to do for the rest of my life. I want to understand living things. And I want to express my understanding in equations. Life is for living and for discovering and I thank you all for helping me during this phase of my journey of living and discovery.

I wrote this thesis using LaTeX (MikTeX) with texniccentre as frontend. I used the pdfpages and hyperref packages among others. For some diagrams I used Ipe and for others I used the GIMP. I wrote RA and then RRiki to manage my growing bibliography. RA and RRiki are open sourced under the GPL and are freely available, like all other tools mentioned here. All the data plots and most of the

other figures are natively in pdf format. Which means that in the electronic version you can zoom in to see great detail. This is especially true of the printed circuit board designs shown in Appendix D.

Funding

During graduate study I was supported for two years by a Jack-Bartlett Fellowship from the Psychology Department and for one year by NIH-NIBIB grant 1 R01 EB00475001 (as part of the NSF/NIH Collaborative Research in Computational Neuroscience Program). Funding for equipment also came from NSF grant IBN0111973 and AFOSR grant FA95500410130.

TABLE OF CONTENTS

LIST OF TABLES

LIST OF FIGURES

দ্বার বন্ধ করে দিয়ে ভ্রমটারে রুখি
সত্য বলে, আমি তবে কোথা দিয়ে ঢুকি?

If you shut the door to all errors, truth will be shut out.

- Rabindra Nath Tagore, *The Same Road*[a]

p 597, *Konika*.

---

[a]The Bengali title is ambiguous, and could also mean *The Only Road*

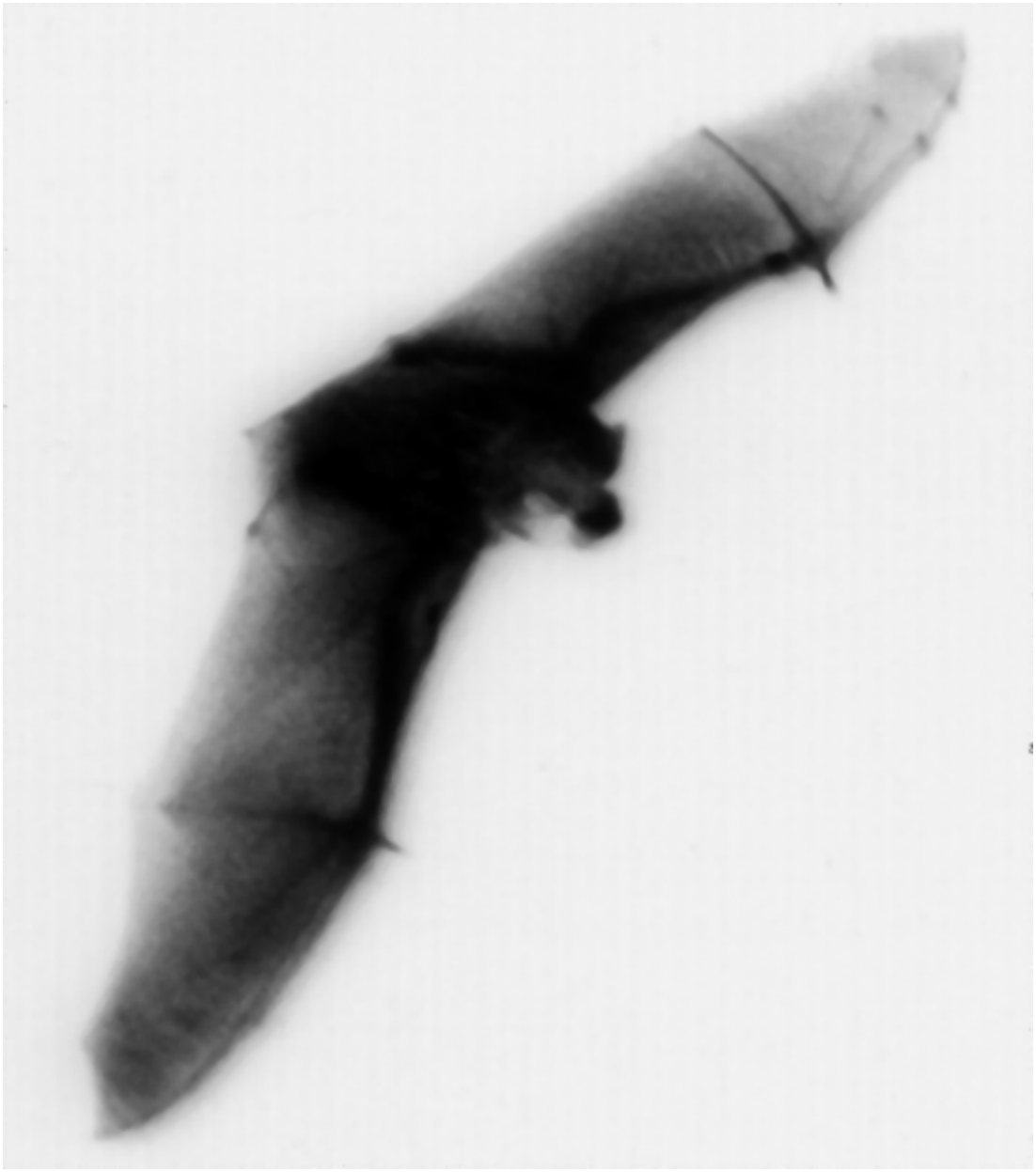

Eptesicus fuscus

Kodak IR film, open shutter, flash (1/60s, $> 650nm$ filter)

Print scanned, inverted and despeckled in the GIMP.

Hobbes : *I suppose research is out of the question.*

Calvin : *Oh, like I'm going to learn about bats and* then *write a report?! Give me a break!*

Bill Watterson

Calvin & Hobbes

1

Introduction

The question of how some bats navigate in darkness has fascinated humans since at least the 1700s. We humans are startled, intrigued and sometimes scared by the idea that something can glide silently past obstacles in complete darkness, in conditions where we can not see our hands in front of our face. Lazzaro Spallanzani and several other researchers, notably Louis Jurine, established during the period 1774-1798, that bats use hearing to navigate in the dark. Galambos (1942) has a synopsis of the painstaking, thorough experiments and the exchange of letters among an international

team of collaborators that led to this discovery. This article also tells of how, for a period, despite Spallanzani's experiments, the "scientific consensus" was that bats navigated through a sense of touch. The primary champion of this (mis)interpretation of Spallanzani's thorough experiments was Georges Cuvier. As late as 1912 Scientific American published an article about the "Sixth sense of the bat" by Hiram Maxim that contained a hybrid conjecture (Maxim, 1912). This article was timed to take advantage of the publicity surrounding the sinking of the *Titanic*. Hiram Maxim, inventor of the Maxim machine gun, outlined a proposal for an infra-sonic fog horn to detect obstacles as sea, such as icebergs. Normal fog-horns could not be made too loud otherwise they would deafen - perhaps permanently - crew and passengers. This shortened their detecting range. The continuous use of audible fog-horns on a luxury liner such as the *Titanic* would also disturb passengers, leading Maxim to propose the use of infra-sound. In one of the earlier attempts to sell the "biomimetic approach" Maxim claimed his infra-sonic foghorn was based on the bat's sixth sense. He suggested that bats produce infra-sound by the beat of their wings and analyze the infra sonic echoes by sensitive organs of touch found on their wings and face.

In the 1920s the scientific method began to reassert itself in this field. Hartridge proposed that bats emit short wavelength tones and listen to the echoes from objects in the environment (Hartridge, 1920). Hartridge refers to some experiments by a researcher called Whitaker, published in *Naturalist* in 1906 that showed that bats could be disturbed by clapping or ripping paper, though they were unconcerned by human speech. Hartridge makes no mention of Spallanzani's experiments. Donald Griffin's interest in bats and the availability of the first ultrasonic microphone led him to perform a series of experiments starting in the 1930s that led to our current appreciation of the bat's mysterious sixth sense as a sophisticated natural implementation of a SONAR

system (Griffin, 1958).

We know now that echolocating bats emit sounds through their mouth or nose. These sounds are mostly ultrasonic and form a beam that travels out into the environment. Objects in the path of this beam reflect echoes that return to the bat. The echoes contain information that the bat uses to form a percept of the world. This percept is so fine that bats can track and capture insects as small as mosquitoes, avoid fine wires less than a millimeter in diameter and locate and enter small cave openings after returning from foraging grounds miles away.

Echolocation demands our attention emotionally and intellectually. Echolocation gives us hope that we may be able to create prosthetics for the blind based on hearing. At the same time it challenges us to conceptualize a world created by sound. Our visual bias is betrayed by a language infested with terms such as 'visualize' and 'imagery'. Echolocation suggests to us a way to broaden our intellectual appreciation of how senses contribute to percepts. Echolocation suggests to us a way to test hypotheses in sensorimotor integration that have been based on experiments in vision.

1.1 Bat Biosonar

The sonar sounds emitted by bats are produced with their vocal apparatus[1] and emitted through their mouth or nose. This acoustic apparatus shapes and restricts the time-frequency and spatial extents of the signal. Different species of bat produce different types of sonar calls. Bats can be classified according to whether they produce calls having Constant-Frequency (CF, pure tone) components and/or Frequency Modulated

[1]The megabat *Rousettus* produces echolocation calls by tongue clicks and is the only megabat known to echolocate (Neuweiler, 2000, Chapter 6, pg 144).

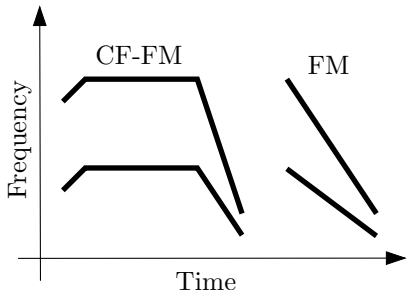

Figure 1.1: Schematic of the time-frequency structure of bat vocalizations

(FM, chirp or frequency sweep) components (see Fig.1.1). Most families of bat use FM calls and they are known as "FM bats". The big brown bat, *E. fuscus*, the subject of this study, is an example of an FM bat. Other bats, such as the horseshoe bat (*Rhinolophus ferrumequinum*), use a combination of CF and FM components in their calls and are known as CF-FM bats (Popper and Fay, 1995, Chapter 1, pg 3-6).

1.2 Active sensing, echolocation and locomotion

Active sensing is the name given to the process whereby animals guide their senses to seek out specific portions of the rich tapestry of information they receive. The study of active vision, for instance, involves the study of eye-movements in the context of different behavioral tasks (Yarbus, 1961). Echolocating bats add a new dimension to active sensing because they produce the initial energy that is reflected back by the environment. Bats can of course orient their head and ears to gather information from different parts of the environment, much like visual animals move their visual gaze around. In addition to this bats also have the ability to modulate various parameters of the outgoing sound to suit their behavioral goals. Bats can change the time-frequency structure of individual calls, the time-pattern of groups of calls, and the direction of their sonar beam in response to different behavioral contexts.

The bat's vocal behavior can be considered an auditory analog to visual gaze - a means by which the animal selects out part of the scene for additional or special processing. This idea leads to the exciting possibility that the bat's vocal behavior during different tasks can be used to study internal processes such as target selection and attention. The time-frequency structure of individual calls, the timing pattern of call groups and the direction the sonar beam is "thrown" may all be related to the behavioral requirements on the bat and may give insight to internal processes, such as attention.

Sensing the environment and moving though it are integral behaviors. Indeed, when our sensory focus drifts from serving our locomotor goal it often leads to perilous situations, as a recent law banning cell-phone use during driving acknowledges. During insect capture in bats the focus of active sensing and the goal of locomotion are likely to be identical - the insect being chased.

1.3 The time-frequency structure of the bat's vocalization as an index of behavioral state

Figure 1.2 shows two sonar calls produced by the same big brown bat during two different behaviors. The first call was made as the bat flew around a laboratory flight-room searching for prey to eat. The second call, recorded about 5 seconds later, was produced by the bat as it chased down an insect. The first call (a) is somewhat shallow (the frequency sweeps slowly with time) and longer in duration than the second call (b). It has been argued that by concentrating a long sound into a narrow frequency band bats can improve the signal-to-noise (SNR) ratio of echoes, improving their ability to detect small and/or distant targets (Popper and Fay, 1995, Chapter1, pg 8-9). A long

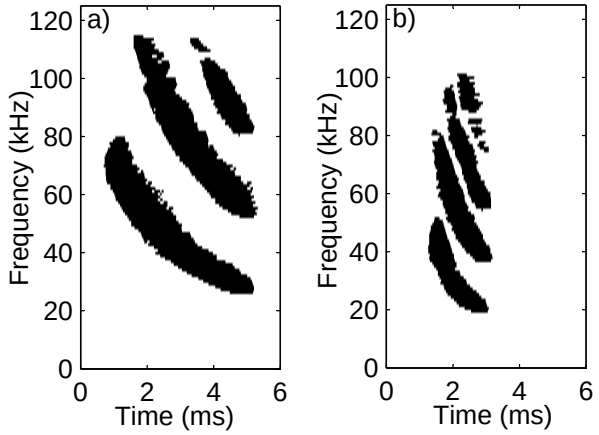

Figure 1.2: Spectrogram of two *E. fuscus* calls made by a single bat flying round a laboratory flight-room. a) A call made as the bat searched for a target to capture. b) A call made during an insect capture. The difference in the time-frequency structure of the calls illustrates the plasticity of bat vocalizations. The two calls have been "cut out" from a train of pulses that the bat produced during its flight in the room.

sound concentrated into one frequency band, however, reduces the resolution of the ranging system. For accurate ranging a short pulse - like the second pulse in Fig. 1.2- is more effective.

Bats also modify the timing of the train of echolocating calls they produce. Figure 1.3 shows the time-waveform of a sequence of pulses produced by a bat as it captures an insect (at time t=0). Initially the bat produces pulses at a rate of 10 Hz. In the field such calls can be as long as 20 ms, though in the laboratory shorter calls are observed (Surlykke and Moss, 2000). This is commonly called the search phase[2]. As the bat detects and then starts to pursue an insect the pulses are produced more frequently. During the terminal buzz, bats will produce calls at rates as high as 200 Hz with durations down to 1 ms or less (Griffin, 1958). During the searching phase of flight bats synchronize their calls to the upward stroke of their wing-beat possibly

[2]It has been argued that, due to the shortness of the calls measured in the laboratory, no true search phase is observed there.

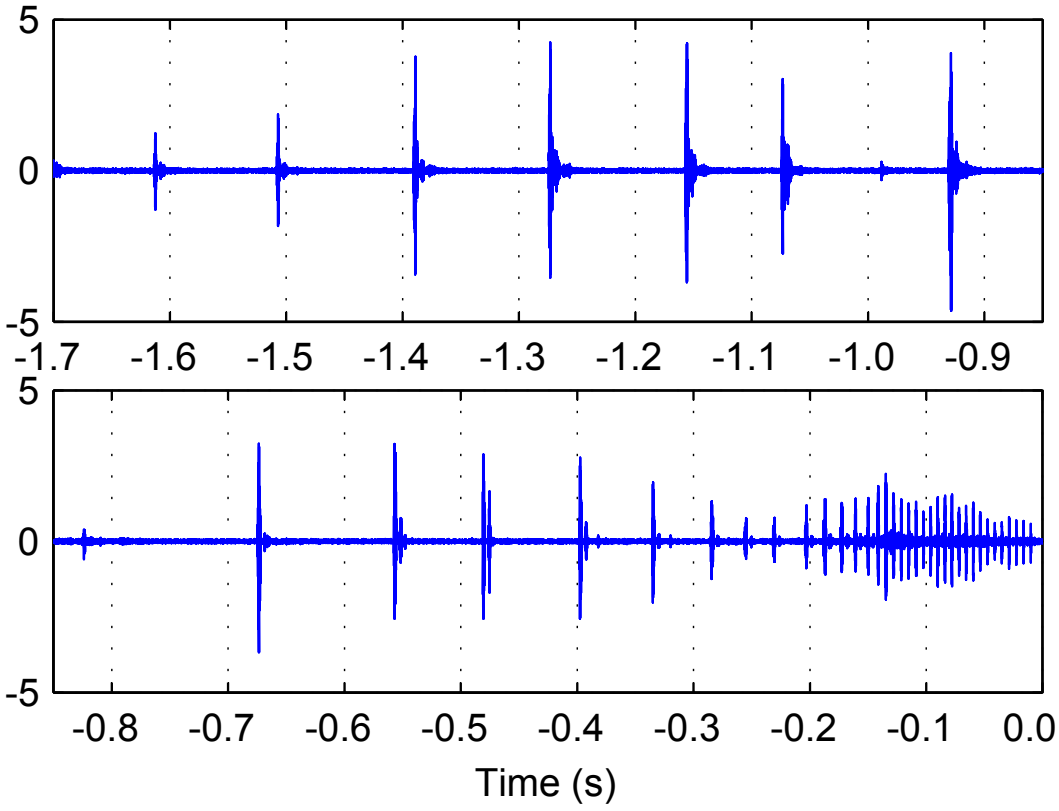

Figure 1.3: Train of echolocation pulses made by *E. fuscus* as it approaches and then captures an insect (capture is at time t=0)

conserving energy (Wong and Waters, 2001). When a prey item has been detected the bat needs to track it till capture. The insect often flies erratically and the bat needs rapid updates of the target position for a successful capture. This requirement is at least one of the reasons why bats increase their pulse repetition rate during insect chases.

There are many studies of the time-frequency structure of bat echolocation calls. A review of such work can be obtained from *Hearing By Bats* (Popper and Fay, 1995, Chapters 1-3), *The Biology of Bats* (Neuweiler, 2000, Chapter 6), *Bats: Biology and Behavior* (Altringham, 1996, Chapter 3) and *Echolocation in Bats and Dolphins* (Thomas, Moss, and Vater, 2004, Chapters 3, 36-38) among others.

1.4 Directionality of the bat's sonar beam

Spatially, the sonar sounds form a directional beam. Objects closer to the beam axis generate louder echoes than identical objects placed further off-axis. The sonar beam of FM bats is likely (see later) to be more frequency rich along the main beam axis. The off-axis sound is effectively low-pass filtered so that lower frequencies dominate to the sides.

Griffin did the first systematic studies of the bat's sonar beam directionality (Griffin, 1958, Chapter 4, pg 104-111). These initial studies were designed to test how directional a flying bat's sonar beam was. Two microphones were used to simultaneously measure the sonar emissions at two different locations as the bat flew through a certain point in space. These studies suggested that the bat's sonar beam, in flight, was directional and the directionality was dependent on the frequency[3]. Simmons (1969) followed up on these experiments by measuring the sonar beam pattern from bats preparing to take-off from a starting platform. The bats were trained to fly from a starting platform and land at a landing platform that had a triangular target. Four microphones were arranged in an array at the starting platform at a 30cm distance from the bat's head. The data were taken from the calls made by the bat a few seconds before take-off. The calls were assumed to have been directed at the landing platform the bat was trained to fly to. In both these studies the primary goal of measurement was to determine how directional the sonar beam of a bat was. Both studies attempted to study sonar beam emission from a behaving, if not flying bat.

All subsequent studies of the sonar beam pattern of the echolocating bat have been on restrained bats. A study of the horizontal beam pattern of a restrained horseshoe bat (Schnitzler and Grinnell, 1977) raised the possibility that the width of the sonar

[3]Griffin studied 50 flights of *Myotis lucifugus* out of which only 9 were analyzable

beam pattern at least for that species (which emits the sonar signal through a complicated nose-leaf apparatus) depends on the intensity of the signal. Hartley and Suthers performed detailed studies in three-dimensions (looking at the shape of the beam in both elevation and azimuth in multiple frequency bands) of the sonar beam in two bats [*Carollia perspicillata* (Hartley and Suthers, 1987), a fruit bat with a nose-leaf and *E. fuscus* (Hartley and Suthers, 1989)]. The bats were not only restrained, but also anesthetized. The brain was electrically stimulated to elicit ultrasonic vocalizations from the bat. These detailed studies revealed complex beam shapes, that could, to an approximation, be characterized has having a large lobe with complex side lobes at higher frequencies (For instance in *E. fuscus* (Hartley and Suthers, 1989), at lower frequencies ($\leq$ 40 kHz) the sonar beam basically consists of one large lobe, while a higher frequencies a prominent ventral lobe appears, with an intensity 6 dB below the main lobe's peak).

1.5 The sonar beam in a flying, behaving bat: An open question

Such previous studies have been concerned, first, with the question of degree ("How directional is the beam?") and, later, with a question of detail ("What is the detailed structure of the sonar beam?"). These studies have shown that the sonar beam is directional, can be described mainly as single lobed, though it has a complex fine structure especially at higher frequencies. These studies have remarked that the combination of directional sonar-beam and directional hearing in bats leads to a fairly directional sonar-system (Grinnell and Schnitzler, 1977). Directionality in this context is not the 2° visual fovea of humans, but rather a more relaxed 60° to 80° wide arc in both az-

imuth and elevation.

Prior work had not revealed how bats orient their sonar beam during flight. The study by Schnitzler (performed in horseshoe bats) includes a section that states bats hold their head level and straight ahead in horizontal flight (Schnitzler and Grinnell, 1977). This statement is repeated in Hartley's study of *E. fuscus* (Hartley and Suthers, 1989). This conjecture, however, had not been tested experimentally at that time. There is a rich literature on the complexity of eye-movements in visual animals and how eye and gaze movements are related to behavioral tasks, reaching and locomotion (Yarbus, 1965). This gives rise to the possibility that studying the direction of the sonar beam in flying echolocating bats will reveal similar, complex relationships between the sonar beam direction and behavioral tasks.

In studies where detailed measurements of the sonar beam shape were taken, the vocalizations were elicited by electrical stimulation of the mid-brain. The sonar beam shape depends, at least, on the frequency content of the signal, the shape of the mouth, the head and possibly the wings and the rest of the body. It is quite possible, therefore, that the sonar beam shapes produced by a flying bat will be different from that measured in stationary, head-fixed anesthetized bats.

This thesis is a collection of studies that examine the sonar beam pattern and direction in flying echolocating bats as they pursue insects in a laboratory flight room.

1.6 Results

The results are presented in the form of self-contained chapters written up (and in three cases, published) as papers.

Chapter 2 presents the apparatus used to record the sonar beam patterns from flying

bats as they perform different behaviors in a laboratory flight room. During insect pursuit the bat directs the horizontal axis of its beam at the target of interest while performing various maneuvers to catch the insect. On occasion the bat will "look over its shoulder", directing its sonar beam at more than 90° to its flight direction. During searching flight, when the bat is not making rapid maneuvers, the bat scans to the right and left of its flight path with its sonar beam. The accuracy of locking of the beam to the target has a standard deviation of 3°. This means that the bat keeps a selected target within an arc of 6° for 60% of the calls during a chase. This arc is one tenth of 70°, the estimated width of the echolocation system (Grinnell and Schnitzler, 1977). This suggests that either previous studies of the echolocation system have over-estimated its spatial coverage, or the bat is tracking targets with its beam with more accuracy than is demanded by purely acoustic considerations (getting a clear echo). Arguments are presented that the sonar beam direction in echolocating bats may be considered a component of the acoustic gaze of bats.

Chapter 3 shows that the vertical cross-section of the sonar beam of *E. fuscus* consists of two almost equally large lobes at 35 kHz. This finding is interesting, since previous studies of the sonar beam in stationary, anesthetized bats indicate that the two vertical lobes of *E. fuscus* calls only appear at higher frequencies ($> 60kHz$). This finding suggests that the sonar beams emitted by behaving, flying bats may be different from the sonar beams measured from stationary, anesthetized animals obtained by electrical stimulation.

Chapter 4 explores the relationship between the bat's sonar beam direction and its flight control. Results are presented supporting the idea that, for stationary targets, the bat's head leads its body. A tight coupling between the angular turning-rate of the bat and the sonar beam direction is found both when the bat is chasing stationary

tethered insects, and when the bat is flying round an empty room searching for a target. Interestingly, the gain of the coupling is higher by a factor of two when the bat is chasing prey, compared to when it is searching and not responding to prey.

Chapter 5 presents an analysis of how bats chase erratically moving free-flying insects. It is shown that bats follow a pursuit strategy that is locally time optimum. In short, the bat adjusts its flight path at every instant of pursuit such that if, from that instant onwards, the target followed a constant velocity path, the bat would intercept it in minimum-time. The strategy the bat follows results in the absolute direction to the target holding constant. That is, the direction of the target, from the bat, is a constant in an external inertial reference frame. This result, in conjunction with the finding that bats lock their sonar beam center to a selected target, suggests an interesting hypothesis for the high accuracy of lock-on. If the bat locks its head onto a target, then any deviations of the absolute direction of the target are signaled by the vestibular system, which is fixed to the head. The bat could then execute its pursuit strategy by flying to null changes in its vestibular system, while simultaneously maintaining head-lock with its target. This strategy is similar to the parallel navigation strategy implemented in guided missiles. In Appendix A it is shown that the result obtained in Chapter 4 is a special case of the minimum-time strategy for the case of stationary targets.

Chapter 6 is a study of the bat's behavioral responses to ultrasound-triggered dives by free-flying mantids. These mantids have a single non-directional ear, tuned to the frequencies of the sounds bat's produce during echolocation. When they detect bat echolocation sounds they initiate a powered dive in order to evade the bat. The mantis dive causes the bat to diverge, in the vertical plane, from the optimum pursuit-strategy described in Chapter 5. The bat will often pursue the diving mantis, recovering the optimal-strategy. When the mantis dives the bat is shown to maintain its sonar-beam

lock on the target (at least in the horizontal plane) as it follows the diving mantis.

1.7 Summary

This is the first study of the sonar beam directing behavior of a flying bat as it searches for and captures insects. This study shows that the sonar beam direction bears a tight relationship with target selection and tracking. As such it is a component of the acoustic gaze of echolocating bats, much like the time-frequency structure of vocalizations and vocalization trains. Also shown are relationships between the flight planning of the bat and the direction of its sonar beam. These relationships underscore the natural linkage between action and perception in the context of the sonar guided flight of bats.

Paper title	The sonar beam pattern of a flying bat as it tracks tethered insects
Authors	Kaushik Ghose and Cynthia F. Moss
Journal	*J. Acoust. Soc. Am.* (2003) 114(2): 1120-1131.

With one hand he held his pipe to his mouth, and in the other a number of lengths of cotton, to each of which was tied an almond-sized rose-beetle, glittering golden green in the sun, all of them flying round his hat with desperate, deep buzzings, trying to escape from the threads tied firmly round their waists.

Gerald Durrell

Ch 3: The Rose-Beetle man

in *My Family and Other Animals*

2

The sonar beam pattern of a flying bat as it tracks tethered insects

This paper describes measurements of the sonar beam pattern of flying echolocating bats, *E. fuscus*, performing various insect capture tasks in a large laboratory flight room. The beam pattern is deduced using the signal intensity pattern from a linear array of microphones. The positions of the bat and insect prey are obtained by stereoscopic reconstruction from two camera views. Results are reported in the form of beam

pattern plots and estimated direction of the beam axis. The bat centers its beam axis on the selected target with a standard deviation (σ) of 3^o. The experimental error is $\pm 1.4^o$. Trials conducted with two targets show that the bat consistently tracks one of the targets with its beam. These findings suggest that the axis of the bat sonar beam is a good index of selective tracking of targets and in this respect is analogous to gaze in predominantly visual animals.

2.1 Introduction

Echolocating bats can orient, forage and perform other perceptually-guided tasks in complete darkness by emitting ultrasonic vocal signals and analyzing the echoes returning from objects in their environment (Griffin, 1958). In this respect, bats provide an opportunity to study the use of audition in spatial tasks, which may be accomplished in other animals by using vision.

We studied *E. fuscus*, a bat species that echolocates with frequency modulated (FM) signals. Each sonar signal consists of several harmonically related frequency sweeps. The *E. fuscus* echolocation call time-frequency structure changes as the bat searches for, approaches and captures insect prey (Fig. 2.1). This species forages mainly in open spaces but has been reported to pursue prey near vegetation (Simmons et al., 2001).

The timing, duration and spectral characteristics of each sonar pulse influence the echo information available to the bat's acoustic imaging system. While searching for prey, *E. fuscus* uses long (15-20ms) pulses with a shallow frequency sweep. The fundamental frequency sweeps from approximately 28 to 22 kHz. The rate of production

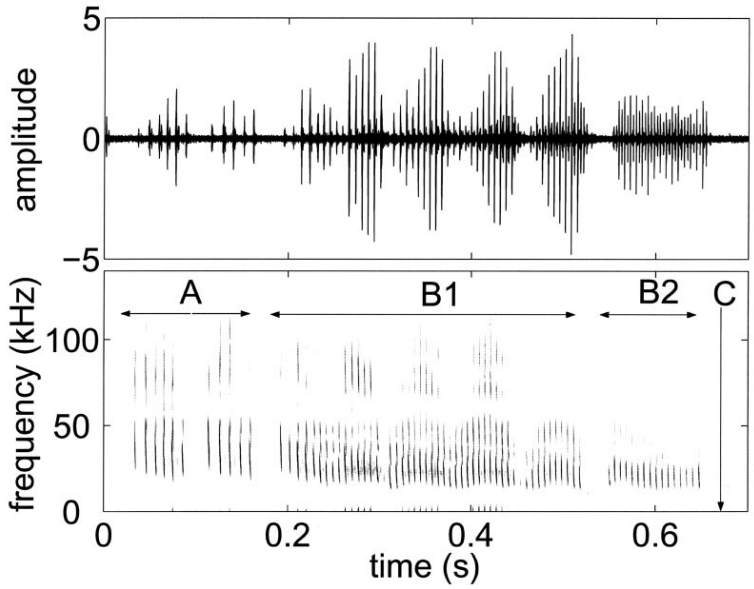

Figure 2.1: The top panel shows the time waveform of a series of *E. fuscus* vocalizations recorded in the laboratory. The bottom panel shows the spectrogram of this signal. Different stages of foraging are marked out. **A** is the approach phase, **B1** is buzz1, **B2** is buzz2, while **C** refers to the time of contact of the bat with the prey.

may be as low as 5-10 Hz. Upon detecting a prey item, the bat approaches it, shortening the pulses to 2-5 ms and increasing bandwidth (fundamental sweeping from 60 to 22 kHz). During the terminal phase the pulses may be as short as 0.5-1ms with the fundamental sweeping from about 40 kHz to 12 kHz and produced at rates of up to 150-200 Hz in the terminal (or feeding) buzz (Griffin, Webster, and Michael, 1960) (see Fig. 2.1). Vocalizations cease when the bat is about 10-15 cm from the prey (which is approximately 30-50 ms prior to contact with the prey). The sequence is completed with a capture attempt using the tail membrane (arranged like a scoop), the wing tips (to push the prey towards the mouth), or in rare instances directly with the mouth. The longer duration search signals have only been recorded from bats foraging in wide open spaces and not in the lab (Surlykke and Moss, 2000).

The spatial characteristics of the sonar beam influence the echoes received by the bat. Hartley and Suthers (Hartley and Suthers, 1989) measured the beam pattern of a stationary, anesthetized *E. fuscus* resting on a platform and stimulated to vocalize by applying electrical pulses to a vocal-motor area of the brain. The results of this study showed that the sonar beam of *E. fuscus* is broad, but not omni-directional. The sonar beam has a main lobe directed along the midline and slightly downwards; its vertical position rising slightly at higher frequencies. The main lobe intensity drops by 3dB at 35° off midline. There is a ventral lobe below the main lobe and weaker by about 6 dB compared to peak intensity.

The directionality suggests that objects closer to the beam axis (the direction of the peak of the main lobe of the beam) will return stronger echoes than objects located more laterally. We propose that the bat maximizes the signal to noise ratio of returning echoes by directing its vocalization beam at the location of a prey item. Therefore, we hypothesize that the bat's aim of its sonar beam in the direction of a target is a natural motor action associated with target selection and tracking. We test this hypothesis by recording the sonar beam patterns produced by bats catching tethered insects in a flight room. We use these data to calculate the direction of the beam axis with respect to the target.

2.2 Methods

2.2.1 Behavioral tasks

Four echolocating bats of the species *E. fuscus* were used for the study. The bats were allowed to fly in a large room (7m x 6m) whose walls were covered with sound absorbent foam (Sonex-1) to dampen reverberation and enable recordings of bat vo-

calizations. The bats were trained to take a mealworm (target) from a tether while in flight. The target could be moved in a circular path by a motor-operated boom positioned just below the ceiling. It could also be dropped into the flight space by a trap door mechanism mounted just under the ceiling. The trapdoor was padded to minimize noise as it opened. Microphones placed on the floor of the room did not pick up any sound when the trap door opened. We cannot, however, rule out there being some sound associated with the trap door opening that the bat could hear.

One behavioral task consisted of releasing the tethered target from the trap door at a random point in time as the bat flew by. In this manner the bat was presented with a target whose location (over an area of approximately 2 m^2) was unknown until the trap door was opened. Analysis of the beam direction before and after the target presentation enabled us to study one aspect of the orienting behavior of the bat as it detects and then attacks prey. The four bats had previously been trained to take targets from a tether and had been used the previous year for studying their vocalization behavior as they caught tethered insects in the laboratory. There was no training time required for the bats during the current set of experiments besides one week of "warm up" flying at the start of the season after which the bats vocal behavior was recorded as they caught tethered insects. Data was collected in the form of insect capture trials setup by the experimenter; each trial consisted of a segment of data that contained one and sometimes more attempts by the bat to capture the target.

2.2.2 Array recordings

The array consisted of sixteen Knowles FG3329 microphones arranged in a planar U-shape along three walls of the flight room (see Fig. 2.2). The linear spacing between the microphones was 1 m, and the height of the microphones was 0.9 m above the floor.

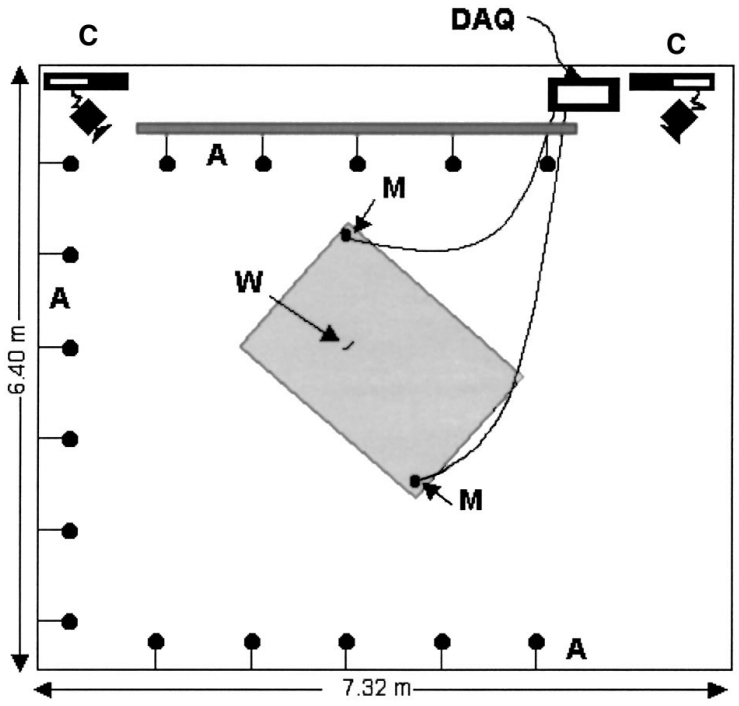

Figure 2.2: Plan view of flight room and array layout. **A**: microphone array, **M**: Ultrasound Advice microphones, **C**: High speed digital video cameras running at 240 frames per second, **DAQ**: Data Acquisition systems; IoTech WaveBook, 2 channels at 250 kHz each and National Instruments AT-MIO-16-E-1 board, 16 channels at 20 kHz each, **W**: Tethered worm. Shaded area represents the calibrated space (within which the path of the bat may be accurately reconstructed from the camera views).

Each microphone was extended from the wall mounting by a thin (3mm dia) steel rod 0.3 m long. This served to reduce the overlap between the original sound and any residual echoes from the sound proofing panels or mounting base. In order to compute the beam pattern for a given frequency band the information required is the intensity of the signal in that band. This information can be obtained from both the band-pass signal as well as the envelope of that signal, provided the signal is narrow-band, or it can be broken up into segments that are narrow-band, as shown here:

Let $f(t)$ be the measured signal, let $f_a(t)$ be the analytical signal for $f(t)$ and let $\hat{f}(t)$ be the Hilbert transform of $f(t)$. Such that

$$f_a(t) = f(t) + j.\hat{f}(t) \tag{2.1}$$

We know that the envelope of $f(t)$ is

$$|f_a(t)| = \sqrt{f(t)^2 + \hat{f}(t)^2} \tag{2.2}$$

Therefore the integral of the square of the envelope from time t_1 to t_2 reduces to

$$\int_{t_1}^{t_2} |f_a(t)|^2 dt = \int_{t_1}^{t_2} f(t)^2 dt + \int_{t_1}^{t_2} \hat{f}(t)^2 dt \tag{2.3}$$

We recognize the first term to be the energy of the signal over the time t_1 to t_2. If we assume that the signal over this time period has primarily one frequency component, then $\hat{f}(t)$ is merely a phase-shifted version of $f(t)$. If we further assume that the time interval $[t_1, t_2]$ is much larger than the period of the signal $f(t)$ then $\int_{t_1}^{t_2} \hat{f}(t)^2 dt \simeq \int_{t_1}^{t_2} f(t)^2 dt$, which gives us

$$\int_{t_1}^{t_2} |f_a(t)|^2 dt \simeq 2 \int_{t_1}^{t_2} f(t)^2 dt \tag{2.4}$$

This result (Eq. 2.4) shows that integrating the square of the envelope of a band-passed version of a bat call will give us the signal intensity in that band. Simulations using recorded bat vocalizations support this result. As described above, the sonar vocalizations of *E. fuscus* are frequency sweeps composed of a fundamental and several harmonics. By band-pass filtering this signal we can meet the required criteria.

The frequency content of the envelope for the echolocation signals is related to the duration of the signals. The shortest signal durations occur during the terminal buzz phase of insect capture and are on the order of 0.5-1 ms, which implies that the upper limit frequency content of the *envelope of the whole signal* is around 2 kHz. Assuming

conservatively that the envelope of a band-pass of this signal has a duration of .25 ms, this places the frequency content of the envelope at around 4 kHz. Therefore, a sampling rate of 20 kHz captures the envelope with good fidelity. This reduces the data acquisition requirements for sonar signal recordings from an array of microphones by a factor of 12.5 (assuming a sampling rate of 250 kHz is sufficient to record the broadband signal).

The frequency band of the sonar signals of *E. fuscus* hunting insect prey in the lab varies widely, with more power at higher frequencies during the early approach phase of insect pursuit and more power at lower frequencies during the terminal buzz phase. By choosing a frequency band centered at 35 kHz we discovered that we could record signals during all foraging stages (The typical Signal to Noise Ratio (SNR) using this method was estimated at 20 dB for the bat vocalizations).

In order to determine the beam pattern from a flying bat, the distance dependent-attenuation of the sonar signals must be corrected (Lawrence and Simmons, 1982). This correction (detailed in the Data Processing section) has two components. One is the spherical attenuation loss and depends only on the distance between the bat and a given microphone. The other is the absorption of energy as the sound is propagated through the air. This is dependent on both distance and frequency.

Keeping these factors in mind, we developed the scheme outlined in Fig. 2.3A. The signal from each microphone was fed to an amplifying band-pass filter which extracts signal components centered around 35 kHz. All circuits were constructed with off-the-shelf components soldered onto custom printed circuit boards. The frequency characteristics of the filter used is shown in Fig. 2.3B. This signal was then fed to a peak detector circuit which extracted the envelope of this band-passed signal. The envelope was smoothed by a low-pass filter and then digitized. Examples of

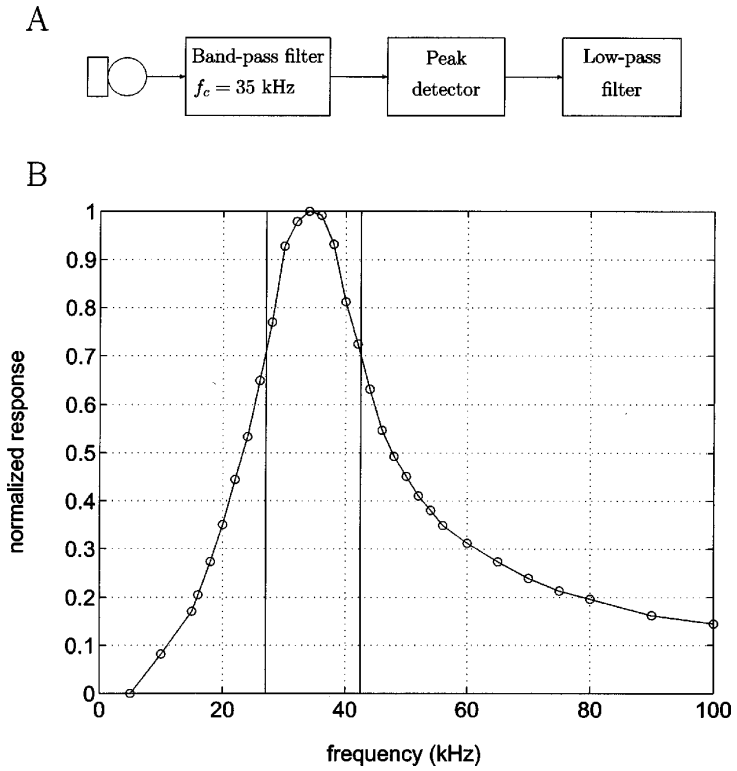

Figure 2.3: A. Schematic of signal processing hardware. B. Filter characteristics of the bandpass filter used. The x-axis shows the frequency, while the y axis shows the normalised response. The vertical bars correspond to the 3dB (half-power) points ie. the start and stop frequency. Examples of band-pass signal and envelope extraction may be seen in Fig. 2.4 A and B.

synthetic and bat sonar signals received at a microphone and their band-pass filtered, smoothened envelopes may be seen in Fig. 2.4 Signal digitization was done by a National Instruments Data Acquisition Board (AT-MIO-16-E-1, 12 bit, 50 ns clock, 8 sec rolling buffer) controlled by a PC running a C program.

2.2.3 Broadband microphone recordings

In addition to the array microphones, we used two Ultrasound Advice SM2 microphones and SP2 amplifiers (flat response up to ($\pm$ 2 dB)40 kHz, 5 dB drop from 40 to 100 kHz). The microphone signal was further amplified and filtered by active fil-

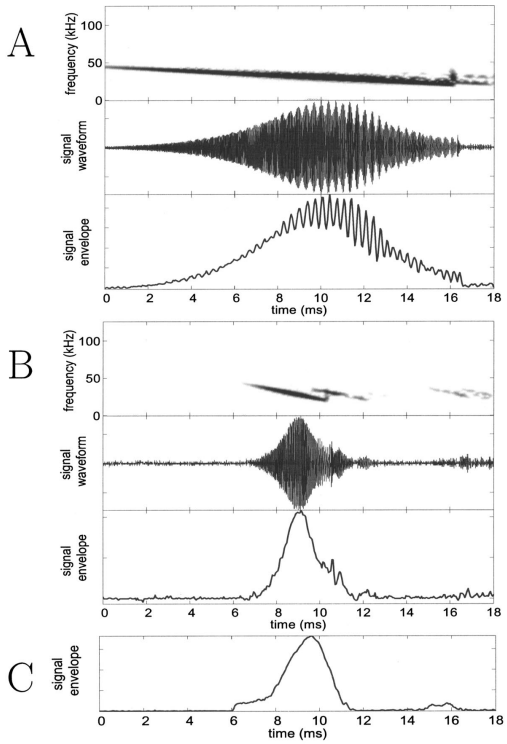

Figure 2.4: Panels A and B show recordings taken by pinging the array with frequency sweeps from an emitter. A shows that for a long (shallow) sweep there is more overlap between the incident sound and the returning echo, and the beats are more prominent. B shows that for short sweeps there is less overlap. The top panel in each is the spectrogram of the bandpassed signal received at one of the array microphones, the middle panel shows the time waveform of that signal, while the bottom panel shows the envelope extracted by the array hardware. The interaction between the incident sound and an overlapping echo shows up as a beat. In both A and B, the emitter was placed in the plane of the array so as to maximize the echo returning to the microphone from the array backend. Due to limitations of the signal generator used to produce the emitted sounds, each frequency sweep has a brief glitch as it resets to the start frequency and this is visible as a vertical streak in the spectrogram. This does not change any results. C shows the envelope signal taken from an array circuit during a trial with a flying bat. In general the bat sounds recorded at the array do not show apparent effects of overlapping echoes. A detailed explanation is given in the text.

ters (Stanford Research Systems Model SR 650 digital filter, band-pass set at 10-99 kHz). These microphones recorded full bandwidth vocalization waveforms. The signals were digitized using an IoTech Wavebook 512 at 250 kHz per channel (12 bit, 8.19 sec rolling buffer) run by a Dell laptop computer.

2.2.4 Cameras and calibration

Two Kodak MotionCorder digital video cameras running at 240 Hz were used to record the flight paths of the bats and the locations of insect targets and microphones. The cameras were operated under long wavelength lighting (> 650 nm, red filters, Reed Plastics, Rockville MD), to ensure that the bats were not using vision in the insect capture task (Hope and Bhatnagar, 1979). The digital frames stored on the camera buffers were downloaded onto analog tape. Relevant sections of the video record were then redigitized using a MiroVideo DC30 capture board. Motion analysis software from Peak Performance Technologies (Motus) was used to convert the images of the bat and other objects from the two camera recordings into 3-dimensional coordinates. A calibration frame supplied by Peak Performance was used for this transformation. Since the array was outside the space covered by the calibration frame, manual measurements were made that enabled us to compute the array coordinates in the camera reference frame.

2.2.5 Triggering and synchronization

Data acquired by the three digitizing systems was continuously stored on rolling buffers. When the trial was judged to be complete (usually after a capture or capture attempt) the same end-trigger was fed to all three systems to capture the last 8 seconds of data.

2.3 Data analysis

2.3.1 Beam pattern computation

The signals from each microphone were segmented to select out the vocalizations and exclude the echoes. The received intensity I_r was computed from the envelope. This intensity value was corrected for spherical loss and atmospheric attenuation to give I_c as shown in Eq. (2.5). Values for the attenuation coefficient were obtained from standard tables [ISO 9613 - 1, acoustics, and cross checked against an ASA Acoustics Handbook (Beranek, 1986)]. The corrected intensity was calculated as :

$$I_c = I_r r^2 . 10^{\frac{1}{10} \cdot r\alpha} \tag{2.5}$$

where r is the distance between the microphone and the bat. Software for this calculation was written in MATLAB.

The overall beam pattern was then reconstructed, as shown in Fig. 2.5.

2.3.2 Beam axis computation

According to our hypothesis, the bat aims its sonar beam at a target of interest. Assuming the beam to be symmetrical, adding up direction vectors from the bat to each microphone, weighted by the corrected intensity at that microphone, results in a vector whose direction is an objective estimate of the beam axis, regardless of the actual profile of the beam. This is given by Eq. (2.6)

$$\overrightarrow{H} = \sum_n \overrightarrow{I}_i \tag{2.6}$$

where $\overrightarrow{I}_i$ is the vector drawn from the bat to microphone i with magnitude propor-

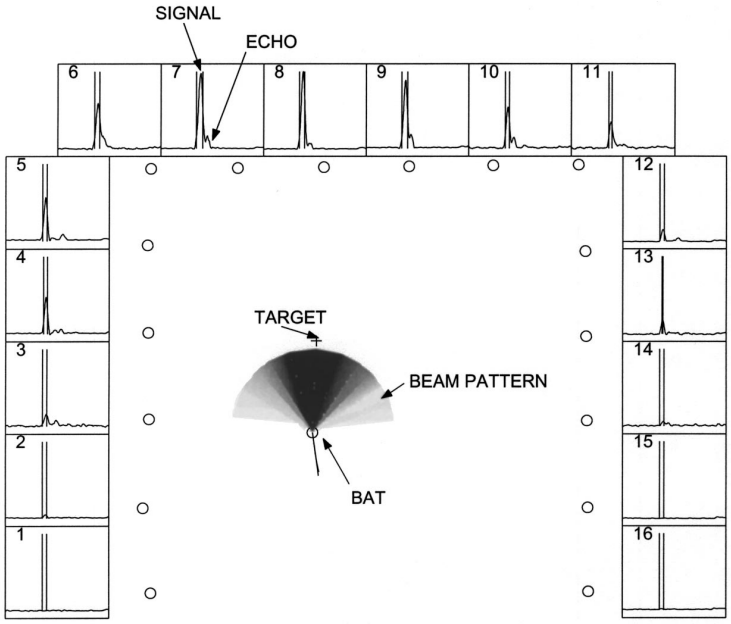

Figure 2.5: Beam pattern reconstruction. Central panel shows the reconstructed beam pattern. The 16 circles along the edges of the panel are the positions of the microphones in the array. The pattern is normalized such that the peak intensity has a value of 1.0 and is colored black. Lighter colors denote progressively lower intensities. The circle at the center of the beam pattern represents the position of the bat. The + symbol represents the position of the worm. The thin curved line terminating at the bat's position is the trajectory of the bat up to that frame. The straight line drawn from the bat represents the direction of motion of the bat (in this frame the two overlap). Surrounding panels (numbered 1 through 16) show the envelope signals digitized from each microphone. All the side panels have the same scales. 20 ms of data are shown. The signal on each panel is time shifted to compensate for the time of travel of the sound from the bat to the corresponding microphone. As a result the direct signal from the bat (first sound) lines up on all the panels. A fairly loud echo (second smaller bump) doesn't as its source is at a different position. This makes it easier to segment the signals and discard the echoes. The segmentation for the vocalisation shown is depicted as two vertical bars bracketing the relevant portion of the envelope trace.

tional to the corrected intensity. $\overrightarrow{H}$ is the resultant, whose direction is the estimate of the beam axis.

2.3.3 Errors due to array geometry

Figure 2.6 shows simulation results for beam axis computations for 6 different head orientations. The simulated beam pattern is shown at the center of the array. This

beam is then "emitted" at different positions in the space enclosed by the array and the estimated beam directions are computed from the signals received by the array elements. The results are shown as black arrows. As can be seen from Fig. 2.6A through E, only if the source of the signal is close to the array (around 1 m) do we see edge effects which warp the estimate. During experiments we only use the data collected within the calibrated space which is more than 1 m from the array boundary. In addition, as expected, if the beam points out of the space enclosed by the array we get a biased estimate of beam direction. This is illustrated in Fig. 2.6F. (If the array were constructed to be a ring, this error would not be present. More microphones were not added because of limitations in the data acquisition hardware and due to difficulties in placing an array segment on the fourth wall of the flight room.)

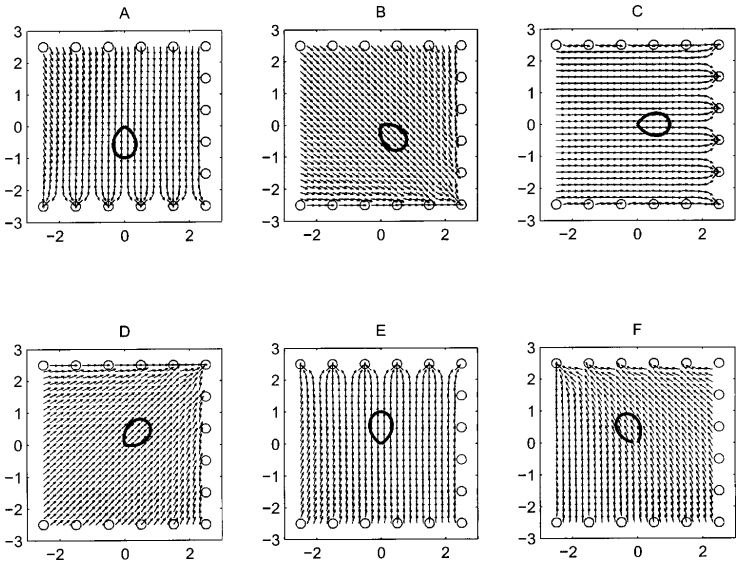

Figure 2.6: Plots of estimated head aim at different points within the space enclosed by the array (small black arrows) with a polar plot of the beam intensity profile (bold pattern) overlaid at the center. The direction the beam is pointing in corresponds to the peak of the profile. Plots A to E demonstrate that errors in computing headaim grow large only when the source is close to the edge of the array (around 1 m). F demonstrates that if the beam is directed out of the space enclosed by the array estimates become biased even near the center of the array. The x and y axes tick marks are in meters.

2.3.4 Calibrations with frequency sweeps

The array was tested using an emitter mounted on a tripod at the center of the array and oriented in different directions. The emitter produced frequency sweeps starting from 50 kHz and sweeping down to 20 kHz. The signals were recorded using the array, and the emitter itself was filmed using the video cameras. Two markers were attached to the emitter, and these were used to reconstruct the direction the emitter was pointing. The signals recorded at the array were analyzed in the same manner as real bat signals and the direction of the beam was computed as described previously. This was compared against the reference direction computed from two markers attached to the emitter.

Three calibrations were done from two positions in the calibrated space and the results of the calibration are illustrated in Fig. 2.7. If the array computation did not need any correction then the traces would be a horizontal line running along zero. The average of these traces between the two vertical dotted lines at -50^o and +120^o was used to create a calibration curve to map the measured beam axis to a corrected beam axis. The final beam axis computation results in an error of $\pm$ 1.4^o

2.3.5 Effect of echoes on the estimate

Echoes that overlap with the original bat vocalization at the array microphone change the envelope of the received signal. The bat vocalizations are frequency sweeps, and the interaction between incident sound and overlapping echo takes the form of "beats" in the envelope. This is illustrated in Fig. 2.4 A and B which show the results of ensonifying the array with an emitter placed level with the array and producing frequency sweeps. Steeper sweeps, shown in Fig. 2.4 B, result in less of an overlap zone and slower beats than shown in A, since the interacting frequencies are further apart.

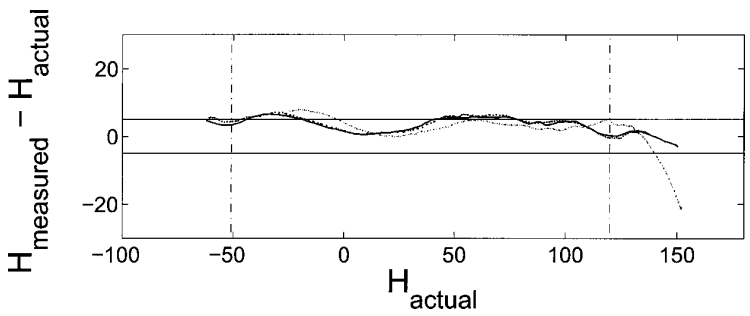

Figure 2.7: This graph summarizes the calibration runs. The y-axis shows the angular difference between the emitter direction observed from the video ($\vec{H}_{actual}$) and the beam center estimated from the array data ($\vec{H}_{computed}$) plotted against $\vec{H}_{actual}$. The two horizontal lines mark $\pm 5^o$. This graph illustrates the edge effect predicted by the simulations (see Fig. 2.6). The edge effect is seen as an increase in bias of the error towards one direction as $\vec{H}_{actual}$ begins to approach the edge of the array. The average of these traces between the two vertical dotted lines at -50^o and +120^o was used to create a calibration curve to map the measured beam axis to a corrected beam axis. The final beam axis computation results in an error of $\pm$ 1.4^o.

The modulation depth of the beats depends on how strong the echo is relative to the direct emission. Fig. 2.4 A and B illustrate the largest echo effects, since the emitter is placed in the plane of the array (.9 m above the ground), and the array microphones received a relatively large echo from the base of the microphone support. In general the bats do not fly so low in the room (the average altitude of the bats is about 1.5m off the ground and this is probably influenced by the height at which prey items are usually presented). Thus the echoes that interact at the array microphones are typically from the walls or floor. These echoes are greatly attenuated (due to the sound absorbent foam used). In addition the path the echo travels is larger and the overlap with the incident sound is less. This is illustrated in Fig. 2.4 C. In practice, modulation of the sound at the microphone array due to loud echoes overlapping with the incident sound is rarely observed. In addition runs were done with the emitter placed in the plane of the array and producing shallow frequency sweeps so as to intentionally corrupt the readings with echoes. Analysis of these runs show that the error introduced by echoes

remain within the tolerance ($\pm 1.4^o$) of the method.

2.3.6 Limitations of a linear array

The sonar beam of the bat extends in both azimuth and elevation. A linear array takes only a slice through the 3-dimensional structure of the beam. Therefore, the exact shape and amplitude of the beam pattern recorded by a linear array depends on the vertical orientation of the beam. This means that absolute measurements of the beam width and intensity cannot be taken from our data. The conclusions about beam axis remain valid for a bat with its head held roughly level with the horizon. The bat's beam is not of circular cross-section (and indeed may have a prominent ventral lobe (Hartley and Suthers, 1989), also see "horns of the bat" section later) and so the beam pattern recorded by a linear array will be distorted if the bat rotates its head relative to the horizontal.

2.4 Results

2.4.1 Beam Patterns

The basic data from the experiments are the beam patterns measured as the bat selects, tracks and then captures a target. A sequence showing beam patterns from successive vocalizations is shown in Fig. 2.8. These show clearly how the bat first scans the space around it with the beam (Fig. 2.8 A, B and C) and then aligns its beam with the target (Fig. 2.8 D, E and F). Also note the "notch" in the beam patterns in A, B and D. The notch may be due to the orientation of the bat's head with respect to the horizontal microphone array and the ventral lobe of the beam. This is discussed in a later section, "horns of the bat."

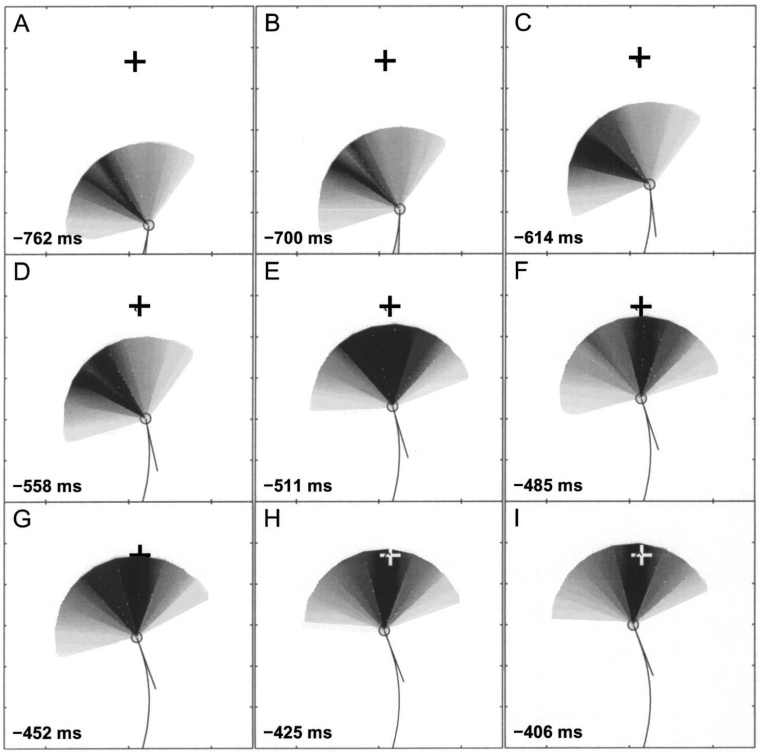

Figure 2.8: Beam patterns of several vocalizations from a bat intercepting a tethered meal worm. The meal worm is denoted by +, the bat is denoted by a circle with a line extending to show the velocity vector of flight, which is assumed to be approximately aligned to the body. The times indicate milliseconds before contact. The circles at the borders of the panels denote the positions of the microphones. Note how a scanning motion (A,B,C,D) narrows down (E,F,G) and then changes to a "lock-on" motion (H,I) as the bat searches for then selects the target. Also note the split that appears in vocalization patterns A and B. This is discussed in the text. Microphone positions are not shown, but the orientation of the plot is identical to that in Fig. 2.5.

We also made animations of the beam patterns recorded from several trials and these are available as `.avi` files on our website *http://www.bsos.umd.edu/psyc/batlab/jasa03/*. A brief description of the animations on the website is given in Table 2.1.

2.4.2 Beam width

The measurements were used to find the half power points of the beam (where the intensity is 3 dB below the peak). Fig. 2.9A is a frequency histogram of the full -3dB

beam-widths obtained by this method. The four traces correspond to data from the four bats. Fig. 2.9B shows a scatter plot of the beam widths against the range from the target when they were obtained. There is no significant correlation between beam width and range to target (r = -0.0252 $p > .1$). Most of the data points are obtained with the bat within 1 m of the target. The mean value of -3 dB beamwidth from all the bats is 70^o.

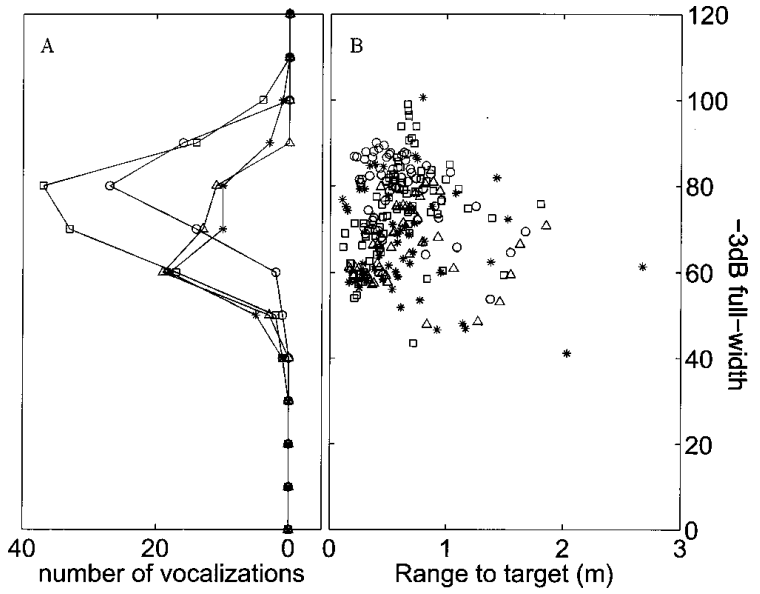

Figure 2.9: A shows a frequency histogram of the computed beam widths over 13 trials and 4 bats. B shows the data from which this histogram was made plotted against the range to target at which the measurements were taken. The data from different bats are shown as different symbols.

2.4.3 Tracking accuracy

Using Eq. (2.6) the axis of the beam can be obtained. The angular deviation between the beam axis and the target (the tracking angle) for 13 trials was analyzed and the results are summarized in Fig. 2.10. Fig. 2.10A shows the tracking angle plotted against time to contact with the target. During the last 300ms of attack the bat locks it

beam with a standard deviation (σ) of 3^o onto the target. Fig. 2.10B shows the tracking angle plotted against range to target. This shows that within .5 m of capture the bat has locked its beam on to the target with a σ of 3^o. Fig. 2.10C shows the interpulse interval plotted against time. Fig. 2.10D and E show the distribution of tracking angles at different stages. D shows data when there was more than 300 ms to contact, while E shows data when the bat was within 300 ms of contact.

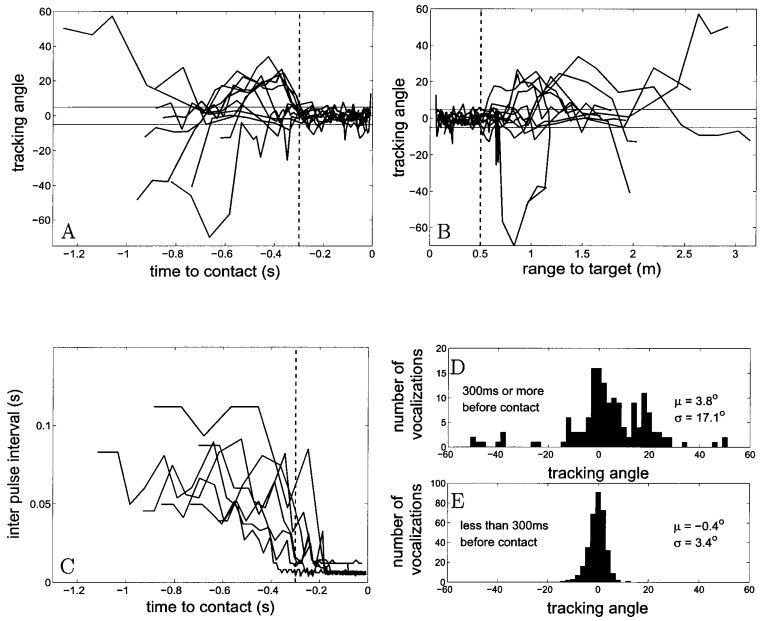

Figure 2.10: This plot summarizes the results of analyzing the angular deviation between the beam axis and the target (the tracking angle) for 13 trials. A shows the tracking angle for each trial plotted against time to contact with the target(zero being time of contact). The vertical dotted line marks 300 ms before contact. B is a plot of tracking angle against range to target. The vertical dotted line marks .5 m to target. In plots A and B the solid horizontal lines mark $\pm\ 5^o$. C shows the interpulse interval plotted against time. D and E show the distribution of tracking angles at different time periods before target contact. D shows data when there is more than 300 ms to contact, while E shows data when the bat is within 300 ms of contact.

2.4.4 The "horns of the bat"

Referring to vocalizations shown in panels A, B and D of Fig. 2.8, the beam seems to be split in two, i.e. displaying two spatially separate energy peaks. The remaining vocalizations seem to have one large lobe. Polar plots of normalized intensity for a single beam and a "notched" beam are shown in the right panels of Fig. 2.11 A and B respectively. The left panels show the image from one of the cameras at the instants these beam patterns were measured. The image of the bat is circled. We confirmed that this notch was not due to measurement error (eg. malfunction in some of the array elements). As shown in Fig. 2.11 B we discovered that in some trials the notch occurred when the bat was clearly banking during a turn. We do not know if the head is tilted during the bank.

2.5 Discussion

2.5.1 Tracking accuracy

From our experiments we conclude that the big brown bat, *E. fuscus*, tracking tethered insects, centers its beam-axis on the target with a standard deviation (σ) of 3^o during the terminal phase of insect capture. The method used here introduced an error of $\pm 1.4^o$. The value of target accuracy we obtain is lower than the accuracy reported by Masters with measurements taken from a stationary bat tracking a smoothly moving target from a platform (Masters, Moffat, and Simmons, 1985) which was given as 1^o. However in the Masters, Moffat and Simmons study the authors applied a lag and gain correction to the bat's actual head motion to arrive at the value. The actual head motion as reported in that paper, appeared to follow the target motion with errors of up to 10^o. The bat seemed to follow the target accurately when it was sweeping past the front of

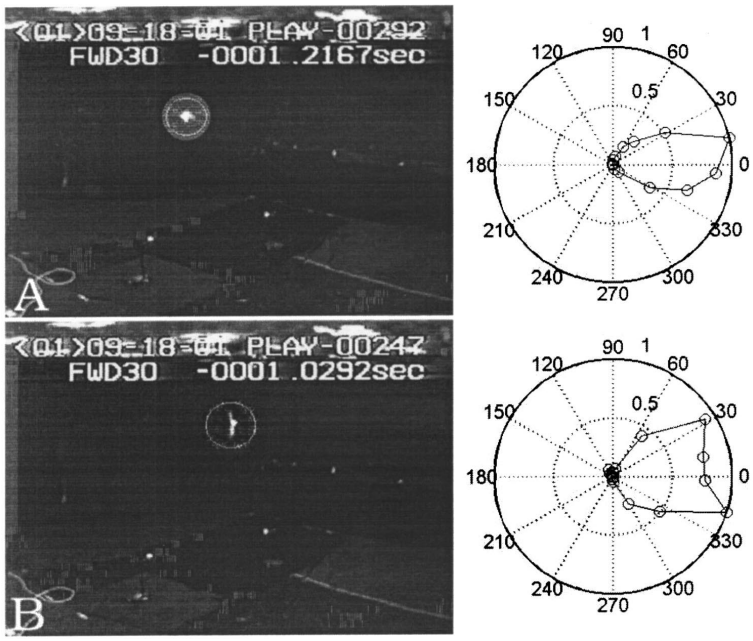

Figure 2.11: The images in the left column are taken from one of the video camera records of a trial. The location of the bat is circled. The images are roughly 190 ms apart in time. The right column shows the polar plot of intensity (maximum intensity normalized to 1.0, and represented by outermost ring of the polar plot) from the vocalizations made during the respective frames. The circles denote actual intensity data points. In A the bat is in level flight, heading parallel to the plane of the camera. Note that the beam pattern has a single large lobe. In B the bat is banking sharply as can be deduced from the relative positions of the wings. It is moving into the plane of the camera. Note that the beam pattern now has a prominent notch. Animations of this trial may be seen at *http://www.bsos.umd.edu/psyc/batlab/jasa03/*. The original grey levels of the camera images have been re-mapped in a nonlinear fashion to enhance the images.

its observing platform, but as the target rotated to more extreme angles the bat did not orient to follow it completely. Webster and Brazier (Webster and Brazier, 1965), using photographs of bats attacking free-flying insect prey, arrived at the slightly looser value of 5^o but the accuracy of the method used was not mentioned.

Given that the 3 dB width of the beam is around 70^o, a standard deviation of 3^o in directing the beam onto the target is unlikely to be due to the bat's need to maintain a good echo return from the target. We cannot say from these experiments what other advantage there may be to centering the tracked target. One review (Simmons, 1987, Chap 8) suggests that the bat's azimuthal localization acuity is greatest in a narrow

($\sim 10^o$) zone directly in front of it. If this is correct, then the bat may be centering the target while tracking in order to keep it in this high localization acuity zone. Neural recordings from the inferior colliculus of the mustached bat show that the thresholds of all binaural neurons are lowest at the horizontal midline independent of the neuron's frequency selectivity (Covey and Casseday, 1995), suggesting that for mustached bats, at least, there is a preference for processing echoes from directly ahead. Studies on the localization ability of the bottle-nosed dolphin indicate that the minimum audible angle (MAA) directly in front of the animal for broadband clicks is around $.9^o$ in azimuth (Renaud and Popper, 1975). The MAA in more lateral positions has not been studied.

Assuming that the axis of the beam bears a constant relation to the bat's head, another hypothesis may be that a type of beam forming operates in the bat's acoustic system. In this beam forming operation, signals that arrive simultaneously in both ears (ie. from the centre line) are enhanced compared to signals from more off-axis targets.

2.5.2 Beam axis as an index of selection and tracking

Our data suggest that the sonar beam direction of an echolocating bat is a useful index of its selection and tracking behavior during prey capture. The bat points its beam around the flight space using a gradual scanning motion while searching for prey. When prey is presented to the bat (e.g. by dropping it into the flight space using a trap door) the scanning pattern shifts towards the position of the target. Finally the bat "locks" its sonar beam onto the target and tracks it closely. The lock-on behavior precedes the high vocalization repetition rates characteristic of the terminal phase by 50-100 ms (see Fig. 2.10A and C). This may reflect a sequential process of first localizing an object, directing the beam towards it and then identifying it as a prey item to capture. It may also indicate different latencies for motor pathways mediating head

orientation and vocalization control.

Animation *http://www.bsos.umd.edu/psyc/batlab/jasa03/2002.08.20.3.02.avi* illustrates that the bat may direct its beam sequentially at different objects before deciding to attack one.

The lock-on behavior is observed even when the prey and bat are moving in a tight circle, and the bat is not within catching distance of the prey, as illustrated in animation *http://www.bsos.umd.edu/psyc/batlab/jasa03/2001.06.12.1.03.avi*. This animation also demonstrates that the bat may orient its beam up to 90^o off its flight path ("looking over its shoulder") in order to maintain lock-on to the target. It appears that pointing its beam at a target of interest is a deliberate strategy adopted by the bat.

It is important, at this point, to note that the relationship between the beam width and the spatial limits of target perception by the bat are unknown. The limits will possibly depend on a combination of the size of the target, orientation of the pinnae and intensity of the vocalization in addition to the direction and width of the beam.

2.5.3 The horns of the bat

We consider here why we observe a notch in some beam patterns. We noted that a) the notch could "travel" from one microphone (or two adjacent microphones) to the other and b) during the same trial we could get a combination of "normal" and "notched" beam patterns, implying that it was not an artifact due to a bad microphone. We hypothesize that the the notch is due to a strong ventral lobe, perhaps more prominent than that measured by Hartley, which was 6 dB below the main lobe intensity (Hartley and Suthers, 1989). Whenever the bat's head is sufficiently tilted with respect to the horizontal, the cross-section of the sonar beam taken by the linear array would pick up the two lobes. In other cases, when the head is level with respect to the array, the

cross-section consists of one lobe. In support of this hypothesis, we noted that in some trials the notch appears during sharp banking turns by the bat (as estimated from the positions of the wings) e.g. see Fig. 2.11B. During a banking turn, it is likely the head is also tilted with respect to the horizon. The notch is probably also not due to a shadowing effect of the beam by the target since it is sometimes observed when the beam is directed away from the target, or when there is no target in the room (e.g. Fig. 2.8)

2.5.4 Comparison with related work

Previous work using microphone arrays to record bat vocalizations have been conducted in the field, and the main aims of these studies have been to estimate bat position and vocalization source levels. Jensen and Miller (Jensen and Miller, 1999) used a vertical array of three microphones to study the variation of bat vocalization intensity with altitude. The array data was also used to localize the bat's position with respect to the microphones in the array. Holderied used two microphone clusters to track bats up to a range of 35m in the field and study source levels. These studies were not designed with the intent of studying the beam pattern directly, but have revealed indirect effects of the beam, such as periodic variations in received intensity, which may be attributed to the bat pointing its beam in different directions (i.e. scanning) while in flight.

Møhl *et al.* (Møhl et al., 2000) recorded Sperm Whale vocalizations using an array of hydrophones. They used these data to localize the animals and deduce the directionality of their emissions. More controlled measurements of the beam patterns of stationary dolphins have been taken (Au, 1993, Chapter 6). In comparison to bats, dolphins have a much narrower half-power beam width (10^o compared to 70^o). The peak of the main lobe seems to be directed upward of the snout axis by 5^o, in contrast

to *E. fuscus*, where the main lobe seems to be directed 10^o below the snout. The differences in the width of the sonar beams of bats and marine mammals may be related to differences in the physical structure of the head as well as differences in signal generation and acoustics in air and underwater. Interaural time and intensity cues for localizing sound underwater are less salient than in air. By producing a narrow emission beam dolphins could conceivably improve their localization ability.

2.5.5 Limitations of a linear array

The apparatus used here, a linear array of microphones, is limited in that it takes only a planar cross section of the bats three-dimensional sonar beam. By using an array that extends in both the vertical and horizontal planes these results may be extended to observe the vertical tracking behavior of the bat and the position of the notch (the region between the ventral and axial lobes of the beam) when the bat tracks prey.

2.6 Conclusion

These experiments are the first measurements of the bat's sonar beam pattern as it tracks and intercepts prey in flight. There has been work on the sonar beam of a stationary anesthetized bat (Hartley and Suthers, 1989) where the sonar beam was described in great detail, but for a non behaving animal. There has been more extensively reported work on the sonar beam of dolphins and other odontocetes (Au, 1993, Chapter 6). In these studies too the subjects were stationary and not using sonar for a target interception task.

The data presented here suggest that echolocating bats of the species *E. fuscus* direct their beam at a target of interest with an accuracy of about 3^o. There may be an

analogy between the orienting of the sonar beam by echolocating bats and the orienting of gaze by visual animals like primates. Early experiments by Yarbus on humans have revealed that when viewing the same scene the pattern of eye movements used is influenced by what information the subject is trying to acquire from the viewing (Yarbus, 1961). Some experiments have also suggested that covert shifts of visual attention are linked to the preparation to make saccades (Rizzolatti et al., 1987). Orienting the eyes to a visual stimulus is an important natural action, even though primates can, if needed, covertly attend to a stimulus without repositioning the eyes (For a review see McFadden and Wallman (McFadden and Wallman, 2001)).

We propose that the orientation of the beam may be used as an index that reveals some aspects of the bat's internal state during different behavioral tasks. Specifically, we think that the orienting of the beam may be used to probe what objects in a complex environment the bat is interested in. We also propose that the orienting behavior may be used to measure latencies in various target detection tasks in echolocation, much like eye movements are used in visual paradigms.

All files are found at *http://www.bsos.umd.edu/psyc/batlab/jasa03/*

File name (.avi)	**description**
2001.09.18.2.01 2001.09.18.2.01split 2001.09.18.2.01splitpolar	The bat flies in from the far end of the array. The black persistent lines represent the computed beam axis for each vocalization. The worm is dropped into the flight space at frame 78. The bat directs its beam initially to the left of its flight path upto frame 132, then starts to ping in the direction of the target (ahead of it) from frame 143 onwards. It increases its repetition rate noticably from frame 169 onwards. The 2001.09.18.2.01split animation shows the view from one of the infra-red cameras. The 2001.09.18.2.01splitpolar animation shows polar plots of the beam pattern
2001.10.02.1.01 2001.10.02.1.01split	The bat takes a sharp turn to its right, flying towards the room center. The target is dropped from the trap door in frame 100. The bat first directs its beam towards the target at frame 199, and makes a sharp turn left to try and intercept it. The bat hits the target but fails to capture it. The target remains swinging on the tether. The bat flies past, then makes a sharp 180^o turn starting at frame 406 and directs its beam in the direction of the target. It picks up pursuit of the target at frame 535, noticably increasing its repetition rate at frame 545. This attempt ends in a successful capture.
2002.08.20.3.02	The bat flies towards the center of the room. The black square represents an inedible block of foam. The bat vocalizes ahead of its flight path. The target is dropped at frame 25. The bat initially "inspects" the inedible foam block (frames 119 to 181) then directs its beam to the target from frame 184 onwards.
2001.06.12.1.03	The bat attempts to capture a tethered meal worm being moved in a circle about .5 m in diameter. The bat keeps its beam centered on the target throughout, even though it gives up pursuit after making a complete circuit. Beam pattern data is not available for part of the pursuit (during which the beam was directed where there were no microphones) .

Table 2.1: Beam pattern animation descriptions

Paper title	Flying big brown bats emit a beam with two lobes in the dorso-ventral plane
Authors	Kaushik Ghose, Timothy K. Horiuchi and Cynthia F. Moss
Journal	for submission to *J. Acoust. Soc. Amer.*

And it would be necessary to prevent Venus being seen round at one time and forked at another, with very thin horns; as well as many other sensory observations which can never be reconciled with the Ptolemaic system in any way, but are very strong arguments for the Copernican.

Galileo Galilei

Letter to the Grand Duchess Christina of Tuscany, 1615

3

The horns of the bat

3.1 Introduction

Insectivorous echolocating bats, such as the big brown bat, *Eptesicus fuscus*, navigate and forage for airborne insects in darkness. They produce intermittent pulses of directed ultrasound and use the information contained in the returning echoes to detect, localize and track flying insect prey, relying on hearing, instead of vision, to guide complex spatial behaviors (Griffin, 1958; Griffin, Webster, and Michael, 1960). The

sonar beam is directional (Griffin, 1958, Chapter 4, pg 104-111) and may serve as a spatial window restricting the region of space the bat gathers information from. The sonar beam in stationary, head fixed, bats has been studied by several people (Grinnell and Schnitzler, 1977; Schnitzler and Grinnell, 1977). Hartley and Suthers performed detailed studies of the sonar beam in *E. fuscus* by measuring the shape of the beam in both elevation and azimuth in multiple frequency bands (Hartley and Suthers, 1989). The bats were anesthetized and positioned on a platform that controlled the position of the head. The mid-brain was electrically stimulated to elicit ultrasonic vocalizations. The sonar beam pattern recorded in that condition consisted of a large main lobe. At frequencies higher than $60\ kHz$ a second lobe appeared, $6\ dB$ less intense than the main lobe. This second lobe was located ventral to the main lobe, at an angle of 30^o.

It is not known whether the sounds elicited by brain-stimulation of a stationary, head fixed bat produce beam patterns similar to that in a flying bat. The sonar beam pattern depends not only on the frequency content of the signal, but also on the shape of the vocal cavity and, potentially, the configuration of nearby surfaces such as wings, during the time of emission. It is important, therefore, to study the sonar beam patterns produced by bats echolocating in flight and during insect capture. Here we recorded vertical and horizontal cross-sections of the sonar beam produced by echolocating bats as they flew and pursued prey in a laboratory flight-room. We were limited by technical considerations to recording a narrow band of frequencies centered around $35\ kHz$. In contrast to the study by Hartley and Suthers we find evidence for a ventral lobe at $35\ kHz$. The size of the ventral lobe is comparable to the frontal "main" lobe. We speculate that the ventral lobe may serve to generate a ground-return that helps the bat to measure its altitude in flight without the need for head movements.

3.2 Methods

3.2.1 Behavioral experiments

We trained two bats of the species *E. fuscus* to fly individually in a large (L7.3m x W6.4m x H2.5m) laboratory flight room (Fig. 3.1). The bats were trained to catch insects (mealworms) suspended from a tether. The tether was attached to a motorized boom placed at random points under the ceiling. The insect could be hung stationary from the boom, or swung in horizontal arcs by the boom to present a moving target to the bat. The walls and ceiling of the flight room were lined with sound-absorbent acoustic foam (Sonex One, Acoustical Solutions, Inc., Richmond, VA) to reduce reverberations. The room was illuminated by dim, long wavelength light (> 650 nm, light from normal incandescent bulbs passed through a infrared filter plate - Plexiglas G #2711, Atofina Chemicals, Philadelphia, PA) to which the bat is insensitive (Hope and Bhatnagar, 1979). Stereo images from two high speed video cameras (Kodak MotionCorder, CCD based cameras operating at 240 frames-per-second ($4.16\ ms$ sampling interval), synchronized to 1/2 frame accuracy) were used to reconstruct the three-dimensional flight path of the bat and the trajectory of the prey. Simultaneously, an array of 20 microphones (Knowles Co, FG 3329, electret) recorded the sonar beam pattern produced by the bat. 16 microphones were arranged in a horizontal U-shape around the room to extract the horizontal aspect of the sonar beam. The remaining 4 microphones were arranged vertically on one wall of the room. These four microphones and one microphone from the horizontal arrangement formed a five microphone vertical array that enabled us to record vertical cross-sections of the emitted sonar beam. The Knowles microphones have a small membrane diameter ($\sim 1\ mm$) and are omnidirectional at $35\ kHz$ ($\lambda_{35\ kHz} = 9.7\ mm$) enabling recording

of the beam pattern as the bat flies around the room (Ghose and Moss, 2003). The

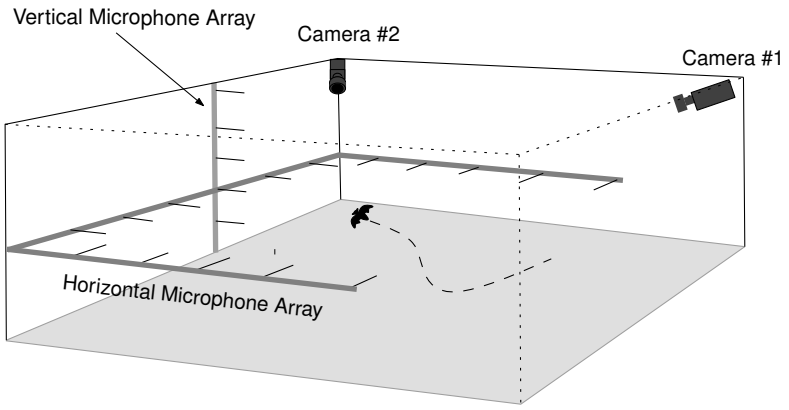

Figure 3.1: Laboratory flight room. The bats were trained to fly in a flight room L7.3m x W6.4m x H2.5m high. The room walls and ceiling were covered with sound absorbent foam to reduce reverberations. Illumination was dim red lighting (wavelength $>$ 650 nm) to exclude the bat's use of vision. Two digital video cameras operating at 240 frames/s recorded the three-dimensional position of the bats and tethered insects during the experiments. An array of 20 microphones (16 microphones arranged in the horizontal plane to record horizontal cross-sections of the sonar beam, four microphones arranged vertically to take vertical cross-sections) was used to record the sonar beam pattern of the bats as they flew in the room.

microphone signals were amplified, band-pass filtered ($f_c = 35\ kHz$, $Q_{-3db} = 2.5$, half-power band ranging from $28\ kHz$ to $42\ kHz$) and then processed through a envelope extractor circuit. The envelopes of the bat vocalizations were digitized at $20\ kHz$ and stored on a computer for later analysis (Ghose and Moss, 2003).

3.2.2 Computation of the sonar beam pattern

The envelope traces were used to compute the received intensity of the sonar beam, I_{r_m}, at each microphone m. This intensity was corrected for spherical spreading loss and atmospheric attenuation to obtain the corrected, normalized intensity, I_{c_m} at each microphone. Previous experiments on stationary anesthetized bats (Hartley and Suthers, 1989) and from flying bats (Ghose and Moss, 2003; Ghose and Moss, 2006)

have indicated that the sonar beam is horizontally symmetrical. In this study we fit the horizontal sonar beam pattern to a Gaussian shape in order to extract the sonar beam-axis direction. The fit is performed by adjusting the direction and width of the Gaussian beam pattern to obtain the least-mean-square error to the observed beam pattern. We have previously used a vector averaging method (Ghose and Moss, 2003) to obtain the sonar beam direction. We observed that fitting the sonar beam to a Gaussian shape before computing the axis direction made the computation less sensitive to edge effects (Ghose and Moss, 2003, Section III C) and less sensitive to variations in the recorded sonar beam profiles from vocalization to vocalization.

3.2.3 Microphone array calibration

The microphone array was calibrated for gain and frequency response by playing ultrasonic frequency sweeps of a fixed amplitude from a speaker placed at a fixed distance and orientation to each microphone. A gain factor was computed for each array channel (microphone and signal processing circuit) that normalized the recordings across all the channels. An ultrasonic speaker with a circular aperture was used as a control emitter to test the microphone array. Recordings of cross-sections of the sonar beam produced by the control emitter appeared as single lobes on the horizontal and vertical arrays.

3.3 Results

We analyzed flight paths, vocalization timing patterns and sonar-beam patterns from a total of 15 flights from two bats as they intercepted insects. Horizontal sonar beam patterns appeared as a single lobe, consistent with previous recordings (Ghose and

Moss, 2003). In all trials, however, we observed notched beam shapes recorded by the vertical array.

3.3.1 The sonar beam has a prominent notch in the dorso-ventral plane

We observed a prominent notch in the vertical sonar beam profile. Fig. 3.2 shows the sonar beam pattern of a single vocalization. The top panel shows the top-view of the flight room. The small black circles are the positions of the array microphones, the black line is the flight-path of the bat, the black circle is the current position of the bat. The dark gray "balloon" represents the smoothened profile of the horizontal sonar beam, with radius proportional to normalized intensity. The intensity at each microphone is normalized to the maximum intensity measured across the array for that vocalization. The measured intensities are shown as connected black dots overlaid with the balloon. The black line is the trajectory of the tethered insect and the black cross is the present position of the insect. The position of the vertical array is indicated by the label 'V' in the upper panel of Fig. 3.2.

The bottom panel shows the sonar beam profile recorded by the vertical array. The dotted lines show the "field-of-view" of the vertical array. These lines show the the angular limits of the vertical array, beyond which we can not measure the sonar beam pattern. As can be seen, in contrast to the single prominent lobe shape of the horizontal cross-section, the vertical cross-section presents a forked shape. This shape is suggestive of two lobes of comparable size arranged dorso-ventrally. At this stage the bat was producing pulses at a low repetition rate ($< 20\ Hz$) which are associated with searching behaviors. The bat's flight maneuvers suggest it was not responding to the target yet.

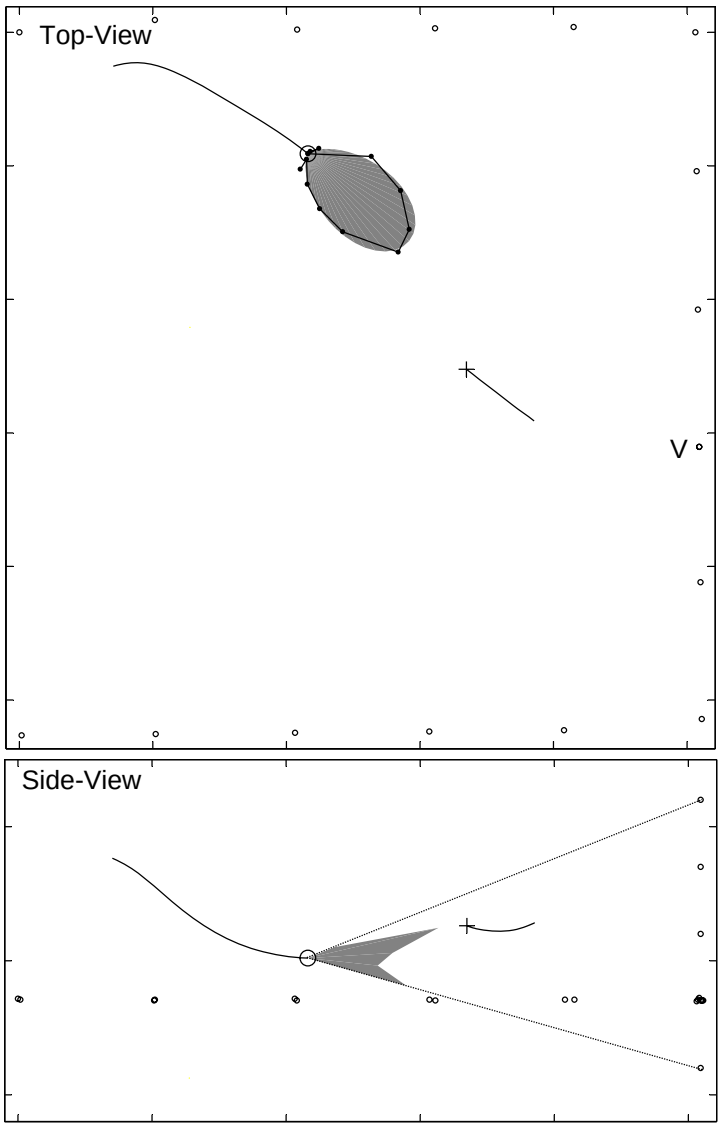

Figure 3.2: The sonar beam of flying *E. fuscus* has a vertical notch. Top panel: The small black circles are the positions of the array microphones, the black line is the flight path of the bat, the black circle is the current position of the bat. The dark gray polar plot represents the smoothened profile of the horizontal sonar beam, with radius proportional to normalized intensity. The black dots joined by a line are the unsmoothened measured intensities. The black line is the trajectory of the tethered insect and the black cross is the present position of the insect. The position of the vertical array is indicated by the label 'V'. Bottom panel: Polar plot of the vertical section of the sonar beam recorded by the vertical array (Gray polygon). Dotted lines show the angular limits of the vertical array measurement. The bat is producing pulses at a slow repetition rate ($< 20\ Hz$) at this stage.

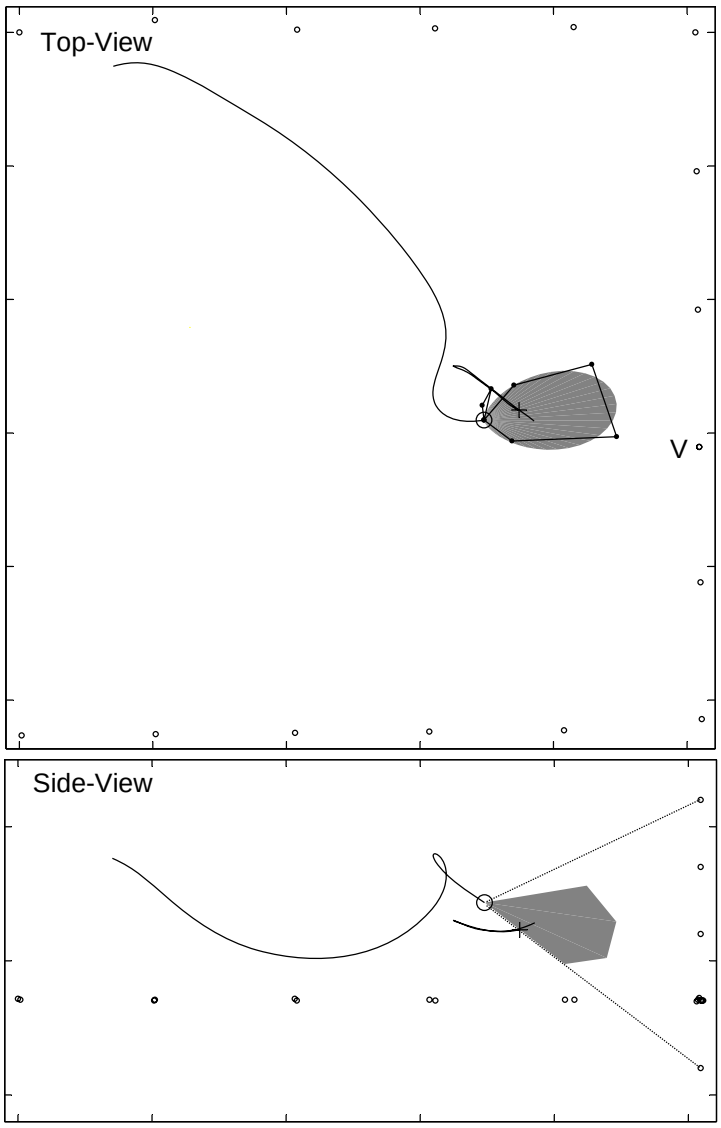

Figure 3.3: The bat may move its sonar beam up and down. This figure shows a sonar beam pattern approximately 1 s after the vocalization shown in Fig. 3.2. The top-view panel shows that the bat is responding to the target by adjusting its flight path and the horizontal aspect of the beam is locked to the target. The side-view panel shows no evidence of a notch in the beam. If the bat's sonar beam had two prominent lobes in the vertical plane and if the bat was directing its sonar beam down at the target (black cross) such that the location of the lower lobe is below the lower angular limit of the array (black dotted lines) this is the expected shape of the recorded sonar beam cross-section.

Fig. 3.3 shows the sonar beam pattern of a vocalization approximately one second later for the trial shown in Fig. 3.2. At this time the bat was producing pulses at a high repetition rate ($> 100\ Hz$) and was responding to the target. The vertical sonar beam profile shows no evidence of a notch for this vocalization. If the bat's sonar beam had two prominent lobes in the vertical plane and if the bat was directing its sonar beam down at the target (black cross) such that the location of the lower lobe is below the lower angular limit of the array (black dotted lines) this is the expected shape of the recorded sonar beam cross-section. Figs. 3.4 - 3.6 present further evidence that the bat moves the sonar beam in the vertical plane, perhaps in order to track the vertical position of the target.

Fig. 3.4 shows six vocalizations from a sequence of calls made by bat#1 as it intercepted a tethered insect. To reduce clutter in the diagram not all vocalizations in the pulse train produced by the bat are shown. Dotted lines in the bottom panel show the "field-of-view" of the vertical array beyond which the shape of the vertical beam could not be recorded. Vocalization samples 1 through 5 show a prominent notch in the vertical cross-section, while the notch is absent in 6. The bat is responding to the target during 5 and 6, and is swooping down on the target during 6. The vertical sonar beam patterns are consistent with the hypothesis that the bat's sonar beam has two lobes arranged dorso-ventrally. During vocalization samples 1 through 4 the bat is directing the beam such that one lobe points up and the other down to the ground. The absence of a notch in 6 is consistent with the bat directing its beam such that one lobe is pointing in the direction of the target.

Fig. 3.5 and Fig. 3.6 show vocalization sequences from bat#1 and bat#2 respectively, each showing the notched appearance of the sonar beam. Initially the bat is producing signals at a low rate ($< 20\ Hz$). In later stages the bat locks its beam onto

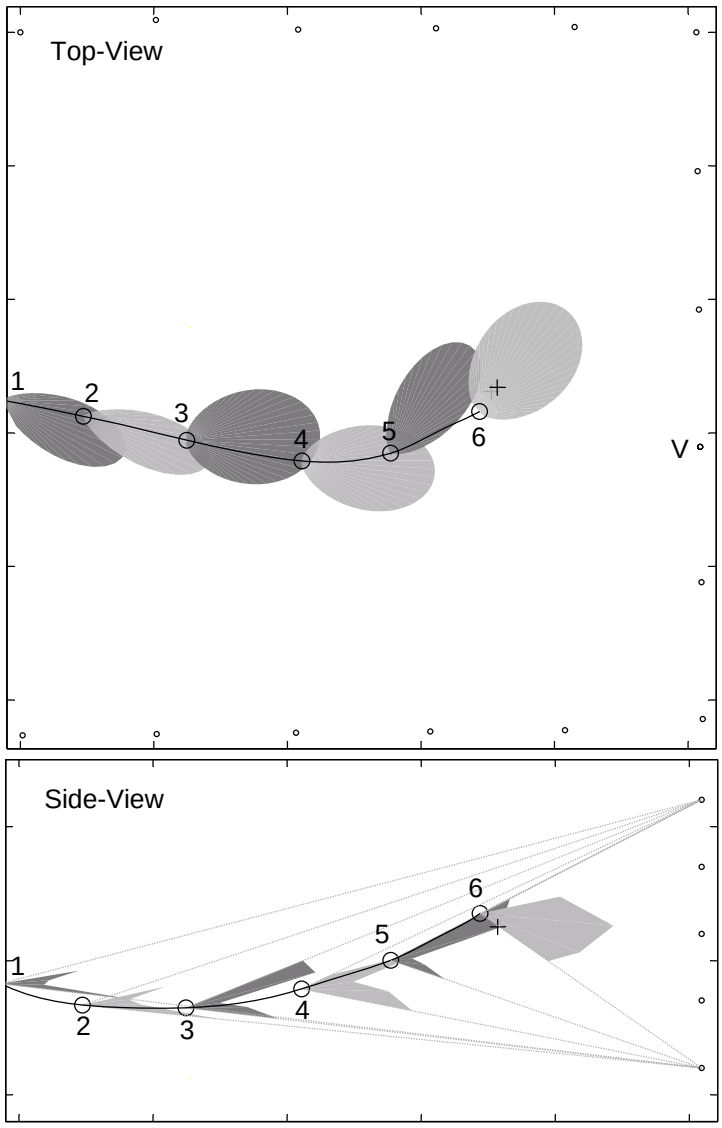

Figure 3.4: The bat may move its beam up and down to track the target. This figure shows some vocalizations from bat#1 during a prey interception. To improve clarity not all vocalizations in the train produced by the bat are shown in the diagram. The top-panel shows horizontal cross-sections of the sonar beam, bottom-panel shows vertical cross-sections. Dotted lines in the bottom panel show the "field-of-view" of the vertical array. Vocalization samples 1 to 4 were produced at a low rate ($< 20\ Hz$) while 5 and 6 are taken from a train of pulses produced at a high rate ($> 100\ Hz$). Samples 1 to 5 show a prominent notch in the vertical cross-section, while the notch is absent in 6. The bat is responding to the target during 5 and 6, and is swooping down on the target during 6. In the side-view the horizontal array is omitted for clarity.

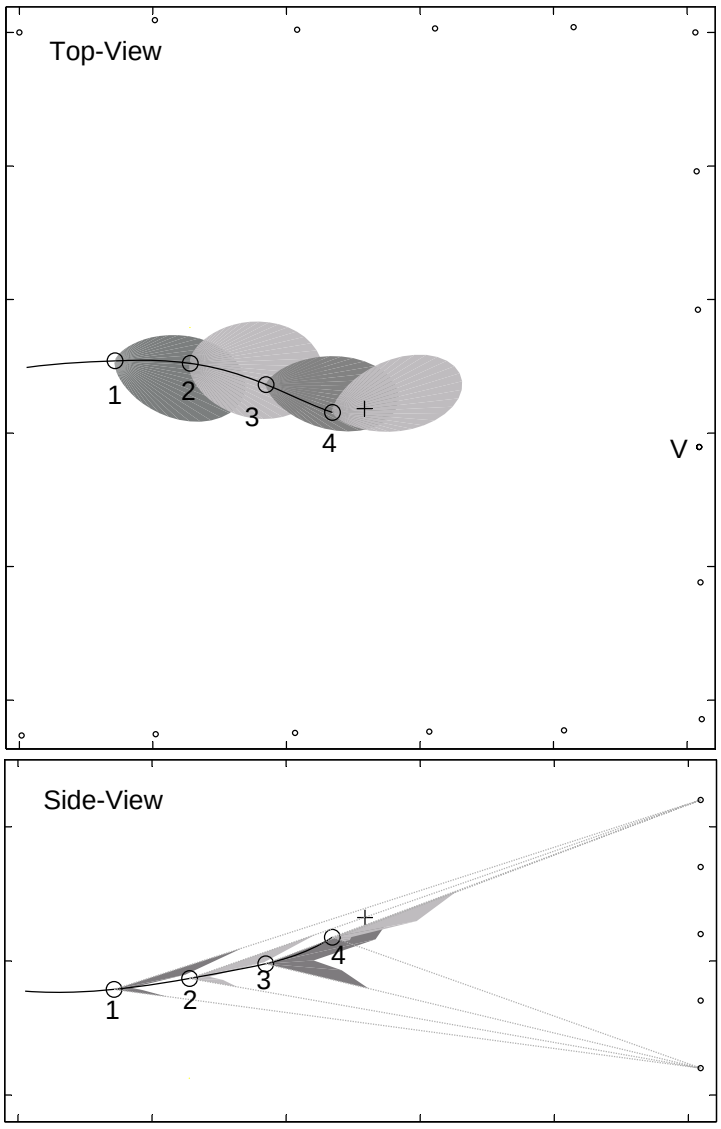

Figure 3.5: A sequence of beam-patterns from bat#2. Beam pattern samples 1 to 3 show the notched beam pattern in the vertical array. The bat is producing signals at a low rate ($< 20\ Hz$) during patterns 1 and 2, and a high rate ($> 100\ Hz$) during patterns 3 and 4. The notch disappears from the recording for sample 4, consistent with the hypothesis the bat is directing its sonar beam up towards the target (black cross).

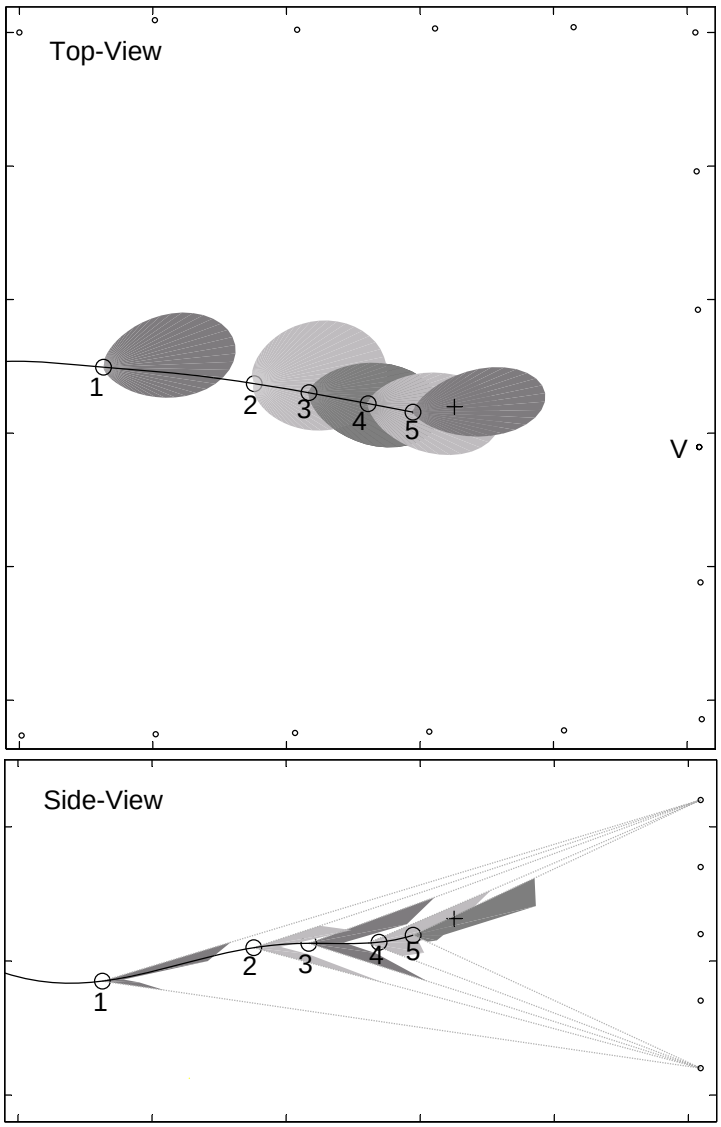

Figure 3.6: A sequence of beam-patterns from bat#1. As in Fig. 3.5, for the last beam pattern shown, when the bat is in the terminal stage of insect capture, no notch is recorded by the vertical array, consistent with the hypothesis the bat is directing its sonar beam up towards the target.

the target (black cross) in the horizontal plane and produces vocalizations at a high rate ($> 100\ Hz$). At the end of both sequences, the vertical array records one lobe. At this point in the pursuit, the target is higher than the bat. The last pattern recorded is consistent with the bat directing its beam upwards, so that only part of one lobe is "visible" to the vertical array (also see Fig. 3.10). This observation suggests that the bat may also track the position of the target in the vertical plane with its sonar beam.

3.3.2 Control measurements

We controlled for the possibility that a systematic error in either the hardware or the calibration procedure lead to one or more of the vertical array microphones giving a consistently low or high reading that gave rise to a notch artifact on the array recordings. We used an emitter with a circular aperture to ensonify the microphone array. The emitter was stimulated by a frequency sweep of the same bandwidth as bat sonar vocalizations. The recorded beam patterns on both the vertical and horizontal array appeared as single lobes. Instances (like Fig. 3.3) where only one lobe is recorded on the vertical array also serve as control measurements to eliminate the possibility of systematic errors with the gain.

If the different envelope detectors had band-pass characteristics that were sufficiently mismatched, then a given vocalization, if sufficiently narrow band, may result in a notch artifact being observed on the microphone channel that is outside the bandwidth of the signal. We controlled for this possibility by testing the frequency response of the envelope detector circuits and ensuring that the peak response did not vary from the designed value by more than $2\ kHz$.

We also inspected the power spectra of full-bandwidth recordings of vocalizations that produced a notch (Fig. 3.7). We verified that notched beam patterns were observed

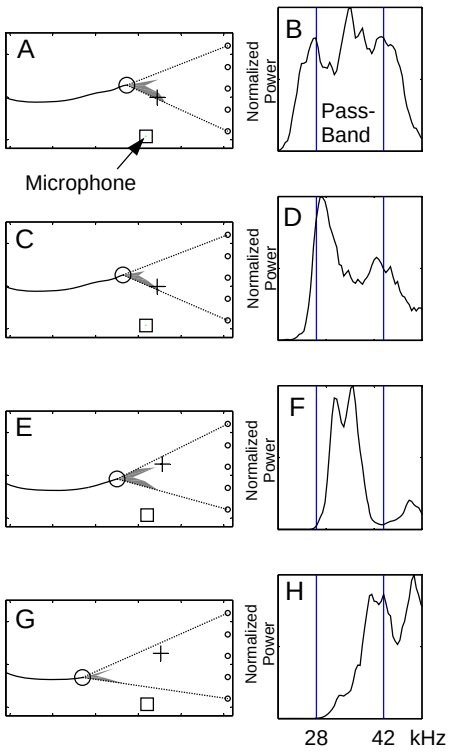

Figure 3.7: Control for bandwidth. **A)C)E)G)** Examples of notched sonar beam patterns. The black line is the bat's trajectory, black circle is the bat's position, black cross is the target position. The black square shows the position of the ultrasonic microphone used to take broad band recordings of the bat calls. **B)D)F)H)** Power spectrum taken from microphone for the notched sonar beam patterns. The band-width of the filter used for the envelope extraction is indicated by vertical lines on the power spectrum plots. Power spectrum of the call spans: **B**) the entire pass-band, **D**) the lower end, **F**) the middle and **H**) the higher end of the envelope-detectors

for vocalization spectra that spanned the entire bandwidth of the filters (Fig. 3.7B). We also verified that notched beam patterns were observed for vocalizations with power in the lower (Fig. 3.7D), middle (Fig. 3.7F) and higher (Fig. 3.7H) ends of the filter bandwidth. Though the microphone used for broad band ultrasonic recordings did not record the exact signal received at the vertical array (The power spectra of the signals recorded at the array are likely to be different due to the frequency dependent directionality of the sonar beam), the examples show that the notch is unlikely to be due to any mismatch of the filters.

Echoes of the original bat vocalization that reached the microphone array to create destructive interference may also create a notched beam for specific positions of the bat. We, however, observed the vertical notch consistently as the bat traveled in different parts of the room, so we believe it to be unlikely that such a consistent observation from different emitter locations would result from multi-path interference.

3.3.3 The sonar beam may consist of two lobes arranged dorso-ventrally

We constructed a three-dimensional model of the bat's sonar beam in an effort to fit the experimental observations via numerical simulations. We found that a model of the sonar beam consisting of two equally-sized lobes oriented dorso-ventrally (Fig. 3.8) could replicate the experimental findings. We modeled each lobe as the emission pattern of a single piston source (Hartley and Suthers, 1989; Kinsler and Frey, 1962) extended to three-dimensions. Let P be the ratio of the sound pressure in the direction θ (azimuth), ϕ (elevation) to the on axis sound pressure. J_1 is the Bessel function of order one. Let k be the wavelength constant, given by $2\pi\ f/c$ where f is the frequency of the sound source, and $c = 340m/s$, the speed of sound. Let a_h and a_v be the horizontal and vertical diameters of the emitter. A single lobe is modeled as

$$P = \left(2\frac{J_1\{ka_h \sin(\theta)\}}{ka_h \sin(\theta)}\right)\left(2\frac{J_1\{ka_v \sin(\phi\}}{ka_v \sin(\phi)}\right) \tag{3.1}$$

Our model consists of two lobes oriented at an angle ζ apart in the vertical plane. They are represented by the equations

$$P_{dorsal} = \left(2\frac{J_1\{ka_h \sin(\theta)\}}{ka_h \sin(\theta)}\right)\left(2\frac{J_1\{ka_v \sin(\phi + \zeta/2\}}{ka_v \sin(\phi + \zeta/2)}\right) \tag{3.2}$$

and

$$P_{ventral} = \left(2\frac{J_1\{ka_h \sin(\theta)\}}{ka_h \sin(\theta)}\right)\left(2\frac{J_1\{ka_v \sin(\phi - \zeta/2\}}{ka_v \sin(\phi - \zeta/2)}\right) \tag{3.3}$$

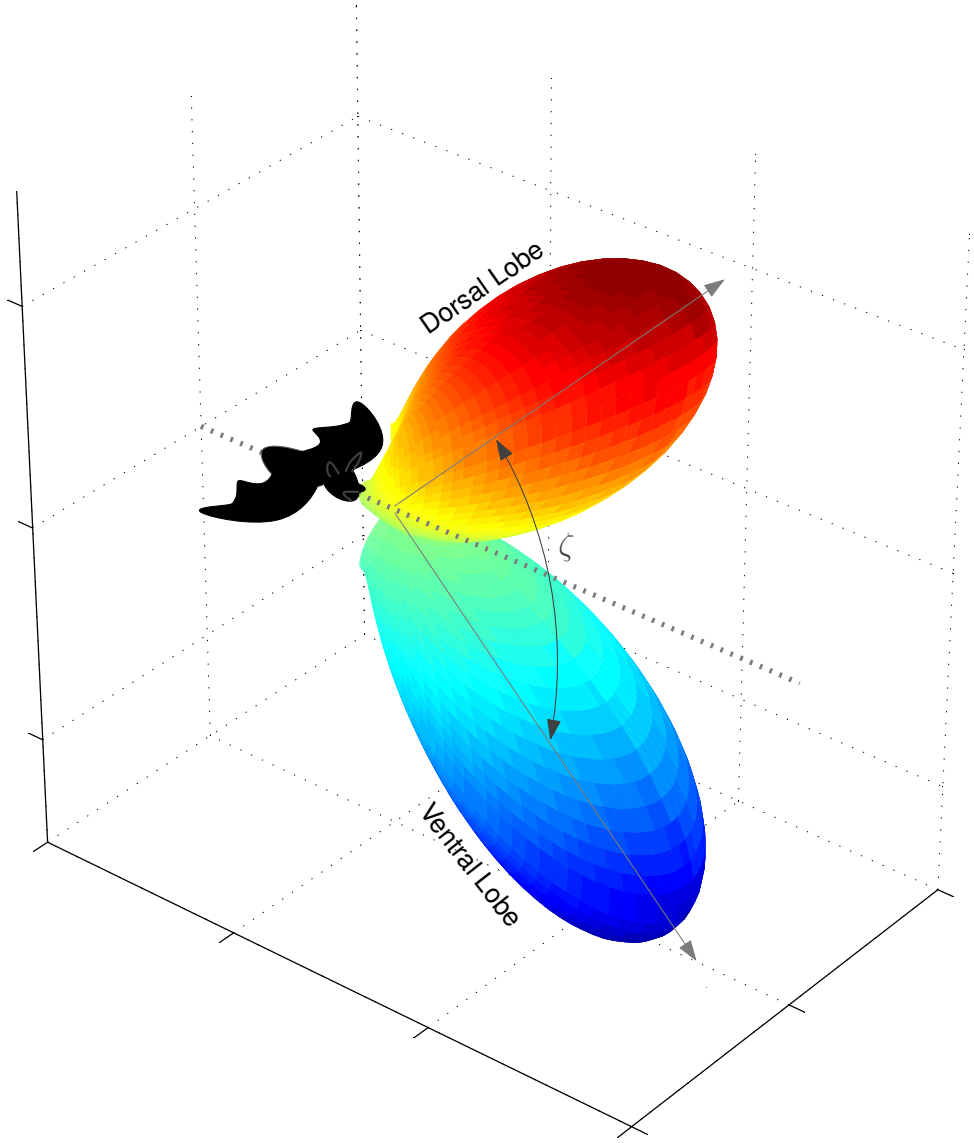

Figure 3.8: Phenomenological three-dimensional model of the bat sonar beam. In this model the sonar beam consists of two equal sized lobes, directed ζ degrees apart in the dorso-ventral plane. Each isolated, individual lobe is modeled as the beam from a piston source. The drawing of the bat is merely schematic. No inference is made about the relation between the vertical orientation of the bat's head and the vertical orientation of the hypothesized beam.

The equations for sound pressure for two lobes are combined to obtain the sound intensity of the complete model as

$$H = P^2_{dorsal} + P^2_{ventral} \tag{3.4}$$

For the simulations we used $f = 35\ kHz$, $a_h = 4mm$ and $a_v = 6mm$ and $\zeta = 90$ degrees. Hartley and Suthers used $a = 4.7mm$ from some measurements of the open mouth of *E. fuscus* in their experiment. We arbitrarily chose two values for a_h and a_v that reflect both the asymmetry of the open mouth (which opens wider vertically than horizontally) and the asymmetry of the beam (which is wider horizontally than vertically (Hartley and Suthers, 1989)).

This is a phenomenological model of the beam and we do not propose any specific structure in the bat that creates this pattern. In the vertical plane it approximates the emission pattern obtained by placing two isotropic sources close together (Strother and Mogus, 1970), but in the horizontal plane it resembles the emission pattern of a piston source (Hartley and Suthers, 1989; Kinsler and Frey, 1962). We define the horizontal position of the beam (0 degrees) to be such that the two lobes are symmetrically above and below the horizontal plane (as shown in Fig. 3.8).

Figs. 3.9 and 3.10 show how this three-dimensional model of the sonar beam is able to replicate the sonar beam cross-sections recorded by both the horizontal and vertical segments of the array. Fig. 3.9 shows simulations of the sonar beam cross-sections that would be recorded by the horizontal and vertical segments of the microphone array. In (A) the model beam is oriented at 0 degrees to the horizontal, such that the two lobes are symmetrically above and below the horizontal plane. The simulated measurement from the vertical array shows a prominent notched shape. In (B) the model beam is directed upwards by 30 degrees. The simulated measurement from the vertical array only captures part of the lower lobe.

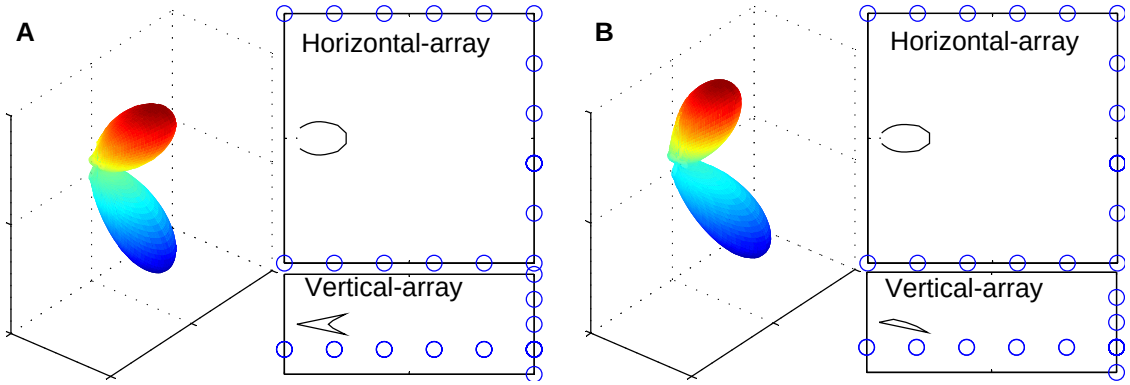

Figure 3.9: Simulated array measurements of the three-dimensional model. **A**) The model beam is oriented at 0 degrees, such that the two lobes are symmetrically above and below the horizontal plane (three dimensional plot). The simulated measurement from the horizontal array (top-panel) shows a single lobe. The simulated measurement from the vertical array (bottom-panel) shows a notched pattern. **B**) The model beam is oriented up by 30 degrees. The simulated measurement from the vertical array only captures part of the lower lobe.

Fig. 3.10 shows the results of sweeping the model beam from -60 degrees to +60 degrees in the vertical plane. When the beam is oriented within ± 5 degrees of the horizontal the vertical cross-section presents a notched appearance. Larger angles result in only part of one lobe being captured, giving rise to a single lobed appearance. The simulated vertical cross-sections shown in this figure are comparable to the measured vertical cross-sections from flying bats shown in previous figures.

3.4 Discussion

The sonar beam pattern of an echolocating bat restricts the spatial region sampled by its echolocation system. Study of the shape and direction of the beam during flight may yield insight into how the bat gathers information to guide behavior. In this study we attempt to infer the three dimensional shape of a flying bat's sonar beam by recording both vertical and horizontal cross-sections of the sonar beam as the bat flew in a laboratory flight-room using echolocation to pursue tethered insects.

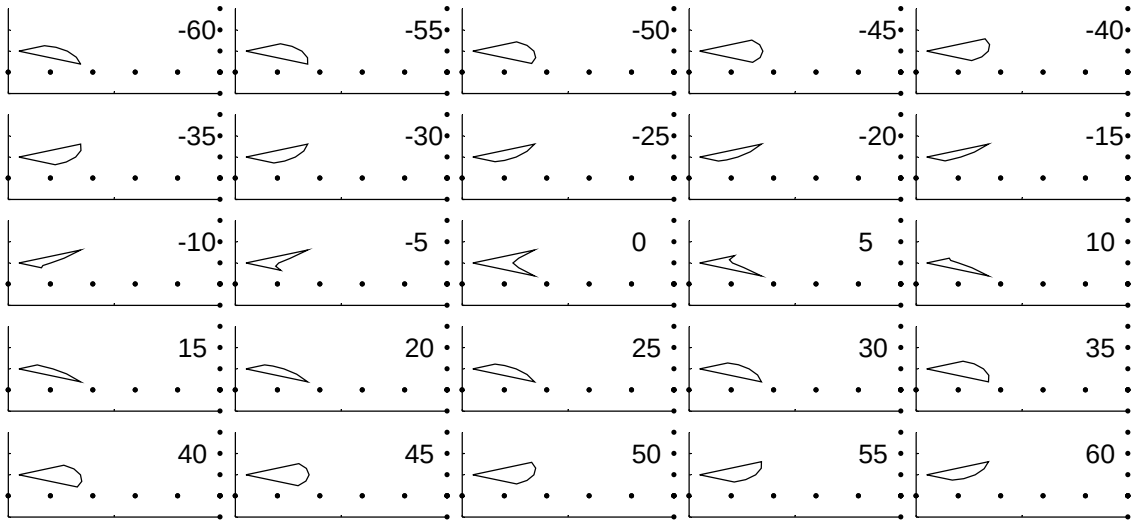

Figure 3.10: Effect of sweeping the model beam in the vertical plane. The model sonar beam is swept from -60 degrees to +60 degrees in 5 degree increments and the cross-section pattern that would be obtained by the vertical-array is simulated. When the sonar beam orientation is within ± 5 degrees of the horizontal the vertical cross-section presents a notched appearance. Larger angles result in only part of one lobe being captured.

We observed a prominent notch in the vertical cross-section of the beam except when the bat was tracking an insect that was positioned either above or below it. Our observations are consistent with the hypothesis that the bat emits a two lobed sonar beam. The two lobes are arranged dorso-ventrally and the sizes of the two lobes are comparable. In our simulation we chose a model with two equal sized lobes directed 90 degrees apart. This model is a representative from a class of two lobed models that fit the observations. It is possible to obtain similar results with lobes 60 degrees apart and with lobes that differ in intensity by a factor of two. Lobes that are closer together and/or have larger intensity differences fail to produce the prominent notch observed in our experiments. Lobes that are much further apart than 90 degrees would produce a shallower "valley" than what we observe in our experiments. The exact beam shape may vary across vocalizations and may depend on the physical characteristics of each individual bat.

A previous study on the beam patterns emitted by electrically stimulated anesthetized *E. fuscus* (Hartley and Suthers, 1989) reported that the sonar beam of these bats consisted of a main lobe and, at frequencies above $60\ kHz$, a ventral lobe $6\ dB$ less intense than the main lobe. The ventral lobe was directed 30 degrees below the main lobe. The authors concluded that, at higher frequencies, the width of the main lobe could be explained by a piston model. This model, however, broke down at frequencies below $25\ kHz$. The bat's beam remained directional at these frequencies, while the model predicted an almost omni-directional beam. The authors also report that the ventral lobe is not explained by any simple model.

In our study, conducted on flying bats, we also observe a splitting of the sonar beam into a ventral and dorsal lobe. However, we observe that this split occurs in the $35\ kHz$ frequency range, and infer that the lobes are of comparable size and separated in direction by a larger angle (ranging from 60 to 90 degrees). We can not infer the shape of the sonar beam at other frequencies because of technical limitations. A more detailed analysis of the sonar beam pattern cross-sections, combined with a denser and wider experimental sampling of the sonar beam is required to determine the exact shape and variability of the sonar beams in flight. A denser and wider sampling of the sonar beam can be implemented in two ways. One is brute force, which is to add more microphones to the array. There are limitations of placement due to the (in retrospect) low height of the flight room. Placing microphones on the ceiling and floor of the room pose challenges related to their small separation of 2.5m. The other method is to generate estimates of the head-direction of the bat in three dimensions and to normalize the recordings of the sonar beam with direction, enabling a three-dimensional picture of the sonar beam to be constructed over a large number of vocalizations. This requires the addition of a head-tracking device, and assumes that the sonar beam pattern is

identical from vocalization to vocalization and over different behavioral states.

Our recordings indicate that in level flight, when the bat is not performing rapid three dimensional maneuvers to chase prey (such as in the initial beam-pattern samples shown in Figs. 3.2, 3.4 to 3.6) the sonar beam is oriented such that the ventral lobe is directed towards the ground in front of the bat. We speculate that one use of the ventral lobe in this configuration may be as a sonar altimeter. Echolocating bats, by using the ground return from the ventral lobe could obtain a measure of the altitude of the ground or vegetation in front of them, allowing them to change flight altitude in response to undulations of the terrain.

Although the echolocation apparatus of the bat could be analyzed separately as emitter and receiver, it makes the most sense to consider them together as a system. The emitter is not just the mouth, but includes the vocal cavity the mouth and possibly parts of the face, head and potentially - at lower frequencies - the whole body. The receiver is not just the mouth, but includes the pinnae, the head, possibly the whole body (Aytekin et al., 2004), the peripheral auditory system and the central nervous system. Just as studies of the evolution, structure and function of the eye make sense only in the full context of the behavior of eyes and what role they play in vision (Land and Fernald, 1992) it is important to study the shape of the sonar beam in flying bats in the context of evolutionary pressures that shape not only the receiver (the bat's hearing and central nervous system) but the emitter (the bat's mouth, face and possibly the rest of its body) as well. This in turn affects and is affected by the bats choice of head and pinna movements as well as general flight behavior. The shape of the sonar beam appears complex enough that it is not the product of a simple model, such as the piston model (Hartley and Suthers, 1989) and gives rise to the interesting hypothesis that details of the bat's emitter have evolved to shape the beam for specific purposes

related to localization and flight guidance.

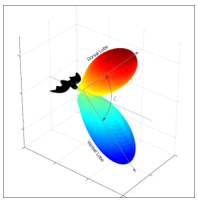

Paper title	Steering by hearing: A bats acoustic gaze is linked to its flight motor output by a delayed, adaptive linear law
Authors	Kaushik Ghose and Cynthia F. Moss
Journal	*J. Neurosci.* (2006) 26(6): 1704-1710

I may have been to blame, I admit it; but nothing excuses violence of language and coarseness of expression, especially in a man who has been carefully brought up, as I know Harris has been. I was thinking of other things, and forgot, as any one might easily understand, that I was steering, and the consequence was that we had got mixed up a good deal with the tow-path. It was difficult to say, for the moment, which was us and which was the Middlesex bank of the river; but we found out after a while, and separated ourselves.

Jerome Klapka Jerome

Ch 6, Three Men in a Boat

4

Steering by hearing

4.1 Introduction

Humans and other animals use information from their environment to guide adaptive motor behaviors such as locomotion. Gaze - the region of the environment a subject explores with the senses - serves to direct locomotion, and much research has addressed how animals use vision during locomotion. Gaze direction restricts the spatial extent of visual information, and the pattern of gaze shifts in humans is related

to task demands (Yarbus, 1961). There have been many studies of how gaze direction in visual animals is related to locomotor planning. Such studies have focused on target-directed motion in which subjects have been required to use specific landmarks in the visual field to guide movement. These landmarks could be presented as a direct goal of locomotion (Land and Collett, 1974; Hollands, Vickers, and Patla, 2002), as a track on which to navigate (Grasso et al., 1996; Land and Lee, 1994; Land and Tatler, 2001) or as obstacles to navigate around (Grasso, Prevost, and Berthoz, 1998; Imai et al., 2001). Such studies have suggested that subjects make anticipatory gaze movements with their head and eyes during locomotion. The relation between gaze and locomotion has contributed to hypotheses of how visual information is used by the nervous system to guide movement (Grasso, Prevost, and Berthoz, 1998; Land, 1999; Wann and Swapp, 2000). Studies on chasing in the housefly (Land and Collett, 1974) and prey pursuit in tiger beetles (Gilbert, 1997) have expressed this coupling in terms of a locomotor gain between visual direction to a target and locomotor output[1].

Current studies on gaze and locomotion have not addressed two issues. One gap in our knowledge is whether gaze and locomotion are similarly related both in the presence and in the absence of an explicit target. For example, when searching for a target the animal may uncouple its gaze from its locomotor plan in order to *scan* the environment without changing its direction of motion. Past studies have, however, focused on how animals move once they have acquired a locomotor target and are moving in response to it. It is not known, therefore, whether the animal adjusts the sensory-locomotor gain in response to behavioral demands. Another gap in our

[1]A study of male whirligig beetles chasing females also reports that the turning rate is proportional to the angular direction to the target (Bendele, 1986). Whirligig beetles also use mechanical waves for active sensing (see Appendix C)

knowledge is how gaze in other sensory modalities, such as audition, is related to locomotion. Echolocating bats emit brief intermittent ultrasonic pulses. Each pulse forms a beam of sound that echoes off objects in its path. Bats compute the direction and distance to obstacles and prey from a spectro-temporal analysis of the returning echoes (reviewed in Moss and Schnitzler, 1995). In contrast to vision, the information from echolocation arrives intermittently in time, yielding snapshots of information. Visual directional information is available explicitly, through the location of an object's image on the retina. Auditory directional information, however, requires a complex mapping of binaural spectro-temporal information into spatial location. The ability to localize objects and navigate via echolocation is very well developed in bats, and the distinctive aspects of echolocation as a sensory system suggest that the study of auditory guided locomotion in bats offers a valuable complement to similar studies in visually guided animals. By comparing and contrasting actions guided by vision and audition we can test hypotheses of sensorimotor integration for their generality and explore modality-specific specializations which animals may have evolved.

The sonar beam direction of each vocalization restricts the region of space from which the bat receives information. In analogy to visual gaze in humans, the sonar beam direction can be considered a component of acoustic gaze for echolocating bats. Additionally, in *E. fuscus*, the sonar beam axis is aligned with the head direction. In this paper we studied the relation between acoustic gaze and flight locomotor output in an echolocating bat during different stages of insect pursuit.

4.2 Methods

Animal model

Insectivorous echolocating bats, such as the big brown bat, *Eptesicus fuscus*, perform complex and rapid flight trajectories to catch airborne insects in darkness. They produce intermittent, pulses of directed ultrasound and use the information contained in the returning echoes to detect, localize and track flying insect prey, relying on hearing instead of vision to guide complex spatial behaviors (Griffin, 1958; Griffin, Webster, and Michael, 1960). The sonar pulses produced by *E. fuscus* are frequency modulated, and consist of multiple harmonics with the fundamental sweeping from about 60 kHz to 25 kHz during the approach stage of insect pursuit (Surlykke and Moss, 2000). Bats change the duration, bandwidth and production rate of their sonar signals with behavioral state (Griffin, 1958). When cruising in open space the pulse production rate (PPR) of *E. fuscus* may be as low as 4Hz and the call duration may be as long as 20 ms (Surlykke and Moss, 2000). As the bat detects and then approaches prey, the PPR rises, terminating in insect pursuit and capture ('terminal buzz') when the PPR may be as high as 150-200 Hz and signals as short as 0.5 ms (Griffin, 1958). Fig. 4.1 shows an example of a bat sonar pulse sequence recorded in a laboratory flight room. The bat is first flying around the room. It then detects and captures a tethered insect.

The sonar beam produced by *E. fuscus* is directional and aligned with its head (Hartley and Suthers, 1989). The directionality of the sonar beam restricts the spatial extent from which the bat's sonar system can gather information. The sonar beam direction of a bat, in analogy to gaze in visual animals, can be considered a component of acoustic gaze (Ghose and Moss, 2003), as it defines the region of space from which the animal's sensory system can acquire information. The sonar beam pattern of the

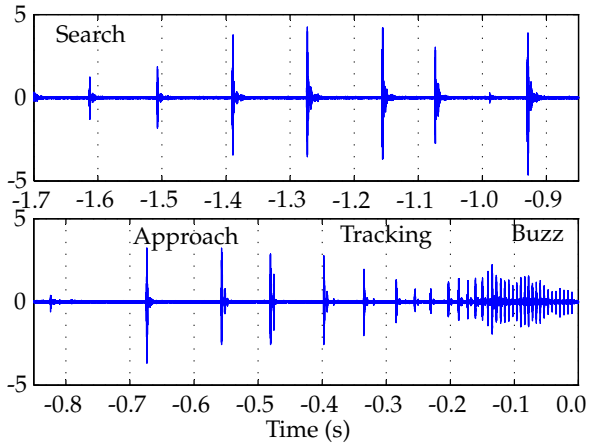

Figure 4.1: Train of pulses produced by *E. fuscus* catching an insect in a laboratory. Insect capture occurs at time 0 s. Initially the bat produces pulses at a rate of around 10 to 20 Hz. In the field such calls can be as long as 20ms, though in the laboratory shorter calls are observed. This is commonly called the search stage. As the bat detects and then starts to pursue an insect the pulses are produced more frequently. During the terminal buzz, bats produce calls at rates as high as 200 Hz with durations as short as 0.5 ms. Several sounds are followed by echoes which are seen in the trace as a second signal of low amplitude after the initial pulse recording.

echolocating bat enables us to measure the gaze direction of an animal that relies on audition as its primary distal sense. The temporal patterning of the sounds produced by the bat also enables us to objectively demarcate different behavioral states during echolocating flight. Echolocating bats, therefore, provide an excellent animal model to study the link between gaze and locomotion, in different behavioral states, in an animal that is not guided by vision.

Behavioral methods

We trained five bats of the species *E. fuscus* to fly individually in a large (7.3m x 6.4m x 2.5m) laboratory room (Fig. 4.2). The room walls and ceiling were lined with sound absorbent acoustic foam (Sonex One, Acoustical Solutions, Inc., Richmond, VA) to reduce reverberations. The room was illuminated by dim, long wavelength light ($>$ 650 nm, light from normal incandescent bulbs passed through a filter plate - Plexiglas

G #2711, Atofina Chemicals, Philadelphia, PA) to which the bat is insensitive (Hope and Bhatnagar, 1979). Images from two high speed video cameras (Kodak Motion-Corder, CCD based cameras operating at 240 frames-per-second, synchronized to 1/2 frame accuracy) were used to reconstruct the three-dimensional flight path of the bat and the trajectory of the prey. Simultaneously, a U-shaped array of 16 microphones (Ghose and Moss, 2003) recorded horizontal cross-sections of the sonar beam pattern emitted by the bat.

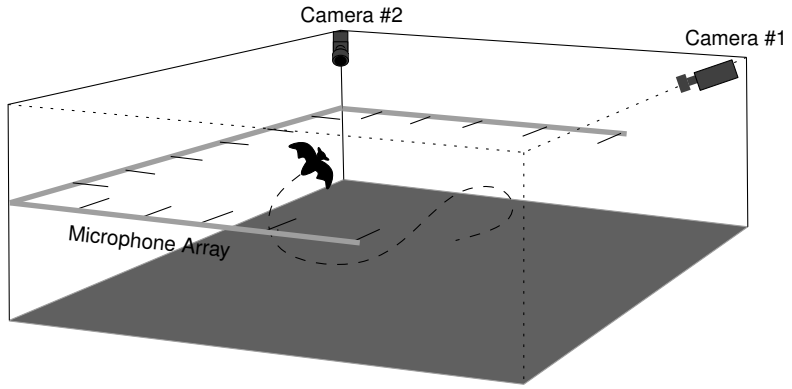

Figure 4.2: Laboratory flight room. The bats were trained to fly in a flight room 7.3m x 6.4m x 2.5m high. The room walls and ceiling were covered with sound absorbent foam to reduce reverberations. Illumination was dim red lighting (wavelength $>$ 650 nm) to exclude the bat's use of vision. Two digital video cameras operating at 240 frames/s recorded the three-dimensional position of the bats and tethered insects during the experiments. An array of 16 microphones was used to record the sonar beam pattern of the bats as they flew in the room.

The bats were trained to catch insects (mealworms) suspended from a tether. The insects were tethered at the end of a 1 m long monofilament line. Each insect was initially concealed in a trap-door mechanism that was placed at random points on the ceiling. After release from the trap-door the insect was held stationary at the end of the tether. The duration of the drop and the jerking motion of the insect at the end of the drop were short compared to the time it took the bat to reorient its flight and capture the insect after detection. This paradigm allows us to study the bat's flight behavior as it attacks a target without having to compensate for target movements (Wilson and

Moss, 2004). Each experimental trial consisted of two parts. During the first part of the experiment, the insect was concealed in the trap-door and bat was allowed to fly in the room. This allowed us to investigate the relation between the bat's acoustic gaze and its flight motor planning when no target was present. After a period of one to 30 seconds the prey was released from the trap-door. This led to the approach and attack stages, in which the bat localized, tracked and intercepted the tethered insect. This allowed us to investigate the relation between gaze and locomotion as the bat progressed through the behavioral states associated with different stages of foraging flight.

Computation of acoustic gaze direction

The sonar beam is horizontally symmetrical about the midline of the bat's head (Hartley and Suthers, 1989). Every time the bat produces a vocalization, the direction of its sonar beam axis can be computed from the reconstructed sonar beam pattern obtained from the microphone array (Ghose and Moss, 2003). The sound intensity incident at each microphone j is corrected for spherical loss and atmospheric absorption to yield the normalized, corrected intensity I_{C_j}. From Fig. 4.3 we see that the axis of the sonar beam may be computed as the *direction* of $\overrightarrow{H}$, where $\overrightarrow{H} = \sum_j \overrightarrow{I_{C_j}}$. Here $\overrightarrow{I_{C_j}}$ is a vector directed from the bat to microphone j with magnitude proportional to the corrected intensity I_{C_j}. The horizontal aspect of the sonar beam axis is also aligned with the head direction of the bat. The spatial extent of the sonar beam limits the region of space the bat can sample with one vocalization and the bat centers its sonar beam axis on a target of interest (Ghose and Moss, 2003). We define the bat's acoustic gaze as the region of space sampled by its beam pattern, and use the sonar beam axis to infer the acoustic gaze direction.

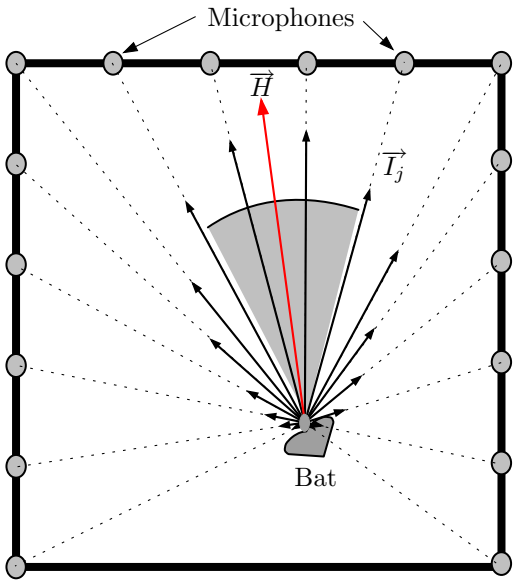

Figure 4.3: Computation of head direction. $\overrightarrow{I}_j$ is a vector directed from the bat to microphone j with magnitude proportional to the corrected intensity I_c for that microphone. $\overrightarrow{H}$ is the resultant of the summation of vectors from all the microphones. The direction of $\overrightarrow{H}$ is the direction of the head.

Computing linkage between gaze and locomotion

From Fig. 4.4, the bat's velocity direction, θ_{flight}, was computed as the direction of the tangent to its flight path. As a measure of the bat's flight motor output we computed the time derivative of this quantity, $\dot{\theta}_{flight}$, that measures the rate of turn of the bat in flight. This was computed by numerically differentiating the changes in the angle of the tangent to the bat's flight path for each video frame. The flight data were smoothed using cubic spline interpolation to remove artifacts introduced when the bat's position was manually digitized from the stereo video data. The computation of $\dot{\theta}_{flight}$ depends only on the kinematics of the flight path and is not affected by vocalization timing. Due to the geometry of the microphone array, only the horizontal component of the gaze direction of the bat could be computed. The axis of the sonar beam in *E. fuscus* corresponds to the direction of the head. We computed gaze angle as the horizontal

angle, θ_{gaze}, between the axis of the sonar beam ($\overrightarrow{H}$) and the bat's flight direction each time the bat produced a sonar call. We studied the relation between gaze angle at any instant t when the bat vocalized, $\theta_{gaze}(t)$, and the rate of turn of the bat at various times τ relative to that instant, $\dot{\theta}_{flight}(t+\tau)$. We considered a range of values of τ, both positive (flight motor output lagging acoustic gaze) and negative (flight motor output leading acoustic gaze).

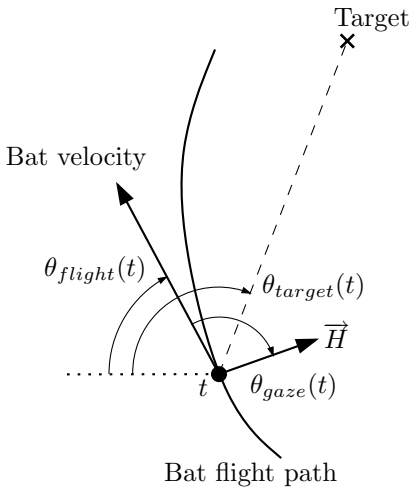

Figure 4.4: Variables considered. The tangent to the bat's flight path gives the velocity direction, θ_{flight}, measured with respect to a fixed world reference (dotted line). The rate of turn of the bat, $\dot{\theta}_{flight}$, is computed as the time-derivative of this quantity at each point on the flight path. The target direction (dashed line from bat to target), θ_{target}, is measured with respect to the common fixed world reference (dotted line). $\overrightarrow{H}$ is the axis of the sonar beam (aligned with head direction). This is computed each time, t, the bat emits a vocalization. The angle between $\overrightarrow{H}$ and the tangent at time t gives the acoustic gaze angle θ_{gaze}, for each bat vocalization. In the analysis $\theta_{gaze}(t)$ is correlated to $\dot{\theta}_{flight}(t+\tau)$ for a range of τ. The value of $\dot{\theta}_{flight}$ depends on the kinematics of the flight path and the value of θ_{gaze} depends on the bat's gaze direction. Both these quantities are not *a priori* dependent on vocalization timing.

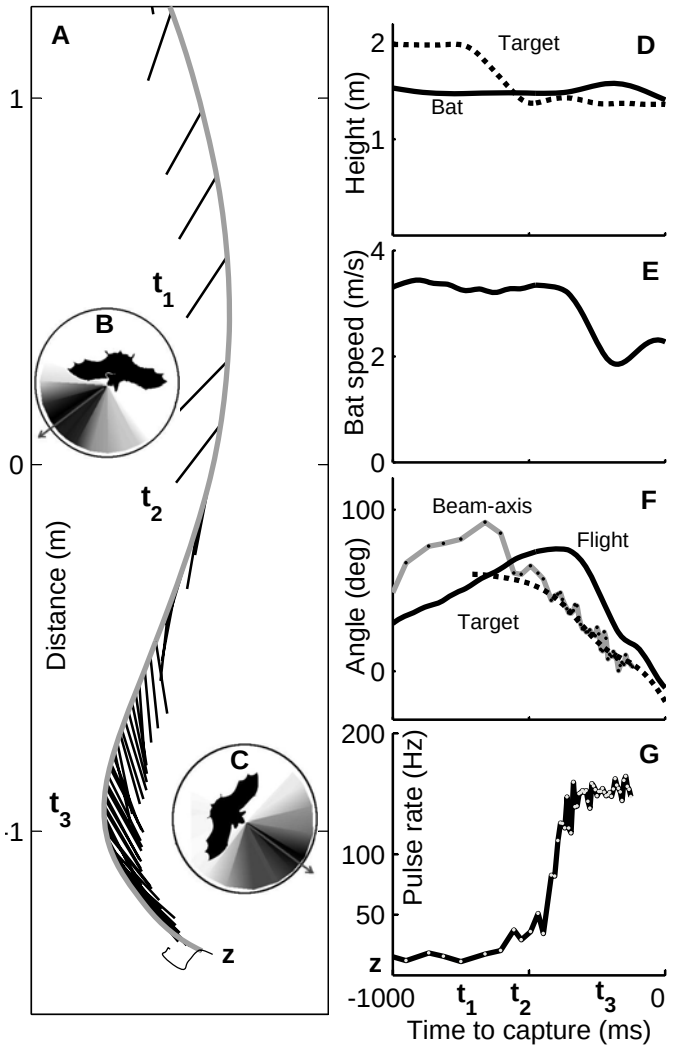

Figure 4.5: Flight path and sonar beam axis of an echolocating bat. **A**) Top view of a bat capturing an insect. The bat (gray line) flies from the top of the panel to the bottom. Straight black lines indicate the sonar beam axis direction of the bat each time it makes a sonar call. When the bat is near **t2** the target is dropped from a trap-door (point **z**). Tick marks are in meters. **B**) and **C**) Schematic insets showing relative orientations of bat's sonar beam axis, flight (body) direction and emitted sonar beam pattern (coded in gray-scale) at points **t1** and **t3**. **D**) The heights of the bat (solid line) and target (dotted line) over time. The target is initially concealed in a trap-door mechanism. **E**) Linear speed of the bat over time. The bat brakes and rises slightly as it turns to intercept the insect. **F**) Bat's sonar beam axis direction, flight direction and bat-to-target direction over time for the trajectory shown. All angles are with respect to an external fixed reference. The bat locks the sonar beam on the target after time **t2**. **G**) Pulse production rate over time. The pulse rate increases as the bat locks the sonar beam onto the target. During the last 50 ms before capture vocalizations were either absent or too faint to analyze reliably and are not shown. For animations of this and other insect interceptions see movies online.

4.3 Results

Flight behavior

An example of an insect capture trial is shown in Fig. 4.5 (Corresponding to movie S1 in the online material). Figure 4.5**A**) is a top-view of the reconstructed flight path of the bat as it intercepts a tethered insect released from a trap-door. The straight black lines denote the direction of the sonar beam axis during each call, the gray line is the flight trajectory of the bat and the thin curved black line is the trajectory of the target. In the example shown, the bat is initially flying in an empty room. Its sonar beam is directed to the reader's left side, and it is also steering to the left (e.g. t_1, also see Fig. 4.5 (B)), producing sounds at a relatively low rate (10 Hz, see Fig. 4.5 (G)). The prey is released from the trap-door at point **z** and suspended from the tether when the bat is at point t_2 (target height drops in Fig. 4.5 (D)). After the prey is presented, the bat turns its sonar beam to lock onto the prey (150 ms after t_2). The bat begins to increase the repetition rate of its sonar calls. During the attack stage the bat redirects its flight to intercept its prey and the PRR rises to high values ($>$100 Hz). During the last 50 ms before capture vocalizations were either absent or too faint to analyze reliably and are not shown. In an earlier study of the sonar beam pattern in flying echolocating bats we reported that the bat centers its sonar beam axis tightly onto selected prey during the attack stage. The accuracy of this lock-on is approximately $\pm 3^o$ (Ghose and Moss, 2003).

Division of stages of bat flight based on PPR

We demarcated the different behavioral states of the bat from its sonar PPR. Griffin first reported the dramatic increase in PPR by echolocating bats during the final attack

of insect prey and termed it the 'buzz' (Griffin, 1958; Griffin, Webster, and Michael, 1960). Subsequent studies in echolocating bats have used changes in PPR to infer changes in the bat's behavioral state (Schnitzler, Kalko, and Surlykke, 1987; Kalko, 1995; Kick and Simmons, 1984). Foraging flight has been divided into four stages, according to the bat's vocal behavior: searching, approaching, tracking and attacking (Kick and Simmons, 1984). The tracking and attack phases correspond to the terminal I and terminal II stages described by some authors (for example see Kalko, 1995). During searching the bat is producing pulses at a very low rate (5-10 Hz). After the bat detects the insect the bat moves into the approach stage and the pulse rate rises (20-50 Hz). It then transitions to the tracking stage (50 Hz, Kick and Simmons, 1984) and finally to the attacking stage (up to 200 Hz). These PPR values are estimates from field studies and vary with species of bat (reviewed in Denzinger, Kalko, and Jones, 2004, also see Obrist, 1995; Fenton et al., 1995).

Here we demarcate the different stages of insect capture behavior of *E. fuscus* under laboratory conditions using the PPR values we obtained in our experiment. Figure 4.6 is a histogram of the pulse production rates of the bats' vocalizations taken during the experiment. In conjunction with observations of the bat's insect pursuit behavior (see Fig. 4.5 (A) and 4.5 (E)) we used the valley points of the distribution as the dividers for the different stages of foraging flight. PPR values less than 50 Hz were assigned to the search/approach stage, PPR values ranging from 50 Hz up to 100 Hz were assigned to the tracking stage and PPR values greater than 100 Hz were assigned to the attacking stage. This demarcation is based on the PPR values of the emitted vocalizations, and is independent of measurements of the sonar beam direction and flight path.

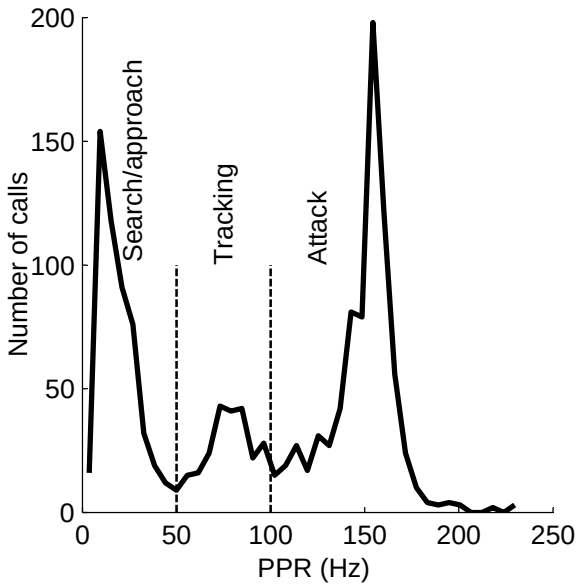

Figure 4.6: Histogram of pulse production rates (PPR) of the sonar vocalizations produced by the bats. The PPR distribution is trimodal. The peak centered around 160 Hz corresponds to the buzz (Griffin, 1958), when the bat is attacking prey. There is a smaller peak around 75 Hz corresponding to the tracking stage (Kick and Simmons, 1984), followed by a large number of calls with pulse rates less than 50 Hz corresponding to periods when the bat is flying in an empty room or has just detected its prey and is begining to increase its PPR (search/approach). We chose the valley points of the distribution as the dividers for the different stages of foraging behavior. Data from 5 bats, 1525 calls, over 38 trials.

Relation between acoustic gaze and flight behavior

The bat can direct its acoustic gaze (sonar beam axis) substantially off its flight path (Ghose and Moss, 2003). However, we noted that during all stages of flight there was a strong linear relation between the acoustic gaze angle at time t and the rate of change of flight direction at a time $t + \tau$, with the gaze leading the flight direction. The gain of linear relation k depended on the bat's behavioral state.

We collected data from five bats and a total of 38 bat flights. We computed the correlation between acoustic gaze angle ($\theta_{gaze}(t)$, which is the angle between the axis of the sonar beam and the bat's flight direction) and flight turn rate ($\dot{\theta}_{flight}(t + \tau)$) for τ values ranging from -200 ms to $+200$ ms, during the different stages of flight

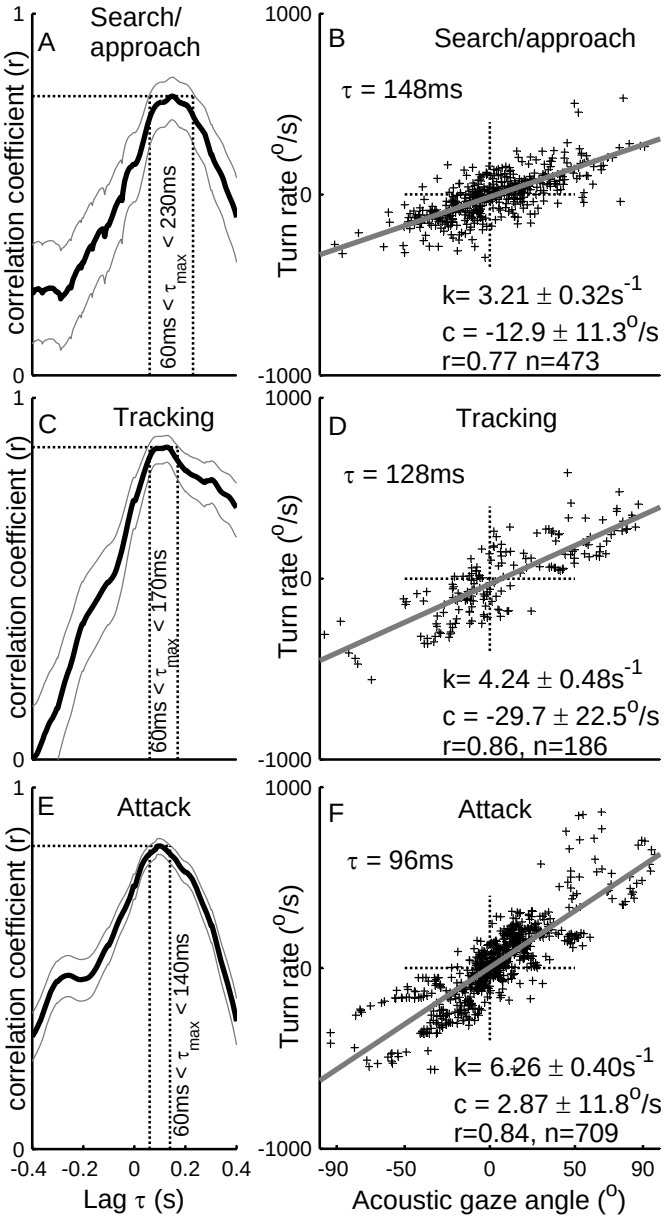

Figure 4.7: Acoustic gaze is adaptively coupled to flight motor-output. **A**), **C**), **E**) The black line shows the correlation coefficient (r) between the acoustic gaze angle (θ_{gaze}) of the bat and the flight turn rate ($\dot{\theta}_{flight}$), for different lag values (τ) for the three behavioral states. The grey lines adjacent to r show the 95% confidence intervals (CI) for r. The vertical dotted lines show the corresponding CI for τ_{max}. There is no signficant difference between the τ_{max} values for the three states, but they are significantly greater than zero, indicating that the acoustic gaze leads locomotor planning. **B**), **D**), **F**) Scatter-plot of θ_{gaze} and $\dot{\theta}_{flight}$ at τ_{max}. Regression line is shown overlaid in gray. The gain (slope, k) increases as the bat progresses from the search/approach to tracking to attack stages of foraging flight. The offset (intercept, c) are negligible. Pairwise comparisons show that the slopes are significantly different from each other with $k_{search/approach} < k_{tracking} < k_{attack}$. This suggests that the bat's behavioral state modulates the gain of the linkage. Data from five bats and a total of 38 flights.

behavior. Figure 4.7 (A) shows how the correlation between acoustic gaze angle (θ_{gaze}) and flight turn-rate ($\dot{\theta}_{flight}$) changes with the lag, τ, during search/approach flight; the correlation peaks at $\tau_{max} = 148$ ms, 60 ms$\leq\tau_{max}\leq$230 ms, 95% confidence interval (CI). Figure 4.7 (B) shows the scatter plot of the sonar beam axis to flight angle versus the flight turn-rate for $\tau_{max} = 96$ ms. The gain, $k_{search/approach}$ (slope of the line), is $3.21 \pm 0.32s^{-1}$, correlation coefficient $r = 0.77 \pm 0.01, n = 473$ vocalizations. Figure 4.7 (C) and 4.7 (D) show data from the tracking stage. In this stage the maximum r occurred at $\tau_{max} = 128$ ms (60 ms$\leq$ τ_{max} $\leq$170 ms) with $k_{track} = 4.24 \pm 0.48s^{-1}$, $r = 0.86 \pm 0.01, n = 186$ vocalizations. Figure 4.7 (E) and 4.7 (F) show data from the attacking stage. In this stage the maximum r occurred at $\tau_{max} = 96$ ms (60 ms$\leq$ τ_{max} $\leq$140 ms) with $k_{attack} = 6.26 \pm 0.40s^{-1}$, $r = 0.84 \pm 0.01, n = 709$ vocalizations.

The value of τ_{max} decreases as the bat progresses from the search/approach stage to the attack stage of flight. The overlap of the τ_{max} confidence intervals between the behavioral states, however, indicates the differences in τ_{max} for the three conditions are not statistically significant. τ_{max} in all stages is significantly greater than zero, indicating that the acoustic gaze always leads the flight motor output. Pairwise comparisons between the gain (k) values for the three stages shows that the gains are significantly different from each other: For search/approach and tracking $t = 4.63$, for tracking and attack $t = 7.2$, for search/approach and attack $t = 12.7$ ($p < 0.001$, Bonferroni correction applied) with $k_{search/approach} < k_{tracking} < k_{attack}$.

These results can be summarized by the following general control law:

$$\dot{\theta}_{flight}(t + \tau) = k\theta_{gaze}(t) \tag{4.1}$$

Here $\theta_{gaze}(t)$ is the acoustic gaze angle, the angle between the sonar beam-axis and flight vector. $\dot{\theta}_{flight}(t + \tau)$ is the rate at which the bat turns in flight, k is a state-

dependent gain factor and τ is the constant time by which the flight lags the gaze direction. The offsets obtained in the data are negligible and are not included in the control law.

The rate of turn for a given gaze angle increases as the pulse interval decreases (larger values of k are obtained during phases when the repetition rate is higher). Since the bat is receiving information from the environment at the rate at which pulses are produced, it might be possible that the bat is keeping the angle it turns per pulse proportional to the gaze angle and independent of the pulse rate. We do not, however, find evidence for this in our data.

Confidence intervals of τ(lag) and r(correlation) values

We utilized the Fisher transform (Howell, 1997, pg 263) to compute 95% confidence intervals on the correlation coefficient r. To compute the confidence interval for τ_{max} we considered the range of τ values for which the experimentally obtained r value was not significantly different from the experimental peak r value (Figs. 4.7 (A) ,4.7 (C) ,4.7 (E) , top gray line).

$$\rho' = .5 \ln \left| \frac{1+r}{1-r} \right| \tag{4.2}$$

$$CI(\rho') = \pm z_{\alpha/2} \frac{1}{\sqrt{N-3}} \tag{4.3}$$

where ρ' is the fisher transformed population correlation coefficient, $z_{\alpha/2}$ is 1.96 for 95% confidence limits. N is the sample size. The confidence intervals on τ_{max} indicate that the τ_{max} for the different behavioral states do not significantly differ. However, they are all significantly greater than zero.

4.4 Discussion

Here we report how the relation between gaze direction and locomotor output changes as an animal progresses from searching behavior to target-directed behavior. We also show a control law linking gaze direction and locomotor output in an acoustically guided animal. We show that during foraging flight the bat's acoustic gaze (direction of the sonar beam axis) leads its flight motor output. This relation may be expressed as a delayed linear law linking acoustic gaze angle with flight turn rate. The gain (slope) of this linkage changes with behavioral state of the bat, as inferred from the repetition rate of its sonar vocalizations.

To the best of our knowledge, this is the first time an adaptive control law linking gaze and locomotion has been described for any species. It requires less energy to maneuver a small part of the body, such as the head, or eye, than to change the orientation or direction of motion of the whole animal. By controlling sensory gaze through a part of the body that is light and independently movable, animals are able to conserve energy when redirecting gaze (see for example Oommen, Smith, and Stahl, 2004). When an animal is not executing target-directed locomotion, therefore, one may expect the gaze direction to be uncoupled from locomotion direction, since the animal may be scanning the environment. Our results show, however, that the linkage between gaze and locomotion in *E. fuscus* exists during all stages of flight, from search to attack. At low pulse rates the bat is either searching for a target, or has just detected a potential target. Dramatic increases in the bat's pulse rate have been interpreted as the animal making a decision to pursue a detected target (Kick and Simmons, 1984). We show that the flight turn rate associated with a given gaze angle increases at higher repetition rate stages.

This is the first study to describe a law linking gaze to locomotion in an auditory

guided animal. An earlier study of spatial memory in bats (*Phyllostomus discolor*) navigating a very small (1m diameter) octagonal arena illuminated with visible light, suggested that the bat's head direction leads its flight direction (Höller and Schmidt, 1996). These experiments were explicitly designed to test spatial memory so the animals were very familiar with the arena. The experimenters concluded that vision and spatial memory were more dominant than echolocation in guiding locomotion under the conditions they set up. Holler and Schmidt's study did not reveal the relation between acoustic gaze direction and flight control in bats pursuing prey or flying in an extended space. In our study, memory effects were minimized, as the bats were required to fly around and intercept a tethered target placed at random locations and dropped at random times in a large (7.3 m x 6.4 m x 2.5 m), empty room. The use of vision in our study was limited by removing light sources visible to the bat. This paradigm allowed us to test flight guidance by echolocation under different behavioral conditions, which is essential to our conclusions.

There are comparable studies, in insects, showing a similar, but constant, delayed linear linkage between vision and target directed locomotion. Studies of chasing behavior in flies (Land and Collett, 1974) and walking tiger beetles (Gilbert, 1997) have quantitatively shown a similar delayed linear relation between *visual target location* and locomotor output. For the fly, the delay between sensory input and motor output is about 30 ms (Land and Collett, 1974), and for tiger beetles, the delay is about 40 ms (Gilbert, 1997). Because of this short latency a hard-wired visual pursuit system has been proposed for flies that links the output of retinal neurons to flight control neurons with only one interneuron stage (Land and Collett, 1974). Neurons sensitive to the position of appropriately sized visual targets are hypothesized to drive flight motor neurons in direct proportion to retinal position, thereby creating a servo-system to control

pursuit. The sensory-locomotor gain for a given fly was considered constant, perhaps a result of the hard-wired nature of the system. The concept of sensory-locomotor gain, as used in these previous studies, though in principle similar to that described in this paper, involves visual target direction, and not gaze direction.

Other studies have linked visual gaze direction with locomotor control, though they have not suggested that the linkage is behaviorally adaptable. Field observations of flying birds have led to the hypothesis that a '*flying bird follows its beak*' (Groebbels, 1929). A study on stationary pigeons demonstrated that there are neck reflexes on wing and tail muscles that cause coordinated movements of wing and tail feathers with deflection of the pigeon's head (Bilo and Bilo, 1983). It is, however, not known whether such coordinated movements also operate in a flying pigeon and result in a behaviorally adaptable linkage of flight path with visual gaze. Studies in humans have suggested a relation between *direction of visual gaze* and future locomotion direction for subjects moving along a fixed path (Land and Lee, 1994; Grasso, Prevost, and Berthoz, 1998; Hollands, Vickers, and Patla, 2002), though there is no evidence for behaviorally adaptable gain in this relation.

The linkage between locomotion and gaze for an echolocating animal, as described in this paper, is similar in principle to that suggested for many visual animals. This finding can be used to consider the generality of theories of sensory-locomotion coordination based on studies of visual animals. For humans the relation between gaze direction and motion has been interpreted in the context of visual cues such as optic-flow (Wann and Swapp, 2000; Warren et al., 2001; Wilkie and Wann, 2003; Fajen and Warren, 2004). One leading hypothesis is that a visually guided animal steers by centering the focus of expansion (FOE) of optic-flow on a locomotor goal (Gibson, 1950; Gibson, 1966). A theoretical paper by Wann (Wann and Swapp, 2000) suggests that

subjects direct gaze toward a locomotor goal in order to minimize errors in computing the FOE.

The echolocating bat receives information from the environment in the form of intermittent snapshots of auditory information. An acoustic analog of optic flow information has been proposed for bats that produce constant frequency (CF) sonar signals in combination with frequency modulated (FM) sweeps (Müller and Schnitzler, 1999). Bats that produce long CF signals are very sensitive to Doppler shifts in the pure tone component of the echo (Schnitzler, 1968; Neuweiler, Bruns, and Schuller, 1980) and may be able to extract flow information from it. FM signals are considered Doppler tolerant (Altes and Titlebaum, 1970), and therefore bats producing only FM signals, like *E. fuscus*, the species used in these experiments, receive echoes poorly suited to carry Doppler information.

We propose that the relation between acoustic gaze and locomotion in the bats studied here is not due to any analog of optic flow for steering control. In *E. fuscus* the sonar beam axis is aligned with the head, which is the auditory reference frame. Researchers who study sensorimotor transformations and those who build mobile robots with movable sensors have grappled with the issue of mapping sensory information into motor commands. Many of these mappings must be learned by the animal or machine (Salinas and Abbott, 1995; Pouget and Snyder, 2000; Cohen and Andersen, 2002). There are often multiple solutions to motor control problems such as locomotion (Bernstein, 1967).

We suggest that the flying echolocating bat constrains and simplifies the conversion of locomotor intention into locomotor action by linking its sensory reference frame to its locomotor output. We speculate that by reducing the gain of the coupling during low signal repetition rate behavioral stages, such as search/approach, the bat is

compromising between a complete uncoupling of gaze direction and locomotor output (conserving energy) and maintaining the computational benefits of coupling gaze and locomotion. As the bat progresses towards capturing an insect, as indicated by an increase in PPR, it increases the gain in the linkage between gaze and locomotion, thereby coupling its flight behavior more rigidly to the target position. The bat, therefore, adapts to different behavioral requirements by adjusting one parameter: the gain of the system linking spatial auditory information to flight motor outputs.

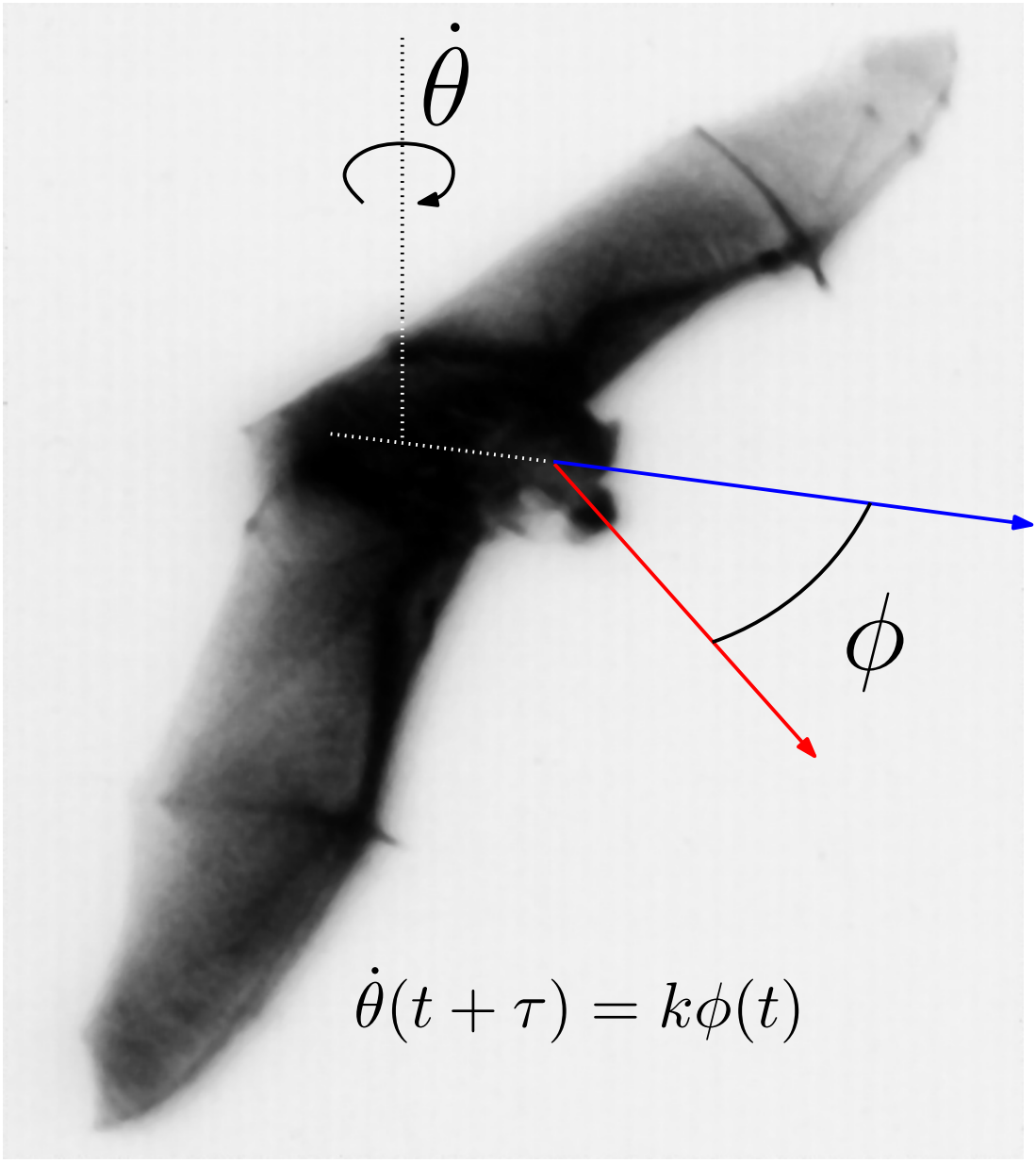
$\dot{\theta}$
ϕ
$\dot{\theta}(t+\tau) = k\phi(t)$

Paper title	Echolocating bats use a nearly time-optimal strategy to intercept prey.
Authors	Kaushik Ghose, Timothy Ken Horiuchi, P. S. Krishnaprasad,and Cynthia F. Moss
Journal	*Public Library of Science: Biology* (2006) *in press*

I learned a great deal about plane geometry from these exercises with The Bull. I discovered that the shortest distance between two points is a straight line, an idea that The Bull either could not fathom or he was reading Einsteinian theory in his spare time. At any rate, he almost always ran in a long, arching curve. This resulted from his knowing nothing about leading a moving target; he always held dead on. Consequently, a diagram of our converging lines of motion would show his course as a long curved line intersecting and merging with my short straight line.

Patrick F. McManus
The Great Cow Plot
in *A Fine and Pleasant Misery*

5

Echolocating bats use a nearly time-optimal strategy to intercept prey

5.1 Introduction

Echolocating bats forage on the wing in darkness. Their primary sensory system for hunting in the dark is echolocation (Griffin, 1958; Griffin, Webster, and Michael, 1960). They emit short pulses of broadband sound, predominantly at ultrasonic fre-

quencies, to derive information from the returning echoes. Bats engage in a natural version of the "homicidal chauffeur" game[1] (Isaacs, 1965), preying upon small, fast, erratically moving insects that may fly in the open only for brief periods at a time (Simmons et al., 2001; Morrill and Fullard, 1992; Lewis, Fullard, and Morrill, 1993). A bat therefore has a fleeting time window within which to detect, localize and capture its prey. A complete insect chase from detection to capture typically takes less than one second (Simmons, Fenton, and O'Farrell, 1979). The short time window available for capturing such highly maneuverable and unpredictable prey would suggest evolutionary pressure for the bat to adopt a pursuit strategy appropriate for its needs. Using high-speed video and audio recordings of the big brown bat (*Eptesicus fuscus*) chasing tethered and free-flying insects in a laboratory flight-room, we show that the echolocating bat uses a previously undescribed pursuit strategy while capturing prey. We argue in this paper that this strategy minimizes time-to-capture of an unpredictably moving insect.

Previous studies in fish (Lanchester and Mark, 1975), dragonflies (Olberg, Worthington, and Venator, 2000) and humans (Chapman, 1968; McBeath, Shaffer, and Kaiser, 1995; Fajen and Warren, 2004) show that a wide variety of animals use a constant bearing (CB) strategy during pursuit. Here, the animal keeps the angle between its heading (velocity vector) and the target a constant as it closes the target range. Additionally, the animal attempts to move in a straight line – a condition that prevents spiral paths about a target (Fajen and Warren, 2004). This strategy, as a means to detect a collision course with another object, has been known anecdotally for hundreds

[1] In this mathematical game, a driver (the "homicidal chauffeur") of a car (faster vehicle with a larger turning radius) attempts to run down pedestrians (slower, with smaller turning radii). This is one of a series of mathematical formulations designed to study various problems involving pursuit.

of years to sailors and more recently to airplane pilots and car drivers and is known as "constant bearing, decreasing range." It was formalized in the 1960s in the human psychology literature (Adams, 1961; Roscoe, 1968). This research has led to the hypothesis that the CB strategy is widespread because it involves the use of a perceptual invariant — by simply nulling the rate of change in the visual angle to a target, animals can pursue a moving object (Cutting, Vishton, and Braren, 1995).

The CB strategy has been successful in explaining pursuit behavior when the target moves at constant velocity and the pursuer moves at constant speed. Under the condition of constant target velocity a pursuer following a CB strategy intercepts the target by moving along a straight line while holding a fixed target bearing (See Figure 5.1A) given by

$$\phi = \sin^{-1}\left(\frac{v_T \sin\beta}{v_P}\right) \tag{5.1}$$

If a pursuer is too slow ($v_P < v_T \sin\beta$) it cannot intercept the target, and there is no solution to Equation 5.1. If $v_P > v_T \sin\beta$ then there are two solutions to Equation 5.1, only one of which causes the distance between the pursuer and the target to decrease.

Under the condition of constant target velocity, when a pursuer follows a CB strategy, it intercepts the target in minimum-time. We offer a proof of this by contradiction: when holding a CB, the pursuer follows a straight path $X'Z$ to intercept the target in time T (Figure 5.1 (A)). Suppose there is another path $X'PY$ (not necessarily a straight line) that would allow the pursuer to intercept the target in shorter time T', at position Y. In that case

$$\begin{aligned}
\sin\phi' &= \frac{XY\sin\beta}{X'Y} \\
X'Y &\leq v_P T' && \text{(since } X'Y \leq X'PY\text{)} \\
\Rightarrow \quad \phi' &\geq \sin^{-1}\left(\frac{v_T\sin\beta}{v_P}\right) && \text{(since } XY = v_T T'\text{)} \\
\Rightarrow \quad XY &\geq XZ
\end{aligned}$$

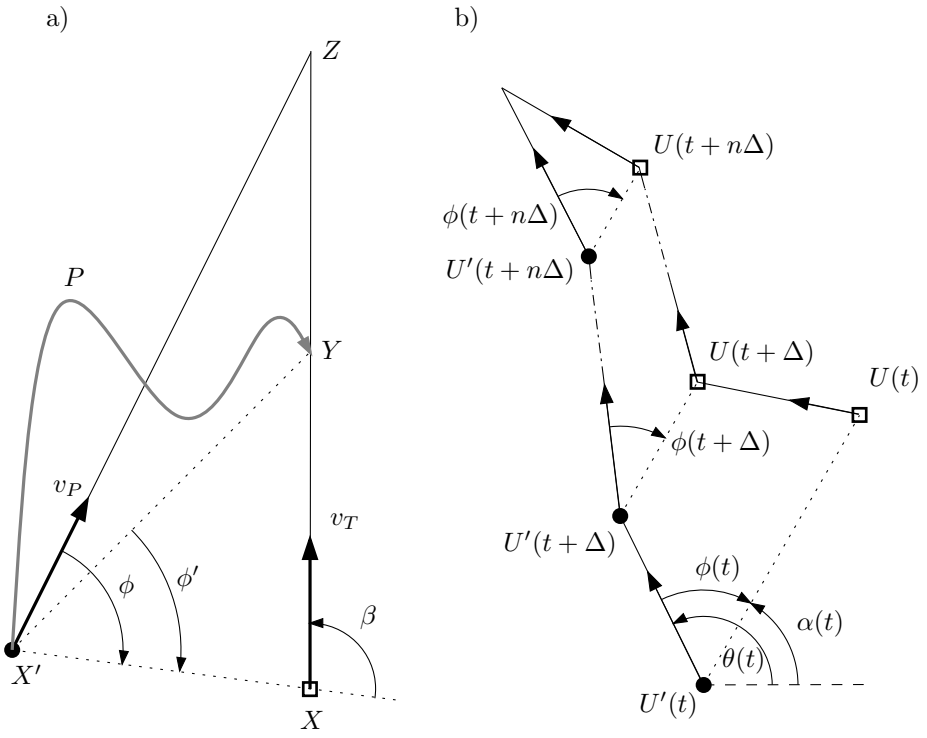

Figure 5.1: Time-optimal strategies to intercept a target. **a**) The target (square), which starts at position X, moves in a straight line at a constant speed v_T. The pursuer (solid disk), which starts at position X', moves at a constant speed v_P. The straight-line intercept $X'Z$, where ϕ is given by Equation 5.1, is the shortest intercept path possible. Quicker intercepts such as $X'Y$ are not possible (see text). **b**) The target (square), which starts at position $U(t)$, moves erratically, changing both speed and direction. The pursuer (solid disk) starts at position $U'(t)$. The erratic target motion can be approximated by infinitesimal constant velocity segments (such as $U(t)U(t+\Delta)$ where $\Delta \rightarrow 0$). There is no globally minimum-time intercept for truly erratic targets. A pursuer can follow a locally time optimum path by adjusting its motion such that ϕ for each infinitesimal segment is given by Equation 5.1. In such a condition the bearing lines drawn from pursuer to target ($U'(t)U(t)$ etc.) remain parallel to each other (α has a fixed value) while the target bearing (ϕ) and pursuer heading direction (θ) may change continually. α and θ are measured with respect to an external, fixed reference frame.

a contradiction, implying $X'Z$ is the shortest interception path available to the pursuer. This demonstrates that ϕ, defined by Equation 5.1, is the optimum bearing that leads to interception in minimum time. Hence we will refer to this value as ϕ_{opt} in what follows.

Bats often pursue targets that move unpredictably. The path of such a target may be broken into infinitesimally short linear segments each of constant velocity (Figure

5.1 (B)). If the pursuer follows an optimum bearing intercept path for each linear segment, then it minimizes time-to-intercept locally, for the duration of that segment. In general the optimum bearing ϕ_{opt} will vary from segment to segment. If the linear segments are long enough then the animal could still use the CB strategy to converge to the optimum bearing (given by Equation 5.1) for each segment. The pursuit will then consist of relatively long periods of CB, interspersed with short periods when the target adopts a new velocity and the pursuer converges to a new CB. A study on dogs catching frisbees supports this idea (Shaffer et al., 2004). If the target motion is sufficiently erratic, however, an animal attempting to execute the CB strategy will never converge to the optimum bearing for any segment.

In the case of an erratically moving target, a pursuer can maintain an optimum bearing using a different strategy. The velocities of the target and pursuer may be decomposed into two components, one parallel to the line joining them (e.g., along $U'U$, Figure 5.1 (B)) and one perpendicular to this line (transverse component). When an animal maintains optimum bearing the transverse component of the velocities of the pursuer and target are matched. This means that the absolute direction to the target (the direction of the line $U'U$, also described by the angle α) remains constant. If the pursuer follows a constant absolute target direction (CATD) strategy where it maneuvers to minimize changes in the absolute direction to the target, the pursuer can maintain the optimum bearing for each instant of the pursuit. The pursuer can follow this strategy by adjusting both its direction of motion and its speed, ensuring $v_P > v_T \sin\beta$ as mentioned previously.

In this study we investigated whether the pursuit of erratically-moving insects by *E. fuscus* is best described as CB (as reported in many other animals) or whether the bat uses a CATD strategy to meet its behavioral requirements. Our results indicate that

E. fuscus follows a CATD strategy.

5.2 Results

We trained eight bats to fly in a large, dark instrumented flight room and capture both tethered and free-flying insect prey. The bat and insect prey were recorded using two high speed infrared video cameras. The flight paths of the bat and its prey were reconstructed from the stereo video frames. Simultaneously a custom built, U-shaped array of 16 microphones recorded horizontal cross-sections of the sonar beam pattern emitted by the bats. *E. fuscus* emits echolocation cries through the open mouth, so the axis of the sonar beam is aligned with the axis of the head. These measurements, therefore, allowed us to compute the horizontal direction of the bat's head as it chased its prey (Ghose and Moss, 2003). The bat was allowed to fly in the room for a random period of time (10–30s) after which the insect prey was released into the room. Each bat was tested individually as it chased a single prey item presented in the room. A trial consisted of the release of the insect and the first attempt by the bat to capture it.

We define for every instant t,

$$\phi_e(t) = \phi(t) - \phi_{opt}(t) \tag{5.2}$$

the difference between the actual bearing to the target, $\phi(t)$, and the optimum bearing, $\phi_{opt}(t)$, given by Equation 5.1.

If the bat were maneuvering to follow the optimum bearing perfectly, ϕ_e should decrease to zero during insect pursuit. If the bat's behavior is better explained by a CATD strategy than a CB strategy, then the rate of change of the absolute target direction should be zero ($\frac{d\alpha}{dt} \rightarrow 0$). From Figure 5.1 (B) we see that $\alpha = \theta + \phi$ (for two-dimensional angles, and for azimuth and elevation components of three dimensional

angles). So

$$\frac{d\alpha}{dt} = \frac{d\theta}{dt} + \frac{d\phi}{dt} \tag{5.3}$$

and for $\frac{d\alpha}{dt} = 0$ we have

$$\frac{d\theta}{dt} = -\frac{d\phi}{dt} \tag{5.4}$$

Conversely, if the bat were following a CB strategy, ϕ should remain a constant ($\frac{d\phi}{dt} \rightarrow 0$).

During insect capture the bat maneuvered to maintain an optimum bearing such that $\phi_e \rightarrow 0$, where ϕ_e (given by Equation 5.2) is the difference between the actual target bearing (ϕ) and the theoretically optimal one (ϕ_{opt}, given by Equation 5.1). The bat maintained the optimum bearing by keeping the absolute direction to the target a constant ($\frac{d\alpha}{dt} \rightarrow 0$). This is illustrated by the example shown in Figure 5.2. In Figure 5.2 the bat chased an erratically flying insect. The numbers along the flight path show time in seconds before capture. Solid lines in Figure 5.2 (d) - 5.2 (g) are for *horizontal* components of motion, while dotted lines are for *vertical* components. The insect (thin black line) made sudden changes in direction (Figure 5.2 (a) , top-view) and height (Figure 5.2 (b)) while continuously changing speed (Figure 5.2 (c)). For the last 500ms before capture the bat (thick gray line in Figs 5.2 (a) - 5.2 (c)) maneuvered such that ϕ_e approached zero (see Figure 5.2 (d)) indicating that it maintained optimum-bearing during its pursuit. During this period the bat did not null $d\phi/dt$ and $d\theta/dt$ (see Figs. 5.2 (e) and 5.2 (f)), as would be consistent with a CB strategy. As expected from a CATD strategy $d\alpha/dt$ was close to zero during this period (Figure 5.2 (g)).

Figure 5.3 shows that the bat's head is stabilized in space when it converges to the CATD strategy. The bat head direction is computed from the recorded sonar beam patterns (Ghose and Moss, 2003). The bat locks its head onto its target during the high

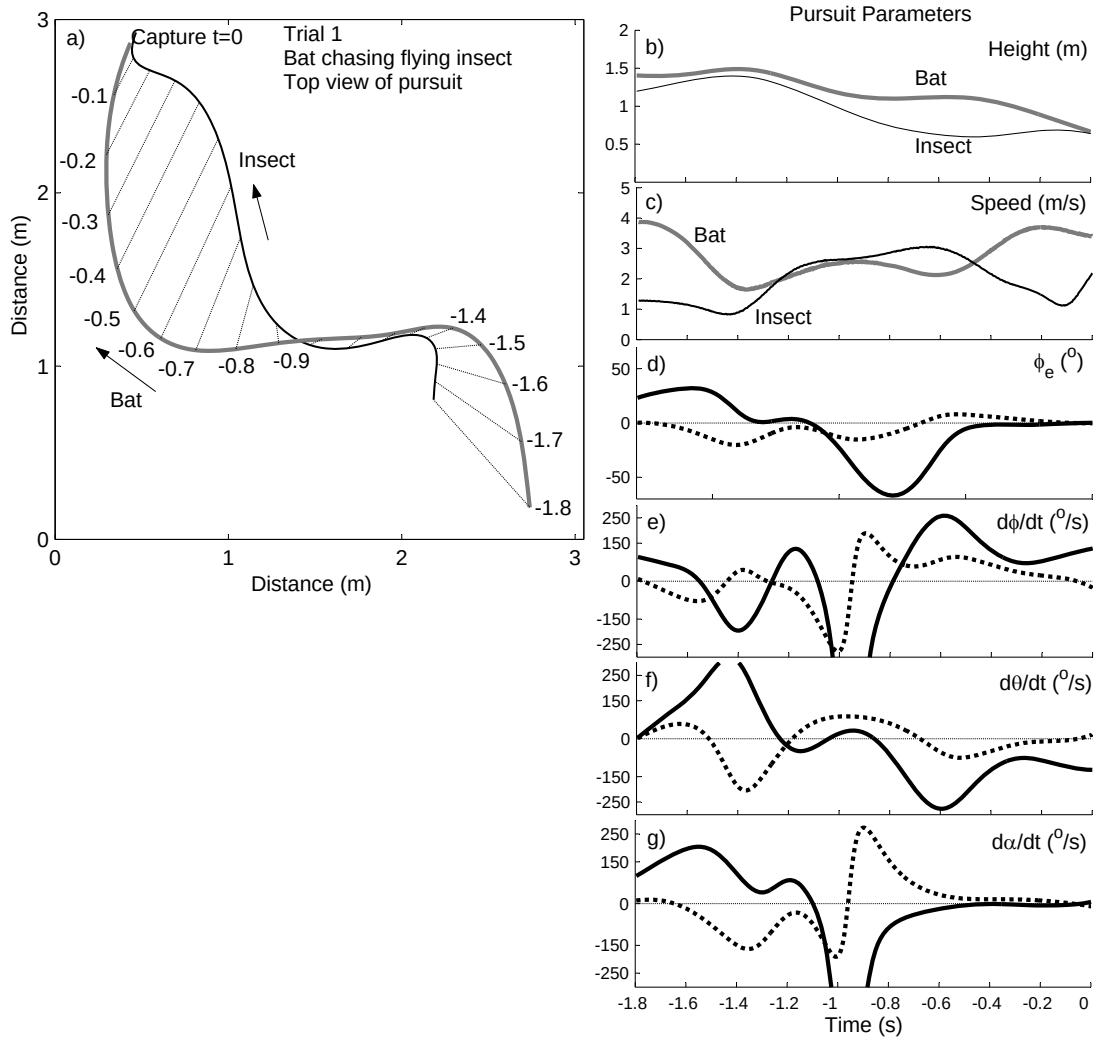

Figure 5.2: Bat chasing a flying insect. **a**) Bat (gray line) chases an erratically flying insect (black line) capturing it at time t=0. Numbers along the flight path indicate the time in seconds to capture. The height **b**) and speed **c**) of the insect varies continually. **d**) The bat maneuvers to drive $\phi_e \rightarrow 0$ in the horizontal (solid line) and vertical (dotted line). **e**) The bearing ϕ is not held constant as $\phi_e \rightarrow 0$ (solid line - horizontal, dotted line - vertical). **f**) The direction of flight (θ) is not held constant (solid line - horizontal, dotted line - vertical). **g**) As $\phi_e \rightarrow 0$ the rate of change of absolute target direction goes to zero (solid line - horizontal, dotted line - vertical). This can also be seen in (a) from the parallel appearance of the dotted lines drawn from the bat to the mantis at 100 ms intervals during the last 700ms of pursuit (see Fig. 5.3). Also see supplementary videos S1-S4

repetition rate stage of insect pursuit. This lock is maintained through out the interception maneuver. This can be seen by inspection in Figure 5.3**a**) and quantitatively

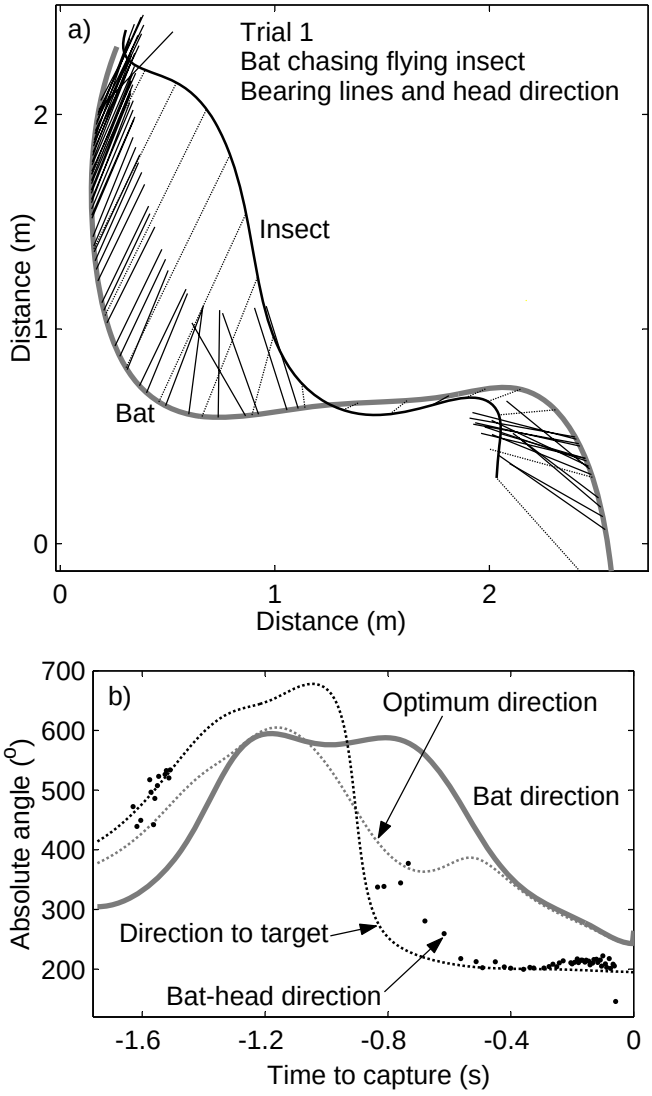

Figure 5.3: The bat's head is stabilized in space during CATD because the bat locks its head onto the target and keeps the absolute direction of the bearing lines constant. **a**) (Similar to Figure 5.2 (a)) Bat (gray curve) chases an erratically flying insect (black curve) capturing it at time t=0. Bearing lines (black dotted) are drawn from the bat to the target every 100 ms. The head-aim of the bat is computed and drawn (straight black line shooting from bat's flight track) each time it emits a vocalization. **b**) The bat's flight direction (thick grey line), the theoretically optimum direction (thin, dotted grey line), the direction to the target (black dotted line) and the bat's head direction (black dots) are shown. Visual inspection of (a) and the computations in graph (b) show that when the bat converges to the CATD strategy (i.e. matches its direction to the optimum direction by maneuvering to optimum bearing) its absolute head direction stabilizes, since it locks onto the target with its head. This can be seen dynamically in supplementary videos S1-S4. We use this observation to suggest, in the discussion, a simple mechanism by which the bat can implement CATD (a functionally predictive strategy) without needing an internal model of target motion.

in Figure 5.3**b**). From Figure 5.3**b**) it can be seen that when the bat converges to the optimum direction, it also converges to the CATD strategy (the absolute direction of the target remains constant, appearing as a flat line in Figure 5.3**b**)) even though its direction of flight keeps changing. Since the bat's head is locked to the target, the absolute direction of the head (black dots) remains constant during this phase of the purusit. We use this observation to propose, in the discussion section, a biologically plausible mechanism by way of which the bat can achieve the computations required by the CATD strategy.

Figure 5.4 illustrates a trial in which the bat chased a tethered insect moving in an arc. Solid lines in Figure 5.4 (d) - 5.4 (g) are for *horizontal* components of motion, while dotted lines are for *vertical* components. Compared to Figure 5.2 the tethered target had less variability in height (Figure 5.4 (b)) and speed (Figure 5.4 (c)). The bat made a U-turn thereby reducing ϕ_e to zero (Figure 5.4 (d)). In this trial, as $\phi_e \rightarrow 0$ the rate of change of bearing ($d\phi/dt$, Figure 5.4 (e)) and flight direction ($d\theta/dt$, Figure 5.4 (f)) also approached zero, making it difficult to discriminate between the CB and CATD models. In this trial note that $d\alpha/dt$ converges to zero earlier (-600 ms, Figure 5.4 (g)) than ϕ_e (-300 ms, Figure 5.4 (d)). From the top-view (Figure 5.4 (a)) we note that during the first 400 ms the distance from bat to target increased as the bat made a U-turn. ϕ_e only approaches zero when the bat is able to both match the target's transverse velocity component and simultaneously decrease distance to the target. In the period -0.6 s to -0.3 s the bat matched the transverse velocity component of the target, but was moving away from it. See supplementary videos S1-S4 to see animations of the bat's pursuit strategy.

To determine if the bat's flight behavior was better described by the CB strategy or the CATD strategy we analyzed 30 successful insect captures by eight bats. Of these,

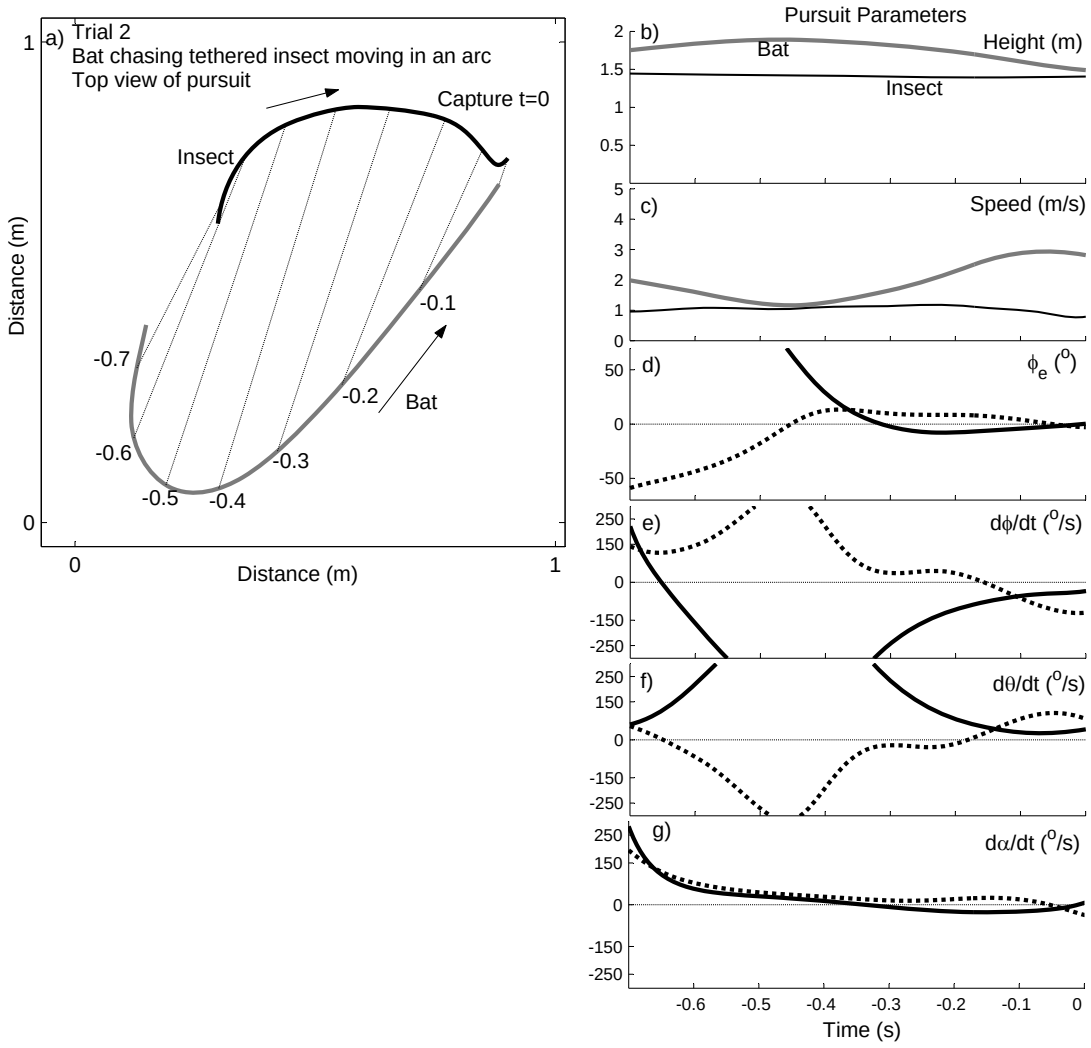

Figure 5.4: Bat chasing a tethered insect. **a**) Bat (gray line) chased a tethered insect moved in an arc (black line) capturing it at time t=0. Numbers along the flight path indicate the time in seconds to capture. The height **b**) and speed **c**) of the insect was more constant than in Figure 5.2. **d**) The bat maneuvered to drive $\phi_e \rightarrow 0$ in the horizontal (solid line) and vertical (dotted line). **e**) The bearing (ϕ) converged to a constant value (solid line - horizontal, dotted line - vertical). **f**) The direction of flight (θ) converged to a constant value (solid line - horizontal, dotted line - vertical). **g**) The rate of change of absolute target direction converged to zero (solid line - horizontal, dotted line - vertical) before $\phi_e \rightarrow 0$. This can also be seen in (a) from the parallel appearance of the dotted lines drawn from the bat to the insect at 100 ms intervals.

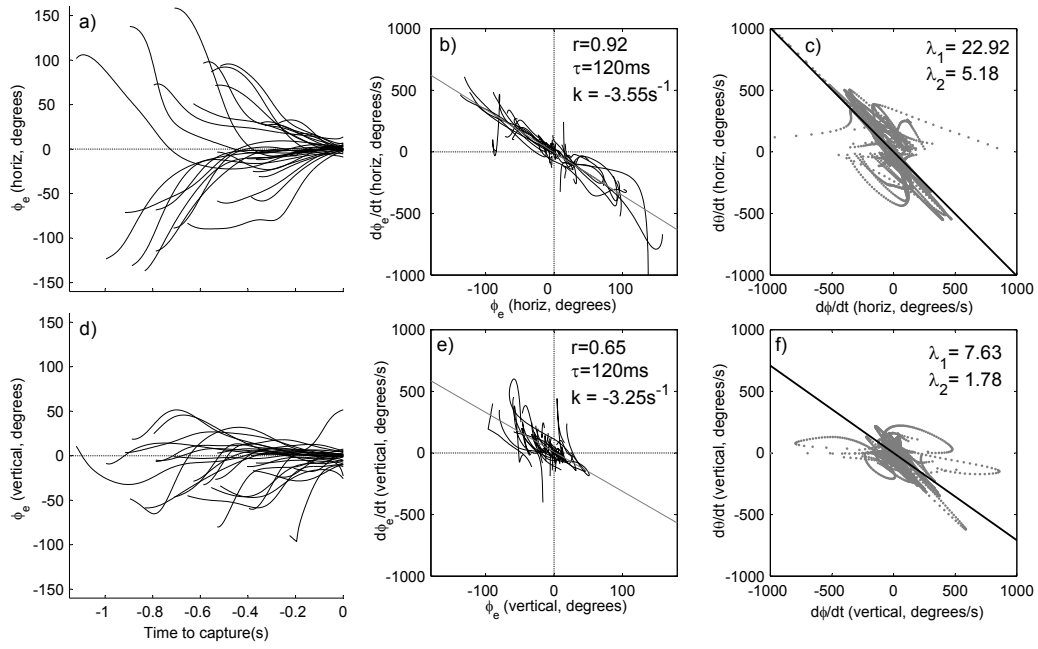

Figure 5.5: Bats maneuver to follow the optimum-bearing by keeping $\frac{d\alpha}{dt}$ low. ϕ_e is the deviation of the target bearing from the instantaneous optimum. Data is shown from captures of both free-flying (15 trials) and tethered insects (15 trials) by 8 bats. **a**) Horizontal component of ϕ_e. Time of insect capture is $t = 0$. The bat reduces ϕ_e during pursuit. For clarity each trial is shown from the instant the bat begins to maneuver to reduce ϕ_e. **b**) The pursuit behavior is captured by a delay-differential equation (Equation 5.5). The gain in the model is given by $k = -3.55s^{-1}$, and the delay is given by $\tau = 120$ ms. The linear fit has a correlation coefficient r=0.92. **c**) The scatter plot of $\frac{d\theta}{dt}$ against $\frac{d\phi}{dt}$ has its principal component (λ_1) (black line) along $y = -x$, indicating that $\frac{d\phi}{dt} = -\frac{d\theta}{dt}$. **d**) Vertical component of ϕ_e for the same trials and same part of pursuit as in (a) . **e**) The bat follows a similar law in reducing ϕ_e in the vertical plane. $k = -3.25s^{-1}$, $\tau = 120$ ms, r=0.65 **f**) The black line shows the principal component (λ_1) of $\frac{d\theta}{dt}$ against $\frac{d\phi}{dt}$ for vertical components of motion.

15 trials were of the bat capturing free-flying insects, and 15 trials were of the bat capturing tethered insects. In each case the bat was observed to maneuver to approach the optimum bearing in both horizontal and vertical planes (Figure 5.5 (a) and 5.5 (d)). As can be seen from the plots of $d\phi_e/dt$ against ϕ_e in Figs. 5.5 (b) and 5.5 (e) , the bat maneuvered to reduce ϕ_e to zero during pursuit. We were able to model the ϕ_e data well by a delay-differential equation

$$\frac{d\phi_e(t)}{dt} = k\phi_e(t-\tau) \tag{5.5}$$

with a negative gain parameter k and a delay τ. The delay, τ, in the model is most likely due to a combination of delays in different parts of the system, including sensori-motor processing time and delay due to the aerodynamics of the bat. It follows from the theory of delay differential equations (Bellman and Cooke, 1963) that solutions to model 5.5 are well-posed and unique given any initial condition $\phi_e^{initial}(t)$, over a time interval of length τ. Moreover, if the gain k is negative and the product $k\tau$ of the gain and time delay is greater than $-\pi/2$, each solution is a weighted infinite sum of decaying exponentials, and the decay rate of each term in the sum is given by the roots of the characteristic exponential polynomial $s - ke^{-\tau s}$ associated to the delay differential equation (5.5) (see Theorem 4.1 and Theorem 13.8 from Bellman-Cooke (1963), a result due to Hayes (1950)). This stability constraint on the parameters of the model is met by the estimates of k and τ in figures 5.5 (b) and 5.5 (e) .

As the bat maneuvers to reduce ϕ_e it faces an erratically-moving target. We recall from Equation 5.4 that if the bat follows a CATD strategy, $d\alpha/dt \rightarrow 0$, resulting in $\frac{d\phi}{dt} = -\frac{d\theta}{dt}$. From the experimental data we see that the bat's strategy is not well fit by a CB model (where $\frac{d\phi}{dt} \rightarrow 0$) but rather by a CATD model (where $\frac{d\alpha}{dt} \rightarrow 0$, or $\frac{d\phi}{dt} = -\frac{d\theta}{dt}$). This can be clearly seen in the scatter plot of $\frac{d\theta}{dt}$ against $\frac{d\phi}{dt}$ in Figure 5.5 (c) . The principal component of the data (λ_1) is along [-1 1] and accounts for

81% of the variance. In the horizontal plane, therefore, the bat keeps $\frac{d\alpha}{dt}$ low ($\rightarrow 0$) at the expense of $\frac{d\theta}{dt}$ and $\frac{d\phi}{dt}$. In the vertical plane the principal component (λ_1) of the scatter of $\frac{d\theta}{dt}$ against $\frac{d\phi}{dt}$ is along [0.82 -0.58], (Figure 5.5 (f) 81% of variance). In the vertical plane, the bat tends to restrict its change in motion ($d\theta/dt$) at the expense of (proportionally) larger changes in bearing angle ($d\phi/dt$) and absolute target direction. One reason for this difference in the bat pursuit strategy along the vertical dimension may be that the bat tends to pounce on the target from above (see Figure 5.2 (b) and 5.4 (b)). So in the vertical plane, the bat may not be trying to match up with the target until it gets very close. At a distance the bat may be aiming for a point slightly above the target. The bat's ability to quickly change altitude may also be less than its ability to change direction in the horizontal.

5.3 Discussion

These results show that the bat maneuvers to approach the instantaneous optimal bearing even when the target is moving erratically. In the horizontal plane the bat prefers to keep the absolute direction to the target (α), rather than the target bearing (ϕ), a constant. Thus the bat, unlike a variety of other animal species, does not use a CB strategy while following its prey. We propose that bats follow a CATD strategy. The bat adjusts its direction of flight and its speed of pursuit so as to maintain the *absolute* direction to the target a constant during pursuit.

When the bat converges to (and maintains) the optimal bearing the absolute direction to the target does not change. The CATD strategy produces a trajectory which, from the viewpoint of the target, makes the pursuer "appear" stationary against a distant background and vice-versa. Such trajectories have been observed in the flights

of male dragonflies engaged in territorial interactions and have been interpreted as camouflaging behavior on the part of the pursuing male (Mizutani, Chahl, and Srinivasan, 2003). Because motion camouflage is primarily useful for defeating visual detection and the bat reveals its presence and direction with the sonar vocalization, the CATD strategy is unlikely to be employed for camouflage. In ongoing work, we are interested in obtaining a sensorimotor feedback law for implementing the CATD strategy, and a recent paper deriving a feedback law for motion camouflage may serve as a useful guide (Justh and Krishnaprasad, 2005). In the field of missile guidance, the CATD strategy is referred to as parallel navigation. Specific guidance laws to achieve parallel navigation have been developed since the 1940's (Yuan, 1948; Zarchan, 1994). It appears that a common constraint – the need to intercept unpredictably moving targets as quickly as possible – has driven both engineers and nature to adopt the same strategy.

We propose a simple mechanism that does not require the bat to explicitly compute the quantities in Equation 5.1 in order to maintain CATD during pursuit. We have shown in an earlier study that the bat locks its head onto a target while chasing it (Ghose and Moss, 2003). When the bat converges to a CATD strategy the absolute direction of the bat's head in space is held constant, independent of the orientation of the body and the bat's velocity vector (see Figure 5.3 for an illustration). The bat could, therefore, maintain CATD by maneuvering to null any changes in head *direction* as sensed by its vestibular system. Because the bat can obtain an accurate estimate of target range through its echolocation system (Simmons, 1971), it would also sense whether it is approaching the target while holding absolute target direction constant. Alternative mechanisms for following a CATD strategy may involve nulling the apparent motion of the acoustic background, assuming the background

sources of noise are distant compared to the target. An interesting possibility is the cross-modal integration of the visual background with the auditory foreground: the bat could follow a CATD strategy by maneuvering such that silhouettes of foliage against the night sky, or the positions of the moon or bright stars (any distant, high contrast object) appear stationary with respect to the acoustically derived position of the target. Some previous modeling studies of bat pursuit behavior have suggested that bats can successfully capture insects using a nonpredictive strategy (Masters, 1988; Kuc, 1994), whereas another modeling study has proposed that bats use an internal model of target motion to predictively pursue an insect (Erwin, Wilson, and Moss, 2001). Our experimental results show that the bat uses a functionally predictive strategy (CATD). The mechanism proposed here, however, allows the bat to implement this functionally predictive strategy without recourse to an internal model of target motion.

From the experiments, we observe that the bat maneuvers to reduce ϕ_e, the deviation from the optimum direction. We model the experimentally observed data using a delay-differential equation (Equation 5.5). In constructing this model we compared linearity between $d\phi_e/dt$ and ϕ_e over a range of delays in steps of 4.2ms (the interval between the video frames) and found that a delay of $\tau = 120\ ms$ produced the best fit (see Figure 5.5). We hypothesize that this time delay is a combination of physical and biological time delays. Such time delays include τ_{echo} (the time delay between the emission and reception of the echo), $\tau_{auditory}$ (the time delay incurred in the central nervous system to process sensory input) and τ_{motor} (the delay due to pre-motor processing and due to the dynamics of the muscular and skeletal system coupled to the aerodynamics). Of these delay components τ_{echo} is the easiest to estimate: the maximum prey distance is about 2m, leading to $\tau_{echo} \leq 12\ ms$ under room conditions. It is harder to

obtain estimates for the other delays. Neural response latencies to echo stimuli in the bat midbrain can be less than $4\ ms$ and greater than $20\ ms$ (Valentine and Moss, 1997; Fuzessery et al., 2003). A conservative estimate of $\tau_{auditory} = 20\ ms$, therefore, still leaves a major portion of the delay (about $90\ ms$ or 75%) to be taken up by τ_{motor}. In this context, bat head movements with a latency of $100\ ms$ are obtained from microstimulation of the bat superior colliculus (Valentine, Sinha, and Moss, 2002) (a midbrain structure implicated in orienting behavior (Moss and Sinha, 2003)). Interestingly, the overall delay of $120\ ms$ that is obtained from our study of bat flight maneuvers is comparable to the latency of $100\ ms$ obtained for human express saccades (Fischer and Ramsperger, 1984).

Since the bat could perform the computations for the CATD strategy by maneuvering to null rotational movements of the head, the bat could link its vestibular system to appropriate flight musculature via a "vestibulo-pursuit-reflex", much like the vestibulocollic reflex. Whereas the traditional vestibulocollic reflex serves to stabilize the head direction when the body posture changes (Wilson et al., 1995), the proposed vestibulo-pursuit-reflex would serve to stabilize the head direction by appropriately changing the bat's flight direction, enabling the bat to use its brainstem to perform the required CATD computations, using cortical input to modulate the computations over longer time-scales.

The bat's strategy is equivalent to following an intercept course to the target at every instant of time, assuming the target will continue moving at its current velocity. The CATD strategy has the important near-optimality property that, under a piecewise linear approximation (Figure 5.1 (b)) it minimizes time-to-intercept of unpredictably moving targets.

5.4 Materials and Methods

We used big brown bats (*E. fuscus*) to study sonar guided flight. The sonar pulses produced by these bats are 2-20 ms long, and consist of multiple harmonics with the fundamental sweeping from approximately 60 kHz down to 22 kHz (Surlykke and Moss, 2000). The bats change their pulse production rate (PPR) with behavioral state (Griffin, 1958). When searching for prey the PPR is low (2-10 Hz), but as the bat detects and then approaches prey, the PPR rises, terminating in the attack phase ('terminal buzz' (Griffin, 1958)) where the PPR may be as high as 200 Hz. We trained eight bats to fly in a large (L7.3m x W6.4m x H2.5m) laboratory room (Figure 5.6). The room walls and ceiling were lined with sound absorbent foam to reduce reverberations. The room was illuminated by dim, long wavelength light (> 650 nm, light from normal incandescent bulbs filtered through a filter plate - Plexiglas G #2711, Atofina Chemicals, Philadelphia, Pennsylvania, United States) to which the bat is insensitive (Hope and Bhatnagar, 1979). Images from two high-speed video cameras (Kodak MotionCorder, CCD based cameras, running at 240 frames/s, synchronized to 1/2 frame accuracy, Eastman Kodak, Rochester New York, United States) were used to reconstruct the three-dimensional flight path of the bats and the trajectory of the prey. The reconstruction was done using commercially available motion analysis software (Motus, Peak Performance Technologies, Englewood, Colorado). Simultaneously, a custom built, U-shaped array of 16 microphones recorded horizontal cross-sections of the sonar beam pattern emitted by the bats. Big brown bats emit their echolocation cries through the open mouth, so the axis of the sonar beam is aligned with the axis of the head. These measurements, therefore, allow us to compute the horizontal direction of the bat's head (Ghose and Moss, 2003).

The bats were trained to catch both free flying and tethered insects. Each bat was

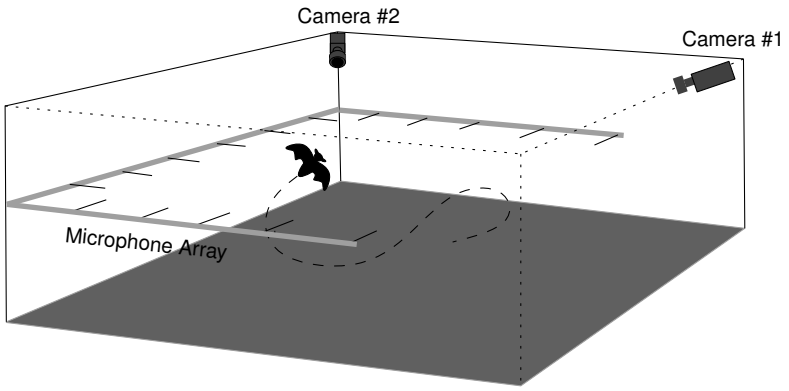

Figure 5.6: Instrumented flight room. The bats were trained to fly in a flight room 7.3m x 6.4m x 2.5m high. The room walls and ceiling were covered with sound absorbent foam to reduce reverberations. Illumination was dim red lighting (wavelength $>$ 650 nm) to exclude the bat's use of vision. Two digital video cameras operating at 240 frames/s recorded the bats and tethered insects during the experiments.

tested individually as it chased a single prey item presented in the room. The free flying insects were a species of praying mantis (*Parasphendale agrionina*). The mantis was released by hand as the bat was flying around in the room. The mantises had their ear plugged with Vaseline to suppress ultrasound triggered diving behavior. The mantises made erratic flight maneuvers after release into the room. The tethered insects were inch-long mealworms tethered by a length of monofilament fiber. The tethered insects were concealed in a trapdoor mechanism that was placed at random positions on the ceiling. The bat was allowed to fly in the room for a period of time (10-30s) after which the the prey was released from the trapdoor. The tethered insect was moved in sections of an arc after release by activating a motorized boom attached to the trapdoor assembly. Each bat was tested individually as it chased a single prey presented in the room. A trial consisted of the release of the insect and the first attempt by the bat to capture it.

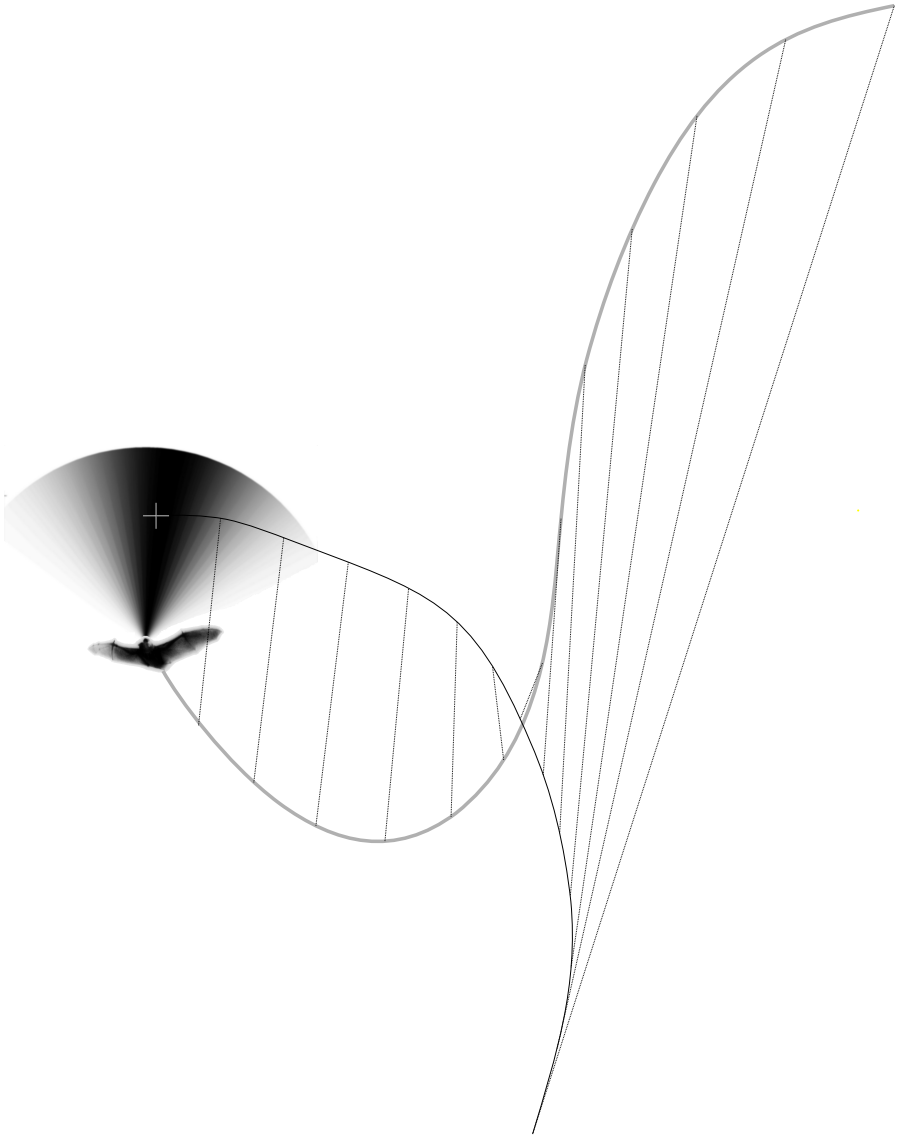

Paper title	Behavioral responses of big brown bats to ultrasound triggered dives by praying mantises
Authors	Kaushik Ghose, Jeffrey D. Triblehorn, Kari Bohn, David D. Yager and Cynthia F. Moss
Journal	for submission to *J. Exp. Biol.*

He roller-coaster he got early warning

He got muddy water he one mojo filter

He say "One and one and one is three"

Got to be good-looking 'cause he's so hard to see

Come together right now over me

The Beatles

Come together

6

Bat flight responses to mantis dives

6.1 Introduction

Insects and echolocating bats are engaged in an evolutionary arms race (Triblehorn and Yager, 2005a). Some nocturnal insects have evolved to take advantage of night skies that are free of visually guided predators such as birds. In turn, a class of mammals, insectivorous echolocating bats, have evolved the ability to fly and forage on insects in darkness, avoiding competition from diurnal predators. Echolocating bats are agile

flyers that sense the environment predominantly through hearing, rather than vision. An echolocating bat emits brief ultrasonic pulses into the environment. Objects in the environment, such as insects, return echoes to the bat. The bat analyzes these echoes to detect, localize and identify the objects (Griffin, 1958). This system of using sound to sense the environment is a natural form of active sonar. A bat's encounter with an insect, from detection to capture, often take less than a second to complete. Insects, under evolutionary pressure to avoid predation, have developed different strategies to evade capture by bats. Some insects limit time in flight (Morrill and Fullard, 1992), reducing the probability they will be in the air when a bat is out hunting. Some insects fly erratically, making it harder for a bat to maneuver and intercept them (Lewis, Fullard, and Morrill, 1993). Some insects have evolved an 'early warning system' – an ear sensitive to the ultrasonic signals emitted by the bat – that warns of potential bat attacks. Through this system, insects detect the bat's ultrasonic echolocation signals and initiate evasive maneuvers. These insects have, therefore, exploited the bat's active sonar system and turned it to their own advantage.

There has been much study of the counter-measures available to insects against bats. In particular, the efficacy of the ultrasound triggered responses to bat attacks has been investigated in great detail, starting with Roeder and Treat's initial work (Roeder and Treat, 1961) and continuing to the present day (e.g. Yager, May, and Fenton, 1990; Triblehorn and Yager, 2005b). Roeder's work on moths suggested that the moth's detection system has a much longer effective range than the bat's sonar, enabling the moth to detect the bat in advance (Roeder, 1967). Further work an lacewings (Miller and Olesen, 1979) and mantids (Yager, May, and Fenton, 1990) suggest that the ranges of early warning systems of several insect species are greater than the range of the bat's sonar, possibly giving an insect equipped with this early warning system, a great

advantage.

In contrast, not much attention has been paid to the other side of this war - the counter-counter-measures adopted by the bat to allow it to successfully forage in spite of the insect's evasive responses. A previous study has shown that the big brown bat (*Eptesicus fuscus*) adopts a time-optimal flight pattern to counter the erratic maneuvers adopted by some insects (Ghose et al., 2006). The strategy adopted by the bat minimizes the time-to-intercept erratically moving prey, and may serve to improve the bat's chances of capturing insects that adopt unpredictable flying as their defense mechanism. Here, we investigate how bats deal with ultrasound-triggered insect dives, adopted by hearing insects as another bat-evasion strategy. In particular, we study the responses of the big brown bat to evasive dives initiated by flying praying mantises in a laboratory flight room.

6.2 Materials and Methods

Instrumented Flight room

We studied the interaction between big brown bats (*Eptesicus fuscus*) and flying praying mantises (*Parasphendale agrionina*) in a large (7.3m x 6.4m x2.5m) laboratory flight room (Fig. 6.1). The room walls and ceiling were lined with sound absorbent foam to reduce reverberations. The room was illuminated by dim, long wavelength light (> 650 nm, light from normal incandescent bulbs filtered through a filter plate - Plexiglas G #2711, Atofina Chemicals, Philadelphia, PA) to which the bat is insensitive (Hope and Bhatnagar, 1979). Images from two high-speed video cameras (Kodak MotionCorder, CCD based cameras, running at 240 frames-per-second, synchronized to 1/2 frame accuracy) were used to reconstruct the three-dimensional flight path of the

bats and the trajectory of the prey. Simultaneously, a custom built, U-shaped array of 16 microphones recorded horizontal cross-sections of the sonar beam pattern emitted by the bats. Previous studies have shown that the big brown bat keeps its sonar beam 'locked-on' to a target during the entire interception maneuver, allowing us to study the target tracking behavior of the bat by observing the direction of its sonar beam (Ghose and Moss, 2003).

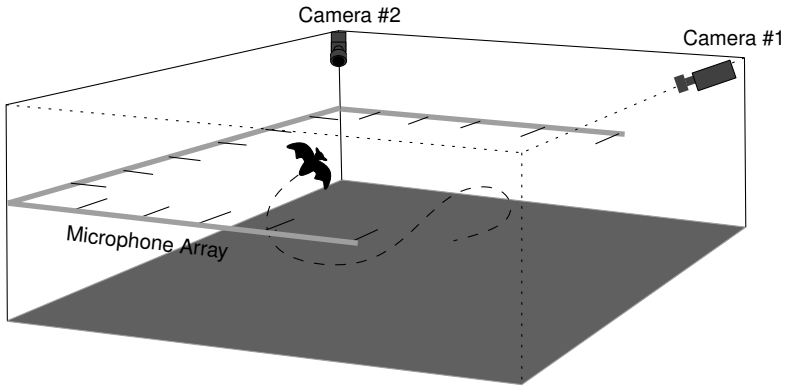

Figure 6.1: Instrumented flight room. The bats were trained to fly in a flight room 7.3m x 6.4m x 2.5m high. The room walls and ceiling were covered with sound absorbent foam to reduce reverberations. Illumination was dim red lighting (wavelength $>$ 650 nm) to exclude the bat's use of vision. Two digital video cameras operating at 240 frames/s recorded the bats and insects during the experiments.

Animals

We used five big brown bats (*Eptesicus fuscus*) collected locally in Maryland. The bats were trained to capture both tethered mealworms and free-flying mantids in the flight room. We tested male *Parasphendale agrionina*(Mantidae; Mantinae; Miomantini) 7-21 days after their molt to adulthood. The mantids were raised in our colony maintained at 25-30 C and 30-50 % relative humidity with a 14 h day length. All mantids were housed individually as adults and fed flies twice a week.

Experimental Paradigm

Each bat was tested individually as it chased a single flying mantis presented in the room. One experimenter (JDT) kept the mantis concealed while the bat was allowed to fly in the room for a random period of time (10-30s). The mantis was then released into the room, starting the experimental trial. The trial ended with the capture of the mantis, the landing of the mantis on the floor or walls of the flight room, or after 8 seconds (The limit of our recording apparatus). Mantises were either untreated or were deafened by applying Vaseline to the ear. The experimenters were blind to the condition of the mantis. Trials were sorted out afterwards into two groups depending on whether they involved deafened or untreated mantises. For analyzes reported here, only trials using untreated (hearing) mantises were considered. Trials with deafened mantises were used to study the bat's behavior to erratically flying prey that did not perform dives (Ghose et al., 2006).

Data Analysis

The flight paths of the bat and mantis were reconstructed using commercially available motion analysis software (Motus, Peak Performance Technologies Centennial, CO, now merged to form Vicon Peak). The flight trajectories obtained were smoothed using a cubic spline technique(`csaps` function, MATLAB, MathWorks, Nanticoke). Instantaneous flight directions were computed as the tangent vector to the curve at each sample time.

The dive time of the mantis was computed as the first time the vertical velocity of the mantis turned negative and stayed negative until the mantis hit the floor, or the mantis leveled off in flight.

6.3 Results

We found that bats captured non-diving mantises in 74% of the cases, whereas they captured diving mantises in 5% of the cases (Fig. 6.2). This is similar to the success rates observed in another study with a larger sample of bat-mantis interactions (n=173, Triblehorn *et al., in preparation*).

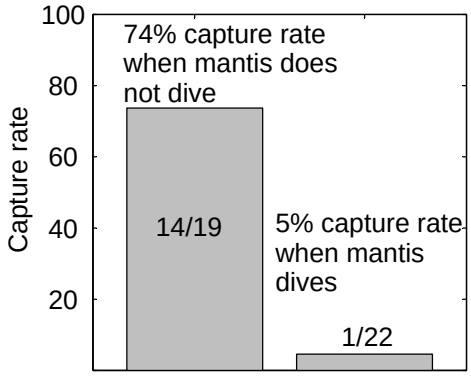

Figure 6.2: Mantis capture rates. When the mantis ultrasound triggered dive was suppressed by blocking the mantis ear the bats were successful in capturing the mantis in 14 trials out of 19. When the mantis was not experimentally manipulated the bat was successful in one trial out of 22 in capturing the mantis after it dove.

We observed that out of 22 trials where the mantis dived the bat initiated a following dive in 14 of these trials (65%). In one another trial the bat initiated a dive 700 ms after the mantis, and the mantis had landed on the floor by then.) An example of a following dive by the bat is shown in Fig. 6.3. After detecting the mantis, the bat initially turns and heads towards it, closing distance. It then adopts a predictive interception strategy (Ghose et al., 2006) where it attempts to minimize the time-to-intercept the target. When the bat converges to its strategy the bearing lines drawn from the bat to the target remain parallel during pursuit. In this trial at time t_{dive} the mantis initiates a dive and heads down to the floor. The bat initiates a following dive approximately $100\ ms$ after the mantid's dive. The bat follows the mantis, but aborts and pulls out of the chase $100\ ms$ before the mantis hits the floor.

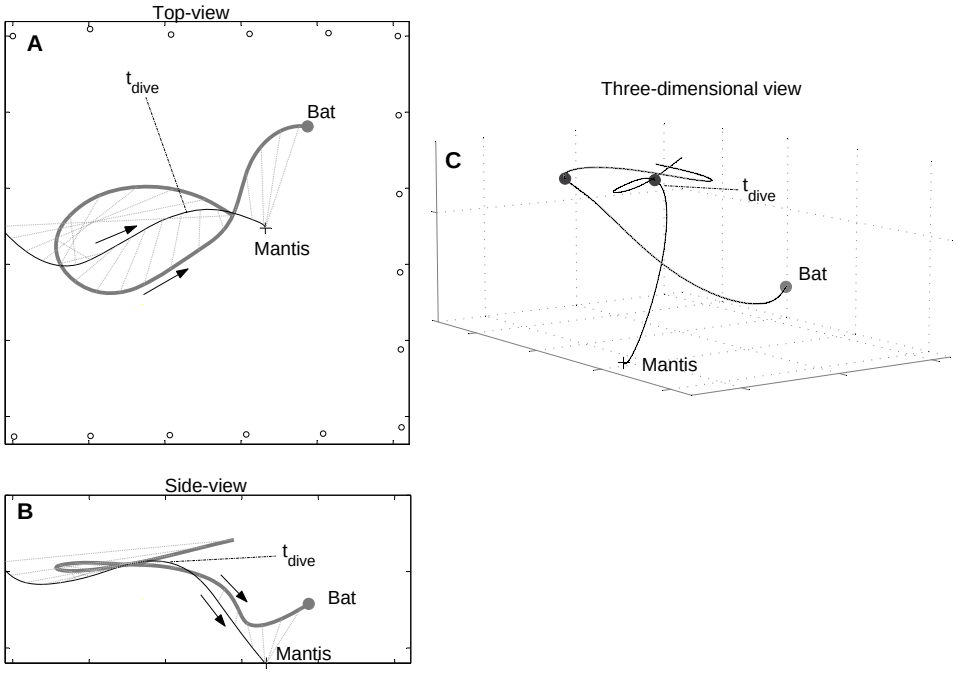

Figure 6.3: **A**) Top-view of bat (solid gray line) chasing mantis (thin black line). Bearing lines from the bat to the mantis are drawn every 100 ms. At time t_{dive} the mantis initiates a dive and heads down to the floor. The bat initiates a following dive approximately 100 ms after the mantis dives. The bat follows the mantis, but aborts and pulls out of the chase 100 ms before the mantis hits the floor. **B**) Side-view of same trial, showing heights of bat and mantis. Each axis-division is 1 m. **C**) Three-dimensional viewo of the trial. Each axis-division is 1 m.

During the entire chase, including the dive, the bat keeps its sonar beam locked onto the mantis in the horizontal plane as shown in Fig. 6.4. Each time the bat emits a sonar pulse the horizontal direction of the sonar beam axis is computed from the array data (Ghose and Moss, 2003). In the initial part of the trial the bat sonar beam was directed away from the recording array, so no sonar beam data is available. As observed in previous studies (Ghose and Moss, 2003; Ghose and Moss, 2006; Ghose et al., 2006), the bat locks its sonar beam onto the tracked target. Here we see, in addition, that the bat maintains the target lock even when the target makes an evasive dive. Our apparatus only allows the computation of horizontal beam direction for these

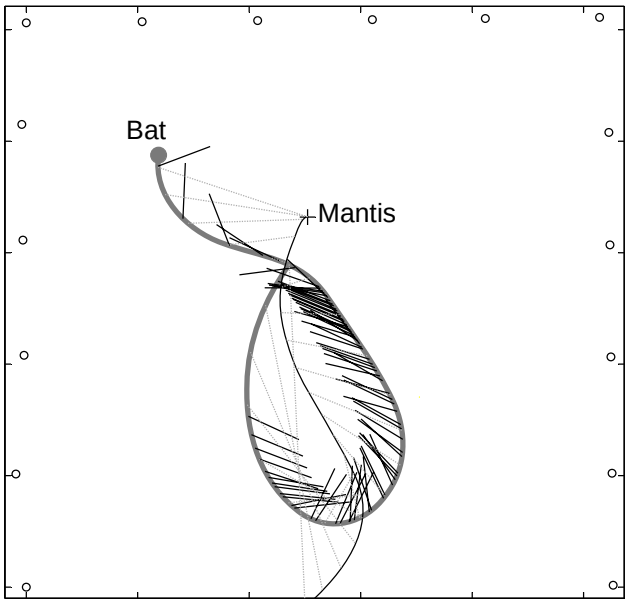

Figure 6.4: This shows the same trial as Fig. 6.3. The horizontal direction of the sonar beam axis is shown each time the bat (gray line) emits a sonar pulse (short black lines). The accuracy of the sonar beam lock on the target can be seen from the correspondence between the bearing lines (thin dotted gray lines) and the sonar beam direction. Note that the sonar beam is locked onto the mantis (thin black trace) during the entire chase, including the dive. Each axis-division is $1\ m$.

trials, so it is not possible to say whether the bat also locked its sonar beam to the target in the vertical aspect.

6.3.1 Mantis dives

Mantis dives are not directionally dependent on the bat's position. The radius of the polar plot in Fig. 6.5 measures time. The center is $-200\ ms$ (before the dive), the thick gray semi-circle is the dive time ($0\ ms$) and the outermost semi-circle is $+200\ ms$ (after the dive). The angle plotted is the angle the horizontal direction of the mantis' flight makes with the bearing to the bat at the time of the dive. When the mantis is

flying directly away from the bat, this angle is 0^o, when the mantis is flying directly towards the bat, this angle is 180^o. If the mantis dive were directionally dependent on the bat's location (i.e. the direction of the source of ultrasound), then each trace would deflect systematically after crossing the gray semi-circle ($0\ ms$, dive time). The deflection would be a function of the bearing angle. We see, however, that the traces, with one exception, show no marked deflection after crossing the gray circle, indicating that when the mantis dives, it continues along its original course. The trace marked with an arrow shows a trial where the mantis quickly turned through 150^o at the start of the dive, before continuing to dive in a straight line.

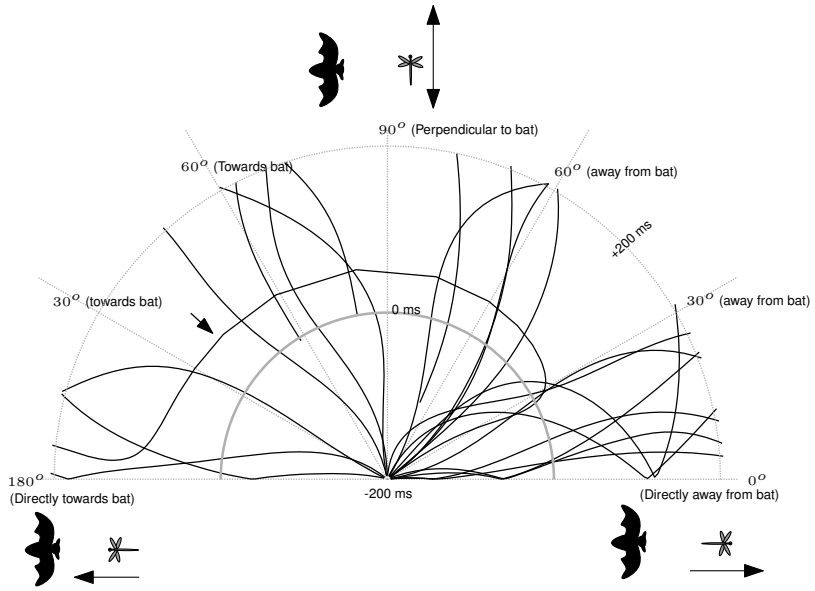

Figure 6.5: Mantis dives are not directionally dependent on the bat's position. The radius on this polar plot marks time with respect to the time the mantis dove. The thick gray semi-circle is the dive time ($0\ ms$). The angle plotted is the angle the horizontal direction of the mantis' flight makes with the bearing to the bat at the time of the dive (0^o = mantis flying away from the bat, 180^o = mantis flying towards the bat). The radial nature of the traces show that the mantis does not respond to the direction of the bat when diving. Rather, the mantis tends to dive in the horizontal direction it was originally flying. The dive marked with an arrow shows a trial where the mantis quickly turned through 150^o at the start of the dive, before continuing to dive in a straight line. N=22 dives.

In the vertical plane, the mantis dive adds large variability to the motion of the

mantis. From Fig. 6.5 it can be seen that before diving mantids fly approximately horizontally, with a vertical motion variability of 15^o. $200\ ms$ into the dive, however, the motion of the mantids spread over a range of 60^o

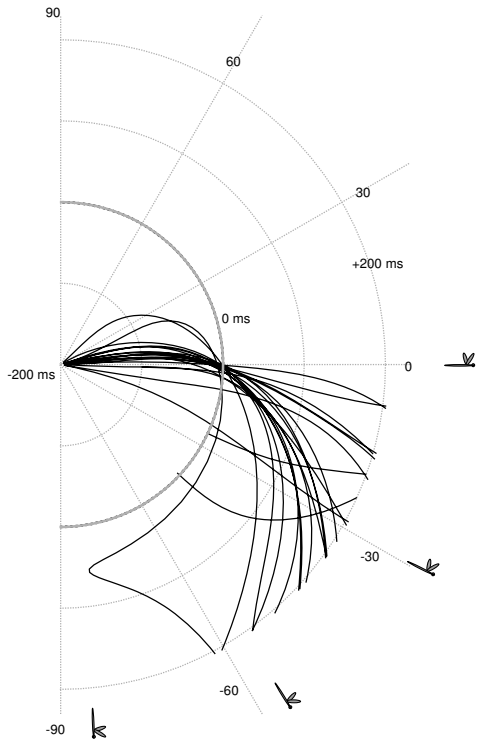

Figure 6.6: In the vertical plane mantis dive angles vary over a range of 60^o. The radius on this polar plot marks time with respect to the time the mantis dove. The center is $-200\ ms$ (before the dive), the thick gray semi-circle is the dive time ($0\ ms$) and the outermost semi-circle is $+200\ ms$ (after the dive). The angle plotted is the vertical angle of the mantis' flight path. Before the dive the mantis' vertical motion is restricted over a 15^o range. $200\ ms$ into the dive this range has increased to 60^o. N=22 dives.

In the experiments we conducted, 68% of the mantis dives (15/22) were initiated when the bat was within $1\ m$ of the mantis (Fig. 6.7). Fig. 6.8 shows that bats were most likely to initiate a following dive when the mantis dive when it was between $0.5\ m$ and $2\ m$ away. Further or closer dives were followed less than 50% of the time. 6.8

Figs. 6.5, 6.6, 6.7 and 6.8 suggest that the mantis' dive "throws-off" the bat, since

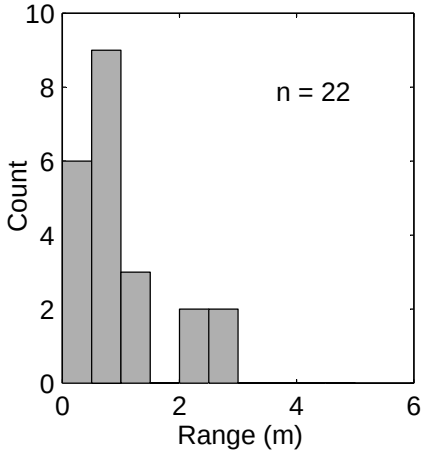

Figure 6.7: Mantis range at dive initiation. The distribution of dives is skewed towards closer ranges, with 68% (15/22) of the dives occuring when the bat was within 1 m of the mantis. N=22 dives.

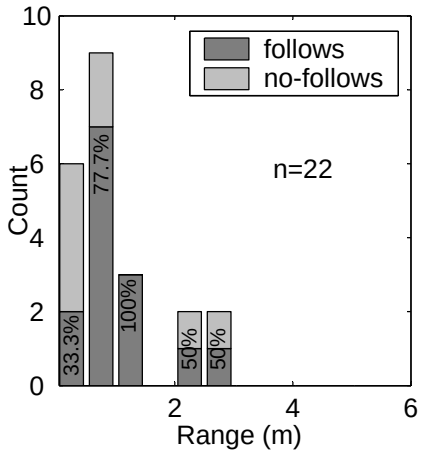

Figure 6.8: The stacked bar graph shows the number of mantis dives at different ranges (same as Fig. 6.7) and the number of instances when the bat followed the mantis dive at those ranges. The bat followed the mantis in 50% or less instances when the mantis dove very close (0.5 m or less) or very far (2 m or more) from the bat. N=22 dives.

it produces a sudden, variable and quick change in vertical motion just as the bat is closing in on the prey. The horizontal motion of the mantis is, however, not altered as much. Fig. 6.8 suggests that the bat decides not to pursue the mantis into the dive if the dive occurs late or early. In cases where the mantis dive occurs late the bat may not be able to maneuver quickly enough to chase the mantis along it's new trajectory. In cases where the mantis dive occurs early, the mantis may reach the ground long before

the bat can reach the vicinity.

6.3.2 Bat vocalization behavior

Echolocating bats change the rate at which they produce pulses with behavioral state (Griffin, 1958; Surlykke and Moss, 2000; Denzinger, Kalko, and Jones, 2004). When searching for prey they produce pulses at larger intervals ($100\ ms$ or more) and when chasing prey they reduce the interval between pulses to low values ($6\ ms$ or less). We studied how the pulse interval (time between the start of sequential pulses) changes as the bat pursues the mantis. Fig. 6.9 shows the pulse interval over time as the bat pursues a diving mantis. The time values are relative to the mantis dive time. Initially

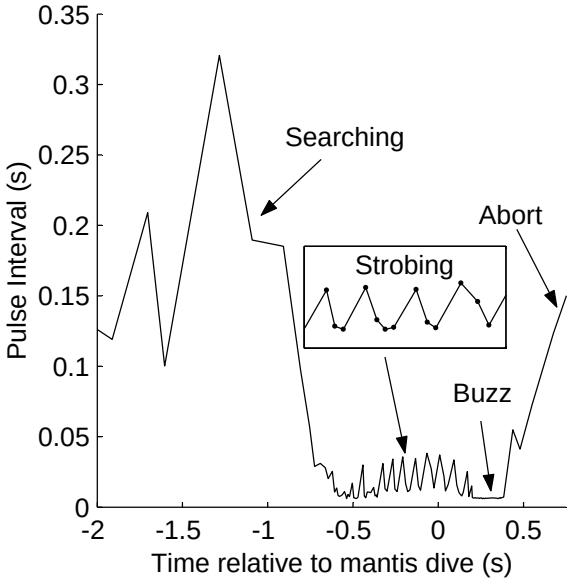

Figure 6.9: Pulse timing during a mantis pursuit. Times are given relative to time of mantis dive. Initially the bat is producing pulses at a low rate with pulse intervals $100\ ms$ or greater ("Search"). At time $-0.75\ s$ the pulse interval drops to less than $25\ ms$ and then, at $-0.5\ s$, drops to less than $6\ ms$. For part of the fast pulse rate phase the bat produces groups of two or three quick pulses separated by slightly larger gaps ("Strobing", see inset for detail). The mantis dove at $0\ s$ with the bat following the dive. During the last part of the attack sequence the bat produces a string of pulses with a short interval ("Buzz"). The bat broke off the chase ("Abort") after the mantis had landed on the floor.

the bat produced pulses at a low rate with pulse intervals $100\ ms$ or greater. At time $-0.75\ s$ the pulse interval droped to less than $25\ ms$ and then, at $-0.5\ s$, droped to less than $6\ ms$. This is the terminal stage of insect attack when the bat is inferred to have committed to capturing the insect. During this phase "strobing" can be observed. This is a phenomenon where the bat produces groups of two or three quick pulses separated by slightly larger gaps. Strobing may be a vocal behavior related to the bat extracting more detailed information about a target (Moss and Surlykke, 2001; Moss et al., 2006). During the last part of the attack sequence the bat produced a string of pulses with a short interval ("Buzz") that is typical of bats at the terminal stage of attack. The bat broke of the attack ("Abort") after the mantis had landed on the floor.

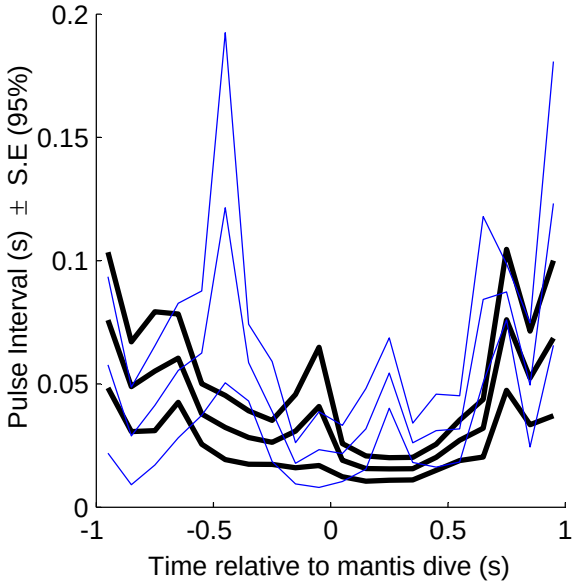

Figure 6.10: Summary of pulse interval variations. $t_{dive} = 0$. Black lines are for trials where bat followed mantis dive, blue lines for trials where bat did not follow mantis dive. Lines show mean pulse interval $\pm$ standard error at 95% confidence level, calculated in 100 ms bins. n=22 dives

Fig. 6.10 shows a summary of pulse interval changes with time across 22 trials where the mantis dove. Time $t = 0$ is the dive time of the mantis. Black lines show the pulse interval changes for trials where the bat pursued the mantis into the dive,

while blue lines show trials where the bat did not pursue the mantis. The lines show mean pulse interval $\pm$ standard error at 95% confidence level, calculated in $100\ ms$ bins. It can be seen that, for those trials where the bat did not follow the mantis dive, $300\ ms$ after the mantis dive there is a significant ($p > 0.05$), but momentary, increase in pulse interval over those trials where the bats followed the mantis dive. There is no significant difference in pulse intervals after that. We use this result in combination with other results to suggest, in the discussion, that even in those cases where the bat does not pursue the mantis into the dive it may still be "monitoring" the mantis until the mantis lands on the floor.

6.3.3 Bat flight responses

Fig. 6.11 shows four example flight paths of individual interactions between bats and diving mantids. In each case a top-view and the corresponding side-view is shown. The solid gray line is the bat, the black line is the mantis, the dotted lines are bearing lines drawn from the bat to the mantis at $100\ ms$ intervals and the black square indicates the dive time of the mantis. (A) and (B) show trials where a bat does not follow the mantis into the dive. In both cases, however, the bat appears to make adjustments to its horizontal motion in order to track the mantis. From the summary of pulse interval variation during pursuit (Fig. 6.10) we note that there is a momentary increase in pulse interval $300\ ms$ after the dive when the bat does not follow the mantis. The pulse interval trace, however, drops back $400\ ms$ into the dive and is not significantly different from that when the bat follows the dive. It is possible that during this period the bat is still "keeping an ear" on the diving mantis, though it is not following it in the vertical plane. **c**) Shows a trial where the bat chases the mantis down, but is unable to intercept it before it hits the floor. **D**) Shows the only trial in which the bat success-

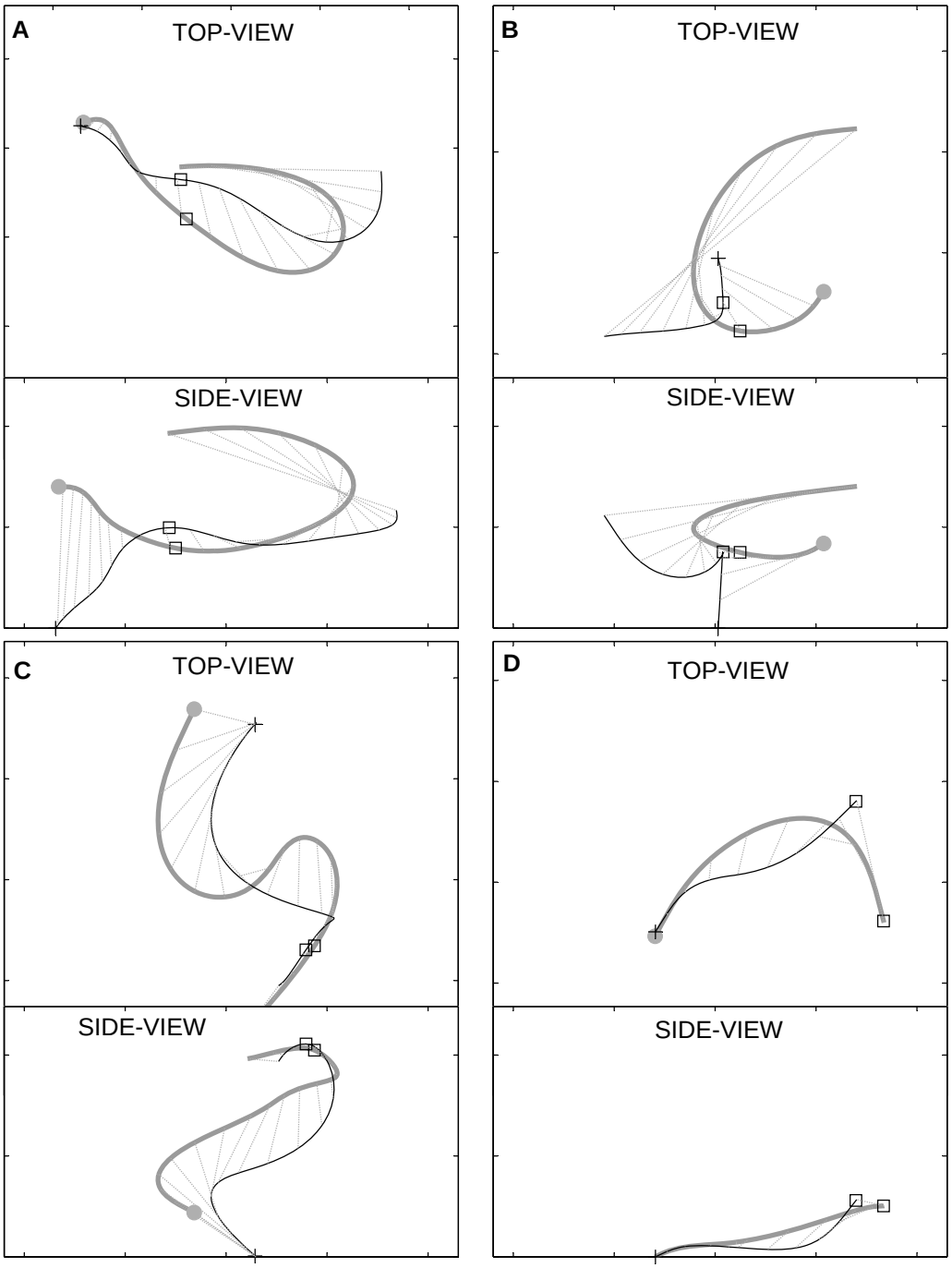
A
TOP-VIEW
SIDE-VIEW
B
TOP-VIEW
SIDE-VIEW
C
TOP-VIEW
SIDE-VIEW
D
TOP-VIEW
SIDE-VIEW

Figure 6.11: Four more examples of bat-mantid interactions. In each case a top-view and the corresponding side-view is shown. The solid gray line is the bat, the black line is the mantis, the dotted lines are bearing lines drawn from the bat to the mantis at 100 ms intervals and the black square indicates the dive time of the mantis. **A**) and **B**) show trials where a bat does not follow the mantis into the dive. In both cases, however, the bat appears to make adjustments to its horizontal motion in order to track the mantis. **c**) Shows a trial where the bat chases the mantis down, but is unable to intercept it before it hits the floor. **D**) Shows the only trial in which the bat successfully intercepted a mantis in the flight-room after it had initiated a dive. In this case the mantis leveled off at the end of the dive and was captured by the pursuing bat.

fully intercepted a mantis in the flight-room after it had initiated a dive. In this case the mantis leveled off at the end of the dive and was captured by the pursuing bat.

In a previous study we have shown that the bat intercepts erratically moving targets by adopting a time-optimal strategy during pursuit (Ghose et al., 2006). We investigated, here, whether the bat attempts to maintain this optimal strategy even when the mantis dives. Given the flight paths of a bat and its prey, it is possible to compute the theoretically optimum direction the bat should adopt for each point on its flight path. The angular difference between the bat's actual flight direction and the optimum direction gives, therefore, a measure of how closely the bat adopts this time-optimal strategy during pursuit. The optimality index, γ, is the cosine of the difference angle between the bat's actual flight direction, and the theoretically computed optimal direction. γ is a number restricted between -1 and +1. $\gamma = +1$ indicates that the bat has converged perfectly to the time-optimal strategy. $\gamma = 0$ indicates that the bat is flying perpendicularly (90^o off-course) to the optimal direction, while $\gamma = -1$ indicates the bat is flying exactly opposite to the optimal direction, completely moving away from the target. We computed γ for the horizontal and vertical components of the bat's motion to investigate how well the bat converged to the optimum strategy in the horizontal and vertical planes.

In 14 of the 22 trials when the mantis initiated a dive the bat followed the mantis

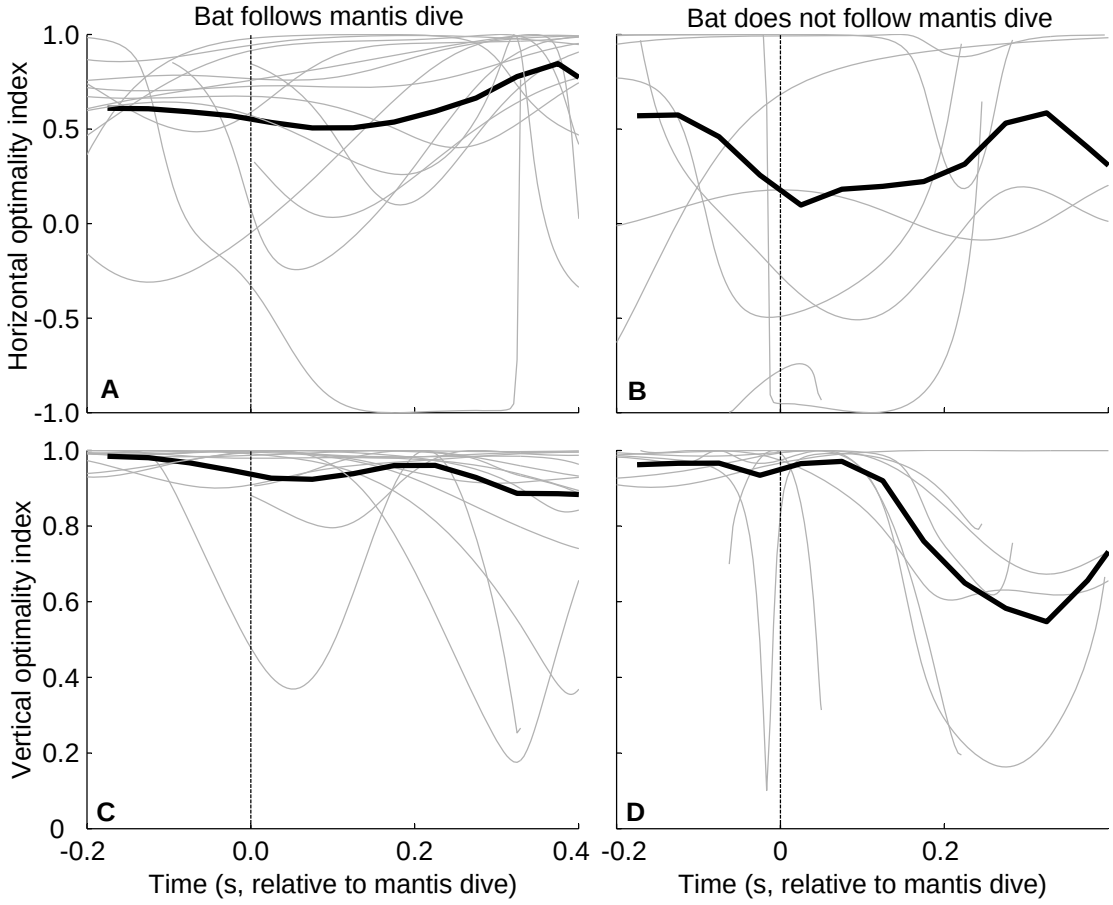

Figure 6.12: When the bat pursues a mantis into the dive, it converges back to the optimal strategy. In all plots, gray lines are individual traces and thick black lines are averages. Time 0 ms is the time of the mantis dive. **A**) $\gamma_{horizontal}$ before and after mantis dive, for trials when the bat followed the mantis into the dive. **B**) $\gamma_{horizontal}$ before and after mantis dive, for trials when the bat did not follow the mantis into the dive. Note that the average $\gamma_{horizontal}$ value even before the dive is lower for the cases where the bat did not follow the mantis. **C**) $\gamma_{vertical}$ before and after mantis dive, for trials when the bat followed the mantis into the dive. **D**) $\gamma_{vertical}$ before and after mantis dive, for trials when the bat did not follow the mantis into the dive. Note that $\gamma_{vertical}$ rapidly drops from $+1$ 100 ms after the mantis dive in cases where the bat does not follow the mantis. In cases, however, where the bat does pursue the mantis, it succeeds in keeping $\gamma_{vertical}$ high. N=14 for follows, N=8 for no-follows.

toward the ground. We computed the optimality index for the horizontal ($\gamma_{horizontal}$) and vertical components ($\gamma_{vertical}$) of motion of the bat both in trials where the bat chased the mantis into the dive, and in trials where the bat broke off the attack, and did not pursue the mantis after its dive (Fig. 6.12).

We show from the trials where the bat did not follow the mantis dive, that the vertical optimality index ($\gamma_{vertical}$) drops from around 1 (bat pursuing mantis in near-optimal fashion) to 0.6 (bat 50^o off the optimal direction) within $200\ ms$ after the dive. When the bat pursued the mantis into the dive, however, the average optimality index does not drop below 0.9 (bat within 25^o of the theoretically optimal direction).

Fig. 6.12 (A) shows $\gamma_{horizontal}$ for cases where the bat chased the mantis into the dive. Fig. 6.12 (B) shows $\gamma_{horizontal}$ for cases where the bat did not chase the mantis into the dive. In the horizontal plane the bat dive does not seem to affect the bat's convergence to the optimal-strategy, as can be seen by both the average curve (black line) and the individual traces. In cases where the bat does not follow the mantis, the bat also appears to be further from the optimum strategy (lower γ value) throughout the trial (even before the dive occurred) than when the bat follows the mantis into the dive. This suggests the hypothesis that when a mantis dives, if the bat is far off from the optimal strategy at that point, the bat aborts its pursuit.

Fig. 6.12 (C) shows $\gamma_{vertical}$ for cases where the bat chased the mantis into the dive. Fig. 6.12 (D) shows $\gamma_{vertical}$ for cases where the bat did not chase the mantis into the dive. We see from both the average trace (black line) and the individual trials (gray lines) that when the bat follows the mantis into the dive (C) , the γ value remains close to +1, indicating that the bat, by following the mantis into the dive, maintains convergence to the optimal strategy. Fig. 6.12 (D) shows the divergence of $\gamma_{vertical}$ that occurs due to the mantis dive when the bat chooses not to follow the mantis.

6.4 Discussion

A previous study has shown that, when pursuing erratically moving insects that do not dive bats adopt a time-optimal pursuit strategy (Ghose et al., 2006). In this study we investigated bat responses to the well-known ultrasound-triggered evasive dives of flying praying mantids (Yager, May, and Fenton, 1990). Our data suggests that immediately after initiating a dive ($200\ ms$) the mantis continues on the original horizontal path it was flying, showing no directional response to the bat. At longer times into the dive, the mantis may occasionally, however, make erratic turns (see Fig. 6.11 (C) for an example). While pursuing the mantis the bat adopts a time-optimal pursuit strategy (Ghose et al., 2006). The mantis dive, consisting of a rapid change in vertical velocity when the bat was typically around $1\ m$ away, causes the bat to diverge from the time-optimal strategy in the vertical plane (Fig. 6.12 (D)). The bat's response, in 65% of the cases, was to pursue the mantis into the dive. This pursuit enables the bat to reduce the divergence from the optimal pursuit strategy (Fig. 6.12 (C)). During the dive the bat keeps its sonar beam locked onto the target, as observed for non-diving and erratically moving prey.

6.4.1 Always keeping an ear on things

We observe that in cases when the bat does not pursue the mantis dive it momentarily increases its pulse interval, suggestive of it breaking off the engagement. The pulse interval, however, subsequently drops back to the levels typical of a bat still pursuing the mantis. From examples shown in Fig. 6.11 we observe that in cases where the bat does not follow the mantis dive it still may adjust its flight path in the horizontal plane to follow the mantis. These observations suggest that the bat, even in cases when it

decided not to pursue the mantis dive (perhaps because the mantis dove too early or too late - Fig. 6.8), still tracks the mantis in some fashion. This enables the bat to attempt a second attack on the same insect if it levels off and stops its dive, returning to level flight.

6.4.2 Hitting the deck

It is not sufficient, however, for the bat to follow a mantis into a dive in order to succeed in capturing it. We observed that in 13 of the 14 following dives that the bat made (93%) the bat was forced to abort the pursuit as the mantis reached the floor of the flight room (Fig. 6.3 and Fig. 6.11 (C)). In one case the mantis levelled of just before hitting the floor, and was captured by the bat (Fig 6.11 (D)).

In the 14 trials where the bat followed the mantis the mean peak vertical closing speed (how fast the bat reduced the altitude difference to the mantis) was 0.55 ± 0.41 m/s. The mean peak mantis dive speed is 2.82 ± 0.64 m/s. Considering that most mantis dives take place about $1\ m$ away from the bat, an estimated value for the time to interception by the bat of a diving mantis is $2\ s$. In this time, if diving continuously at peak speed, the mantis will cover about $5.6\ m$. We hypothesize, therefore, that mantids of this species, flying above approximately $5.5\ m$ are in greater danger of being captured by bats, than mantids flying below this “safe-altitude”. Mantids flying lower that this altitude are likely to be able to ”hit the deck” before the bat has a chance to capture them, thereby living to fly another night.

It is better to know some of the questions than all of the answers.

James Grover Thurber

Attributed

7

Future directions

7.1 Suggestions for array expansion

7.1.1 Low risk

1. More dense sampling. The present National Instruments board (6071E) has a capacity of 64 channels. At 20 kHz each, about 48 channels can be safely used on the board. A more dense dense sampling (say at .5m intervals, rather than 1m intervals) may lead to some increase in beam-axis computation accuracy,

however I do not think it will increase proportionally (due to the broadness of the sonar beam).

2. Close the loop. Adding a movable ”barricade” of microphones to cover the fourth wall of the flight-room will be invaluable, especially if more free-flying insect pursuit studies are done.

3. Vertical array. From the vertical array data I would recommend that a much more dense and extended sampling be done. Using the present system, I would recommend adding microphones on the floor and ceiling.

7.1.2 High risk: Scalable Wireless Array

This is my dream array. I have just worked out a skeleton. I estimate one month of researching and six months of prototyping before the design can work. This design is intended to

1. Address problems with the large volume of wiring for large arrays

2. Make the array painlessly scalable

3. Take care of the tedious process of calibrating the array

4. Make use of the full bandwidth of the bat's sonar call

The array is made of multiple units (nodes) of identical design (Fig. 7.1 a)). Each node carries a Knowles FG3329 microphone on a stem. At the base of the stem is a discrete active filter/amplifier built around the TL074. The output of the filter is fed to an Analog Devices AD7813 analog-to-digital converter running off a 250 kHz clock signal. This data is then transmitted using the WiFi protocol (IEEE 802.11g) to the

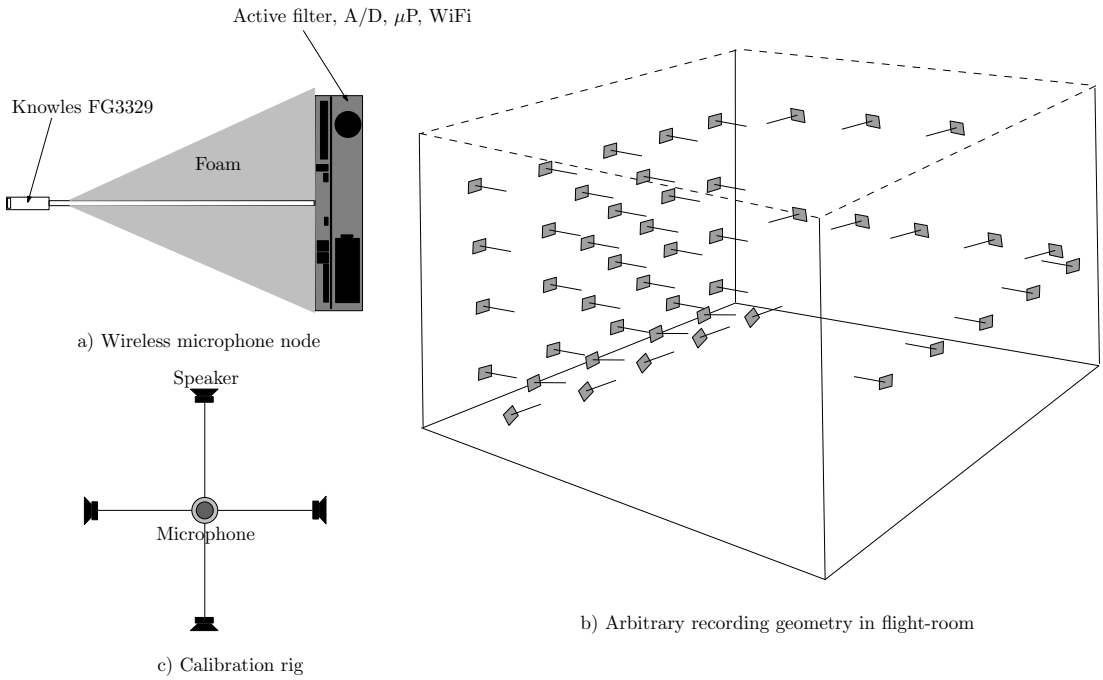

Figure 7.1: Scaleable wireless array

recording computer, which also has a WiFi card. Getting the data off the AD7813 and into the WiFi card will probably require a micro-processor running a program (the Array Operating System - AOS) stored in EEPROM. Each node is allocated an IP address that is hardwired (DIP switches, jumpers or burned into EEPROM). The recording computer is given a list of IP addresses that it polls, retrieving digitized data from the nodes. The limitation in size of the array is now set by the bandwidth of the WiFi protocol and the overhead of the two way communication between the base computer and the nodes.

Given that the fastest rate of an *E. fuscus* pulse train is 200Hz, one implementation could involve a threshold detector built into the AOS that will store data into a RAM buffer at each node when the received signal exceeds the threshold value. The AOS then sends a ”data ready” packet to the base computer, which then retrieves the buffer

of data, time stamps it and stores it. This strategy will enable the addition of more nodes in the array than a strategy involving continuous data transfer from all nodes to the base computer (Since we are effectively ”piecewise off-lining” the data transfer, and we only transfer data from the small percentage of microphones that get a signal from the sonar beam during one vocalization). The data transmission should be prioritized according to the magnitude of the received signal.

The array geometry is flexible - the nodes may placed anywhere (Fig 7.1 b)) in the room. The array is calibrated using a set of four speakers directed to four corners (Fig. 7.1 c)). There is a microphone placed at the center of the speaker assembly that is able to pick up the emission from all speakers. The central calibration microphone is placed in view of both flight-room cameras so its position can be digitized in camera coordinates. Each speaker is activated in turn. Multiple readings are performed with the calibration rig placed at different points of the flight-room. The time difference between the signal reception at the calibration microphone and the array microphones is used to triangulate each array microphone and convert its position to camera coordinates.

A standard calibration setup will be used to periodically calibrate the gain and frequency response of each array node. The calibration setup will allow the node to be placed in a standard orientation and range from a calibrated emitter. The node will be brought in from the flight room, placed in the setup and tested.

7.2 The complete beam pattern of a flying bat

From Chapter 3 we see that the big brown bat likely has a sonar beam pattern consisting of two lobes. Our knowledge of the detailed shape of the beam comes from studies

on stationary, head fixed bats electrically stimulated to elicit vocalizations. It is quite possible that not only does the beam pattern emitted by a flying bat differ in shape, but also the beam pattern from a flying bat is plastic. Since the beam shape depends on both the frequency content of the signal and the shape of the mouth (at least), the bat can potentially modify the beam shape to match its behavioral requirements. Detailed measurements of the complete beam pattern as the bat flies, avoids obstacles and captures insects may reveal evidence for plasticity in beam shape with behavioral tasks. The bat's sonar beam may not just be a $ 2 flashlight bought from the grocery store, but a $ 100 adjustable, multiple mode, programmable flashlight from a specialty camping equipment shop.

7.3 The sonar beam axis, acoustic gaze and task demands

Following his invention of the suction-cap, Alfred Yarbus performed a series of experiments that showed how human eye-movements are influenced by the type of information a subject is attempting to gather from a scene (Yarbus, 1965).

Some experiments performed with a bat navigating a gap in a mist net suggest that the bat inspects the edges of the gap with its sonar beam before passing through. The bat shortens the duration of its vocalizations to avoid over lap with the echoes from the net, but increases the duration before passing through the net - "looking beyond" the net, as it were.

It may, therefore, be fruitful to study the sonar beam direction and the vocalization duration (an analog of eye vergence in the sense that it may indicate the range at which the bat's gaze if focused) as the bat performs behavioral tasks that require it to extract

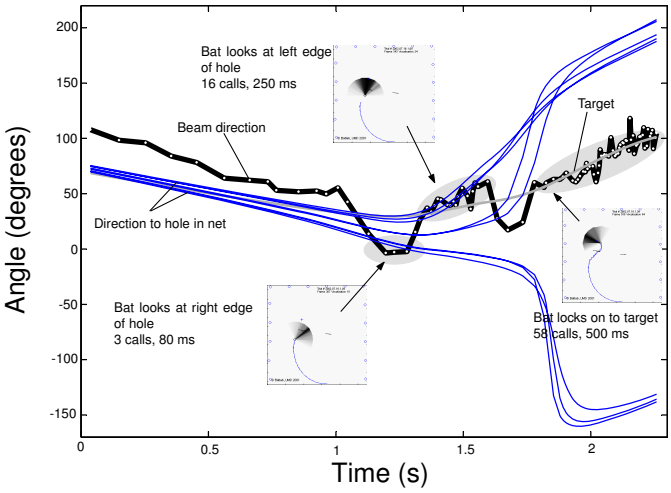

Figure 7.2: Sonar beam aim as the bat navigates an obstacle to capture an insect. The bat navigates through a gap in a fine mist net at time $t = 1.5$. It directs its sonar beam to the right edge of the gap and then to the left edge of the gap before passing the gap and locking on to the target.

information from different spatial locations simultaneously and sequentially.

The essence of science is that it is always willing to abandon a given idea, however fundamental it may seem to be, for a better one; the essence of theology is that it holds its truths to be eternal and immutable.

Henry Louis Mencken

quoted in *Minority report: H.L. Mencken's notebooks.*

A

Reconciling the results from Ch 4 and 5

From Ch 4 we see that, isolated from any target dynamics, the bat turns to head straight for a single stationary target, steering to reduce the target bearing to zero. This steering can be summarized in the form of a control law (Eq. 4.1), given again below

$$\dot{\theta}_{flight}(t+\tau) = k\theta_{gaze}(t) \tag{A.1}$$

From Ch 5 we see that, when target dynamics are introduced, the bat adjusts its flight to follow the optimum bearing continuously during pursuit. This result can be

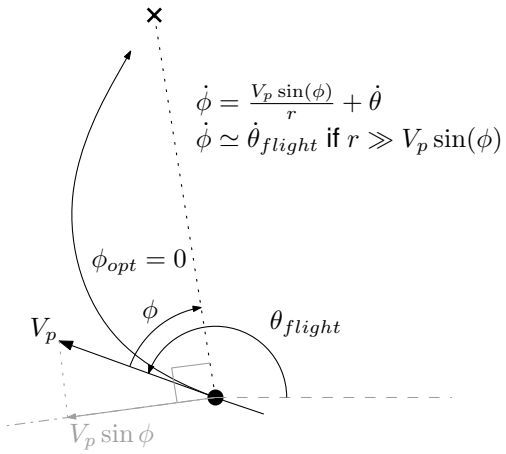

Figure A.1: Reconciling the results from Ch 4 and 5.

summarized by Eq. 5.5, given again here

$$\dot{\phi}_e(t+\tau) = k\phi_e(t) \tag{A.2}$$

Can these two results be reconciled? It can be shown that, to an approximation, Eq. 4.1(A.1) is a special case of Eq. 5.5(A.2) for the condition where the target has no motion. From Eq. 5.1 we see that for the case of a stationary target

$$\phi_{opt} = 0 \tag{A.3}$$

So, to chase a stationary target according to the optimum-time strategy described in Ch. 5, the bat needs to head straight for the target, and, indeed, this is what the bat does (Ch 4). Now from Fig. A.1 we see that, for a stationary target, the target bearing changes as a result of both the bat's linear motion and its turning about its flight path. If the bat, for instance, flew in a straight line past the target (keeping V_p in Fig. A.1 constant) the target-bearing would change according to the equation

$$\dot{\phi} = \frac{V_p \sin(\phi)}{r} \tag{A.4}$$

If the bat remained stationary, and turned in place, then the target bearing would merely change in response to the bats own turning, and this is expressed simply as

$$\dot{\phi} = \dot{\theta}_{flight} \tag{A.5}$$

The combined effect of the bat's motion (speed along flight path and turning in flight) gives us

$$\dot{\phi} = \frac{V_p \sin(\phi)}{r} + \dot{\theta}_{flight} \tag{A.6}$$

In Eq. A.1 $\theta_{gaze} = \phi$ when the bat has selected and is intercepting an insect, since the bat locks its head onto a target. Replacing this value in Eq. A.1 along with the value for $\dot{\phi}$ from Eq. A.6 we have

$$\begin{aligned}
\dot{\theta}_{flight}(t+\tau) &= k\theta_{gaze}(t) && \text{(A.7)} \\
\dot{\theta}_{flight}(t+\tau) &= k\phi(t) && \text{(A.8)} \\
\dot{\phi}(t+\tau) - \frac{V_p \sin(\phi(t+\tau))}{r} &= k\phi(t) && \text{(A.9)} \\
\dot{\phi}_e(t+\tau) &= k\phi_e(t) \text{For } r \gg V_p \sin(\phi) && \text{(A.10)}
\end{aligned}$$

From Eq. A.10 we see that for $r \gg V_p \sin(\phi)$, the two models of bat behavior are the same. The condition $r \gg V_p \sin(\phi)$ is approximately satisfied for stationary target intercepts, because ϕ is likely to be high when the bat first spots a target, and since this is at a distance, r is likely to be large. After detection the bat steers to face the target ($\phi \rightarrow 0$) before closing the target ($r \rightarrow 0$).

Eq. (4.1) may be considered a *control equation* modeling a sensorimotor control system. This equation directly links a sensory variable (head direction) to a motor variable (rate-of-turn). Eq. (5.5) is *not* a control equation since it does not directly link a sensory variable with a motor one. In order to derive a control system model that would *result* in the behavior expressed in Eq. (5.5) we could hypothesize that the bat

changes its rate of turn ($\dot{\theta}$, a motor variable) to minimize the change in absolute target direction ($\dot{\alpha}$, a sensory variable, obtainable from the vestibular system, sonar system or visual system - see Ch. 5). Such a control system model may take the form of

$$\dot{\theta} = f(\dot{\alpha}) \tag{A.11}$$

with f passing through the origin, since the bat would stop maneuvering ($\dot{\theta} = 0$) when the absolute target direction is constant ($\dot{\alpha} = 0$).

Happy families are all alike; every unhappy family is unhappy in its own way.

Leo Tolstoy

Anna Karenina

B

Individual variability between bats

The data in Chapter 4 was obtained from 38 trials with five bats. In Fig. B.1, the pulse production rate histogram obtained from the data (Fig. 4.6) is decomposed to show the individual histograms for each bat.

In Fig. B.2 the relationship between acoustic gaze angle and flight turn rate (Fig. 4.7) is decomposed by bat and behavioral state. The demarcations of the behavioral states and the lag values (τ) are the same as that used in Chapter 4 The general trend of gain increasing as the bat progresses from search/approach to tracking and then to

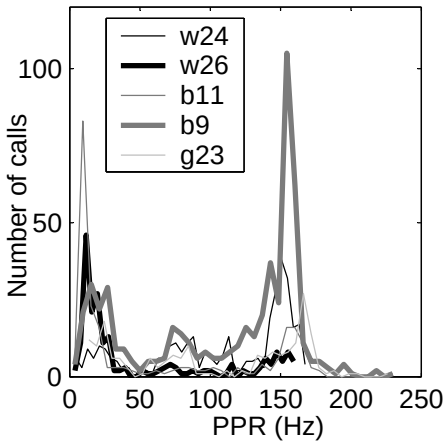

Figure B.1: Pulse rate histogram from Ch. 4 decomposed by bat.

attack holds except for b11 and gr23. For b11 the tracking phase gain is larger than that for theother two states, but the standard error is also large (reflecting less data). For gr23 the search/approach gain is higher than the other two stages, though the standard error is not much larger.

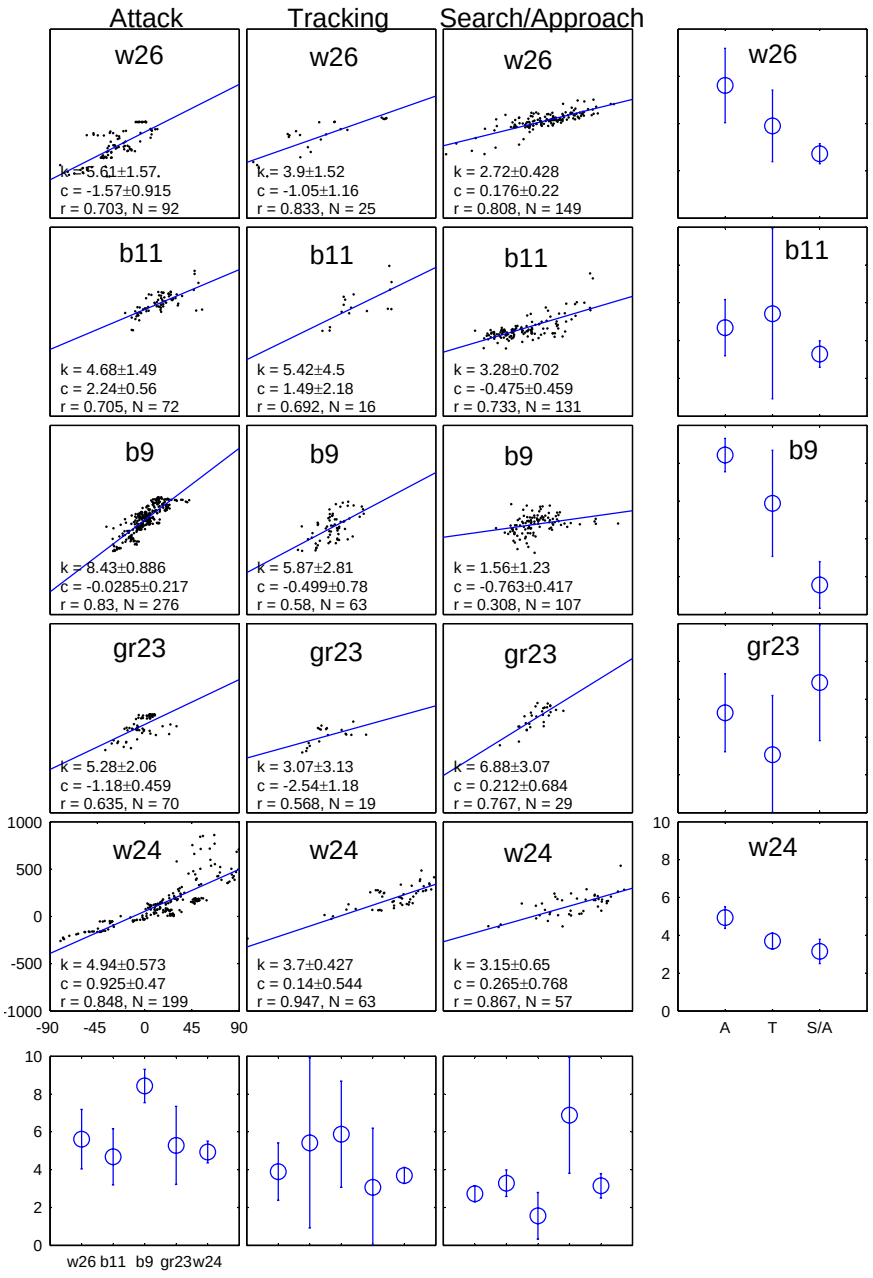

Figure B.2: Final results from Ch. 4 decomposed by bat and behavioral mode. The first three columns show the three behavioral states (labeled) while the first five rows show the five bats used in the study (labeled). The last column shows the gain values (open circles) and standard error (error bars, 95%) for each bat across the three behavioral states. The last row shows the gain values (open circles) and standard error (error bars, 95%) for each mode across the five bats.

"That's it!" said Huck; "they done that last summer, when Bill Turner got drownded; they shoot a cannon over the water, and that makes him come up to the top."

Mark Twain

The Adventures of Tom Sawyer.

C

Other Echolocators

The work presented in this thesis focused on part of the echolocating system of the big brown bat. There are several other animals that are thought to send out vibrational mechanical energy and use the returning echoes to sense the environment. Donald Griffin's book, Listening in the Dark (Griffin, 1958), has a marvelous account of such animals in the chapter titled "From Whales to Water Beetles". The book "Echolocation in Bats and Dolphins" (Thomas, Moss, and Vater, 2004, Part six) also has some information on less well known echolocators, or animals thought to echolocate. Here,

I summarize echolocation (or its possibility) in four species not so widely associated with echolocation.

C.1 The bow wave sensor of the whirligig beetle

The earliest reference to a study of these beetles (Whirligig Beetles, *Gyrinus substriatus*) is of Eggers (1927). This and some subsequent work is in German and is summarized in "Listening in the dark" (Griffin, 1958, Chapter 10, pg257). Whirligig beetles can sense mechanical surface waves using their antennae. Eggers' work shows that whirligig beetles can navigate in darkness or with eyes covered. The hypothesis supported by Eggers' work is that these beetles produce surface waves by their swimming motion and use the reflected waves to navigate.

More recent work by Bendele (1986) (published in English) suggests that whirligig beetles use a servo-like mechanism to orient towards sources of surface waves. This servo-mechanism, much like that of the tiger beetle (Gilbert, 1997) and the bat (Ghose and Moss, 2006), can be expressed as a delayed linear proportional control law linking stimulus position with turning response.

C.2 The bark of the catfish

Research done by Tavolga (1976)[1] indicates that catfish can navigate solid transparent mazes in a fish tank. While navigating the maze the catfish makes continual short vocalizations. If the catfish is experimentally manipulated to remove its vocal cords (so it is made mute) the catfish starts to bump into the walls of the perspex maze. Interestingly, catfish make calls only when in the presence of other catfish, and the use

[1] I thank Dr. Richard Fay for referring me to this research

of the vocalizations seem to primarily serve a social purpose; to locate other catfish and school together.

C.3 The squeak of the oilbird

Both the Oilbird of Caripe (*Steatornis caripensis*) and some swifts (*Collocalia*) navigate in dark caves while emitting clicks. Oil birds emit clicks in the 6 to 10 kHz range. Such birds lose the ability to navigate if their ears are blocked, supporting the hypothesis that the clicks are part of an echolocation system (Griffin, 1958, Chapter 11).

C.4 The bellow of the baleen whale

Though dolphins (Au, 1993, Chapter 1) and other toothed whales (*Odontoceti*) (Miller, Johnson, and Tyack, 2004; Johnson et al., 2004) have been shown to echolocate it is not clear if baleen whales (*Mysticeti)*) also echolocate. Baleen whales produce low frequency sounds (peak energy below 1 kHz) and are well suited to listen at such low frequencies (Au, Popper, and Fay, 2000, Chapter 4). Such sounds may be suitable for detecting large obstacles at great distances, like underwater cliffs, or the sea floor and sea surface. However a controlled study on the ability of humpback whales to use sonar to avoid obstacles returned a negative result (Beamish, 1978).

...her own mother lived the latter years of her life in the horrible suspicion that electricity was dripping invisibly all over the house. It leaked, she contended, out of empty sockets if the wall switch had been left on.

James Thurber

My Life and Hard Times

Ch2, The Car We Had To Push

D

Notes on array hardware

Each microphone is a Knowles FG3329 electret. I chose the Knowles FG3329 for three reasons.

1. It is small, with the membrane measuring 1mm in diameter. The small size gives it a broad receiving beam at 35 kHz ($\lambda_{35kHz} \simeq 1$ cm). A broader beam for the microphones is advantageous since the bat, as it flies around, will be at different and changing angles to each microphone.[1]

[1]This small footprint ensured minimization of the echoes from the microphone itself. This was an

2. It has a simple ”support circuitry”. The only support circuitry this microphone needs is a steady DC supply not to exceed 1.5v. I initially used AAA batteries to power the microphones. For the 16 and 20 microphone arrays I used a 1.25v voltage regulator to power the microphone.

3. It was cheap - it cost $25 a unit, and I actually made most of my first arrays using samples the company provided.

The only tricky thing about the FG3329 is that it is designed for human hearing aids and its performance is only documented upto 10 kHz or so. In the ultrasonic range it requires a fairly high gain (I used a gain of the order of 130x). The response is not quite flat, but Murat Aytekin has successfully used the microphones out to 120 kHz in Head Related Transfer Function (HRTF) studies where the uneven response can be factored out. The array circuits are tuned to a single frequency - 35 kHz - and their gains are calibrated.

The microphones are positioned at the tip of a 30cm long steel tube. Wires carry the signal from the microphone to the envelope detector circuit which is placed as close as possible to the microphone to reduce noise pickup.

The microphone signal is amplified and filtered to extract components around 35kHz using an active filter built around one TL074(Fig. D.3). The envelope of this signal is then extracted using a full-wave rectifier and a leaky peak-detector. The leak of the peak detector is adjusted to smoothen out ripples near 35 kHz (the center frequency of the band-pass filter) but to be responsive to changes in the 5 kHz range - the expected frequency content of the bat signal envelope. The extracted envelope is sent over a signal line bus that serves all microphones. The signal bus ends at an anti-aliasing board. I discovered that even though the signal cable is shielded it picks

important consideration when I was envisioning hundreds of them.

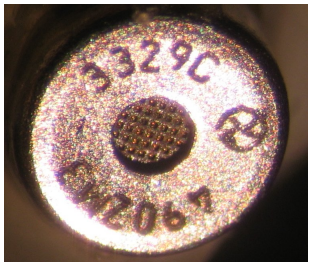

Figure D.1: Knowles FG3329

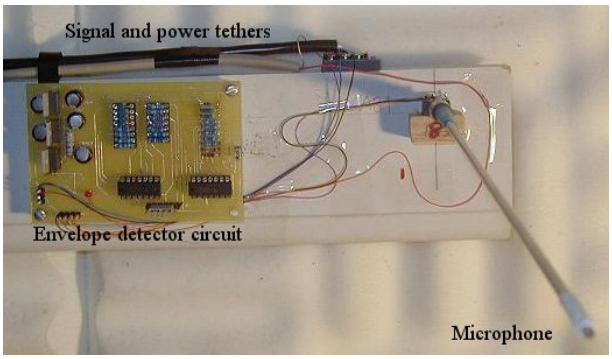

Figure D.2: Array microphone and circuitry

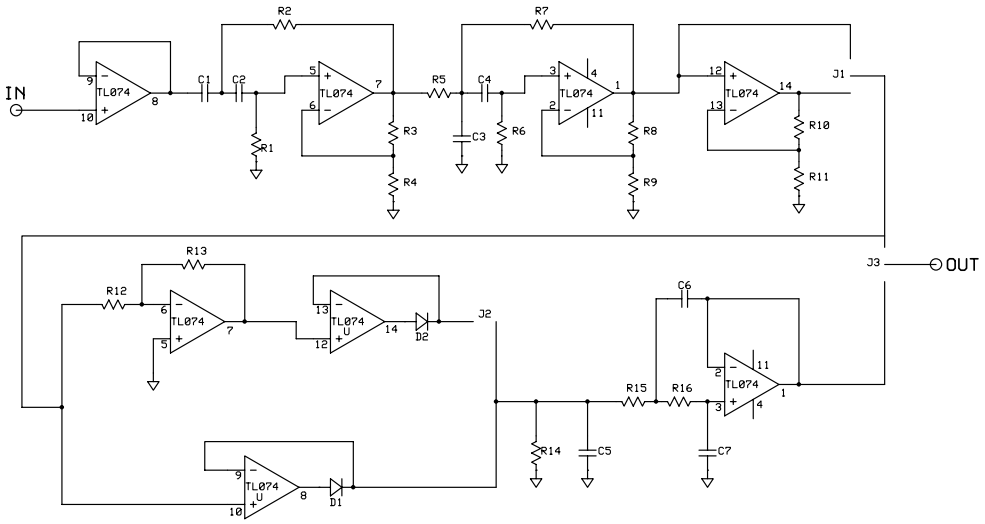

Component	Value	Component	Value	Component	Value
C1	1nF	R2	18.2 kΩ	R10	20kΩ
C2	1nF	R3	28 kΩ	R11	10kΩ
C3	1nF	R4	3.92 kΩ	R12	20kΩ
C4	1nF	R5	4.53 kΩ	R13	20kΩ
C5	10nF	R6	6.49 kΩ	R14	10kΩ
C6	3.3 nF	R7	10 kΩ	R15	20kΩ
C7	1 nF	R8	20.5 kΩ	R16	20.5kΩ
R1	3.92 kΩ	R9	4.53 kΩ		

Figure D.3: Envelope Detector Schematic

up noise in the form of short (submilisecond) spikes of 300-500mV amplitude. The anti-aliasing board filters out these spikes before passing the signal onto the 6071E National Instruments Data Acquisition board (NIDAQ). I could not find the source of

these spikes.

D.1 Printed Circuit Boards

The envelope detectors for each microphone and the antialias board are implemented on custom fabricated printed circuit boards (PCB) from ExpressPCB. The layouts for the envelope detector (Fig. D.4) and the anti-alias board (Fig. D.5) were done "by hand" and then sent to the ExpressPCB website. ExpressPCB now has a circuit schematic tool that can help check the correctness of the layout. The circuits use commercially available components that were bought from Digi-Key.

Though there is no documentation about it, I found that the NI trigger pin is susceptible to noise unless it is grounded through a 2-10kΩ resistor. If left floating, the voltage on the pin rises to around 2V, which may be close enough to the high logic level for transient noise to trigger the board.

D.2 By-pass capacitors

I ran into trouble while implementing the envelope detector circuit on a printed circuit board. The circuit had a tendency to oscillate. I followed Timothy Horiuchi's suggestion to add by-pass capacitors (small tantalum capacitors with very short leads, in the picofarad range) between the integrated op-amp power pins and the ground. This solved the problem. The by-pass capacitors short any high frequency noise on the power bus to ground, preventing the noise from adversely affecting the operation of the chip. The by-pass capacitors are placed as close as possible to the power pins of the IC. The component holes for them can be seen on the PCB layout for the envelope detector(Fig. D.4) next to the '+' and '-' signs for each IC.

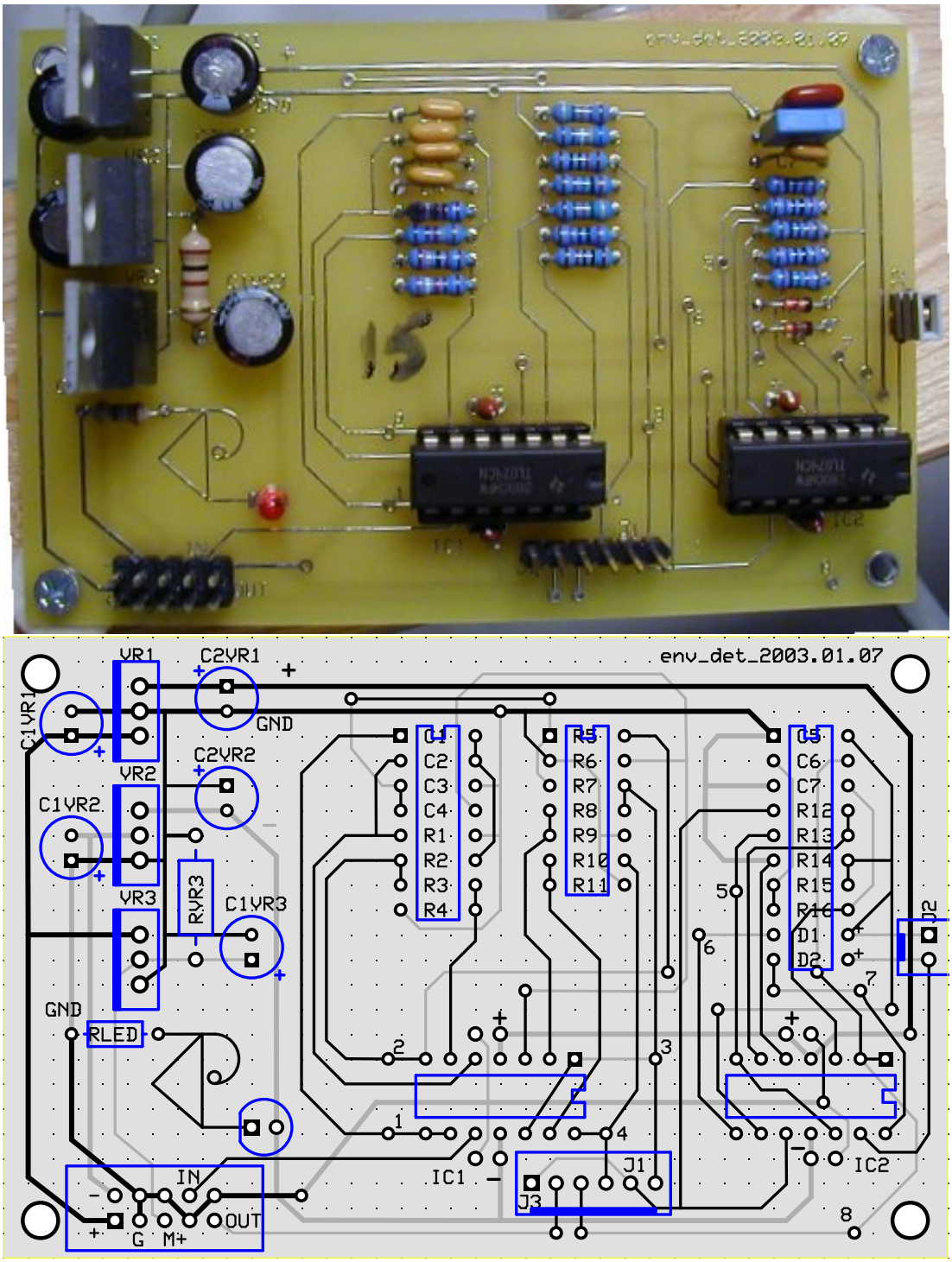

Figure D.4: Envelope Detector PCB

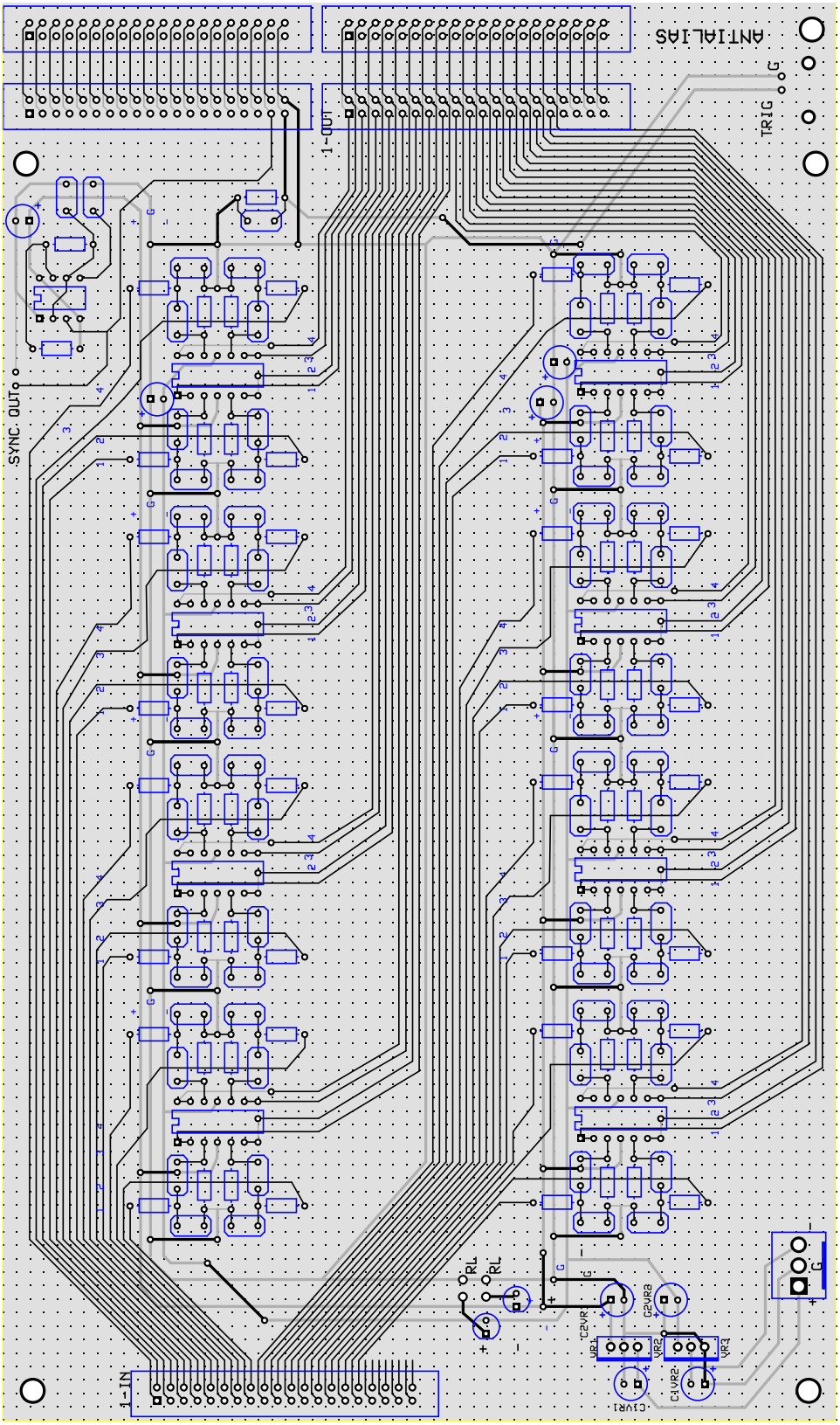

Figure D.5: Anti-aliasing breakout board

... It's a thing that scientists are ashamed of–this history–because it's apparent that people did things like this: When they got a number that was too high above Millikan's, they thought something must be wrong–and they would look for and find a reason why something might be wrong. When they got a number close to Millikan's value they didn't look so hard. ...

Richard Philips Feynman

Surely You're Joking, Mr. Feynman!

E

Array data analysis tools

I wrote graphical user interfaces(GUIs) to analyze the array data using Matlab. MATLAB allows fast and very interactive prototyping of GUIs and the ability to chase down bugs during runtime. I am familiar with MATLAB, as are many members of the Batlab. Writing the array analysis tools in MATLAB therefore enables multi-generational use of the software.

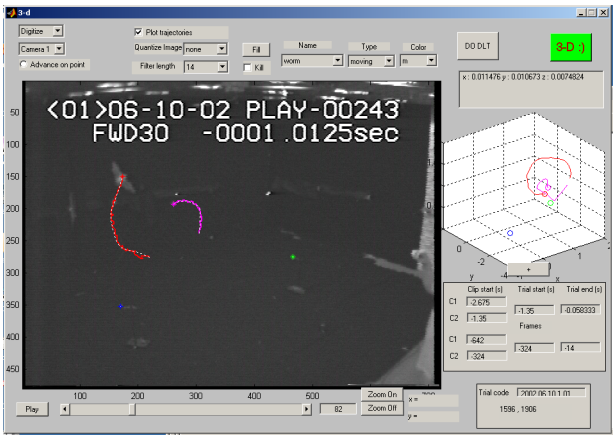

Figure E.1: D3. Used to digitize video data.

E.1 *D3*

D3 is used to digitize the raw video data to extract three dimensional flight paths of the bat and target. D3 was written together with Murat Aytekin. For the DLT engine we used KineMat. KineMat is a set of MATLAB function files written for the analysis of three-dimensional kinematics and turned out to be ideal for our requirements. KineMat is freely available from the web[1] and is written by Christoph Reinschmidt of the Human Performance Laboratory, The University of Calgary.

Users can import avi files from any source (In the case of my experiments I used a Hi-8 player with a fire-wire interface to transfer the Kodak MotionCorder analog video into a digital DV format) into D3, crop the video segments appropriately, perform the video calibration, digitize points on both cameras and then generate a three dimensional path. This path can be saved as a matlab binary file (`.mat`) or a file format compatible with the tab delimited format exported by motus.

[1] http://www.isbweb.org/software/movanal/kinemat/index.html

E.2 *Sunshine*

Sunshine is as important as the array hardware. It is used to go through the digitized array traces, segment out vocalizations and compute the sonar beam pattern. *Sunshine*

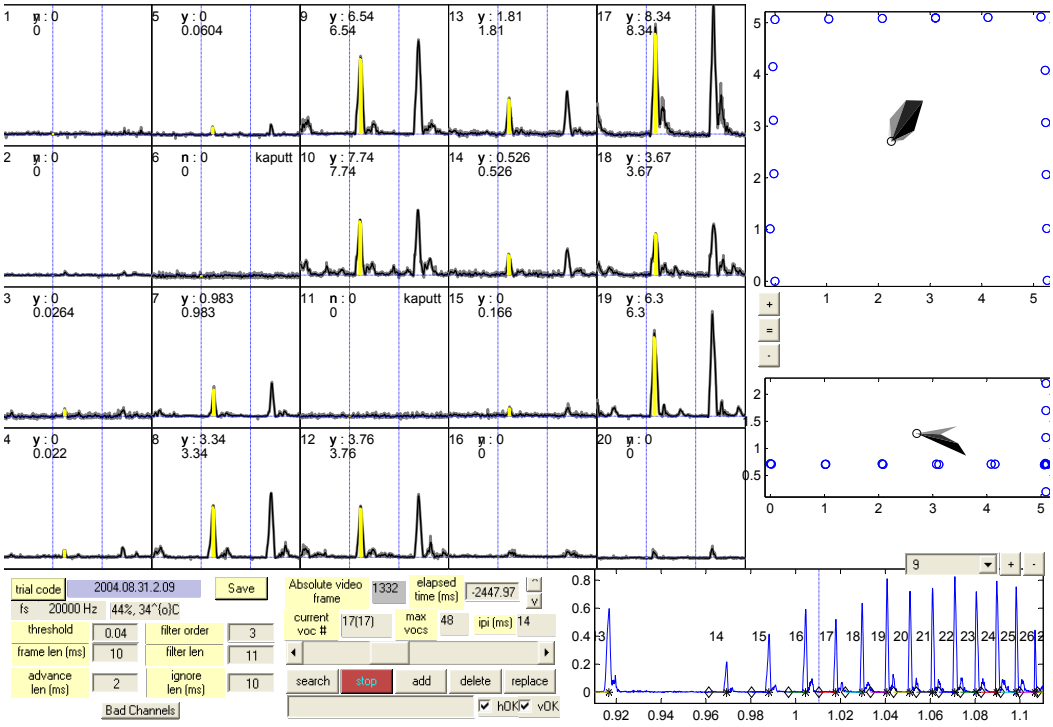

Figure E.2: Sunshine. Used to segment vocalizations from the raw array data.

automates all these tasks via an algorithm that is uniformly applied across all channels. The user only has to accept or reject a section of the data as a valid vocalization. The user can adjust several variables to affect exactly how the algorithm segments the vocalization. The user can adjust the threshold of the noise floor to avoid getting mired in the bumpiness of the noise. The user can adjust the order and window length of the Savitzky-Golay (Savitzky and Golay, 1964) filter used to smoothen the data. It is recommended to keep both at the default values (3 and 11) since these appear to preserve the peakiness of the array signal while smoothing out the noise in the

baseline (quiet) periods. The value chosen to represent the intensity is taken as the peak value of the segmented vocalization[2]. The horizontal and vertical sonar beam patterns are shown on the right part of the GUI. The flight path of the bat and the positions of the target(s) are not shown to avoid bias. The user should tweak the segmentation parameters to make sure the signal envelopes on the 20 channels are correctly segmented. The sonar beam pattern is a quick way to make sure of this. The user should not be influenced by the bat's flight path or the position of the target(s) while tweaking the segmentation.

E.3 *Moonbeam*

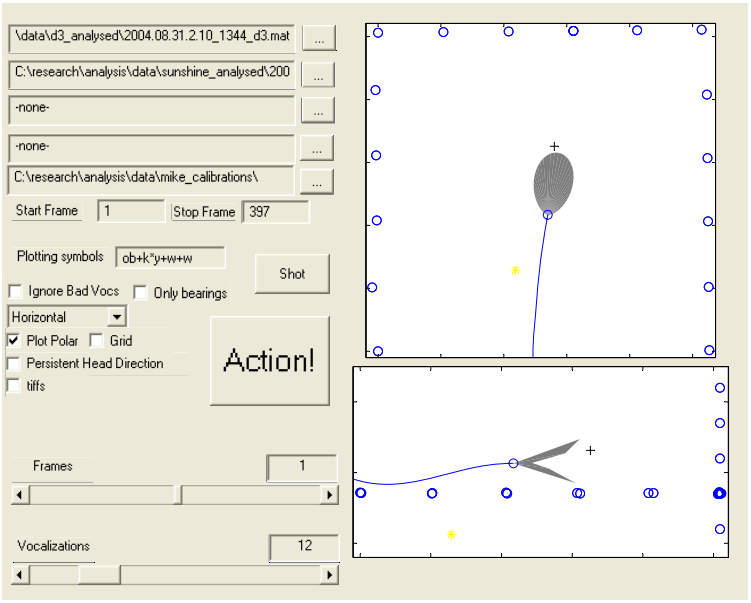

Figure E.3: Moonbeam. Used to make movies and figures for publication

Moonbeam is used to inspect individual analyzed sonar beam trials, to create

[2]Using the average value of the segmented vocalization does not alter the sonar-beam pattern, though it affects the intensity values

movies and figures for publication. It has options to display the sonar beam using different representations.

The first list we made out had to be discarded. It was clear that the upper reaches of the Thames would not allow of the navigation of a boat sufficiently large to take the things we had set down as indispensable; so we tore the list up, and looked at one another!
George said: "You know we are on a wrong track altogether. We must not think of the things we could do with, but only of the things that we can't do without."

Jerome Klapka Jerome

Ch 3, Three Men in a Boat

F

List of files on accompanying CD

The accompanying CD contains several infra-red video clips and data animations that illustrate bat behavior in the experimental paradigms used in this study. The video files are in audio video interleaved (`.avi`) format. They are compressed using the XViD compressor codec (http://www.xvid.org/). The XViD codec is an excellent, free, open source MPEG-4 video codec. For Windows and Mac the codec can be obtained from http://www.xvidmovies.com/codec/. Packages for linux are also available, though if you run linux, you may want to compile the source code on your system. The source

code for version 1.1.0 and the installer for windows is included.

F.1 List of infrared videos on accompanying CD

The videos play at $1/10^{th}$ real speed and show the view from one of the infra-red video cameras. While the bat and free-flying insect are easy to spot some practice is required to follow the mealworm.

`tailflip1.avi` The bat tries to capture a praying mantis, mis-times and brushes it with its tail-membrane.
`bat_mantis_long_chase.avi` The bat tries to capture a praying mantis that makes multiple eavsive maneuvers.
`wingtip_gather1.avi` A bat knocks a mantis with its right wing into its tail membrane. Camera #1 view.
`wingtip_gather2.avi` A bat knocks a mantis with its right wing into its tail membrane. Camera #2 view.
`bat_mantis_capture.avi` A bat captures a mantis after a frenzied chase.
`singletarget_jerk.avi` A bat is about to capture a tethered meal worm when the mealworm is retracted. The bat executes a tail-flip into thin air.
`plenty_of_mealworms_in_the_air.avi` The bat is presented with two mealworms. It mistimes catching the first one and immediately turns to capture the other one.
`wingbeatflutter_as_it_chooses.avi` The bat is presented with two mealworms. There is a "flutter" in its wingbeat pattern before it commits to chasing one of them.

Table F.1: List of infrared videos on accompanying CD

F.2 List of sonar beam animations on accompanying CD

The animations play at $1/10^{th}$ real speed and show the top-view of the flight room. The bat is represented as a circle, the target as a cross. Sonar beam patterns are coded with gray scale, with black as the most intense sound direction. The computed sonar beam axis direction is shown as a line from the bat's flight path.

`animation_circle.avi` The bat tries to capture a tethered insect being moved in a circle.
`animation_twice.avi` The bat tries to capture a tethered insect dropped from a trapdoor. It misses, flies around and captures it the second time.
`animation_search_destroy.avi` The bat initially flies in an empty room producing sounds at a low rate. A tethered mealworm is dropped from a trapdoor. The bat centers its beam on the mealworm, increases its repetition rate and then turns to intercept the insect.
`animation_notarget.avi` The bat flies in an empty room, producing sounds at a low rate.
`animation_bearing_doubleweave.avi` The bat chases a free-flying insect that performs two weaves. The bat performs matching weaves, attempting to bring the bearing lines parallel before aborting the attack.
`animation_bearing.avi` The bat captures a free flying mantis that performs two weaves. Bearing lines are parallel during the last $500\ ms$ of pursuit.
`animation_headaim.avi` The bat captures a free flying mantis that performs two weaves. The bat keeps its head locked onto the target throughout the pursuit.

Table F.2: List of sonar beam animations on accompanying CD

When a bat flies about in total darkness, the beat of its wings sends out a series of pulsations or waves after the manner of sound waves, but of too low a frequency to be considered as sound. These waves strike against all surrounding objects, and, like sound or light, are reflected back to their source of origin. ... The extremely delicate nature of the bat's wings, together with the sensitiveness of its organ of the sixth sense, enables it to judge the distance to any object by the lapse of time between sending out and the receiving of the waves ... We know that this is the mechanism that gives to the bat what is practically a sixth sense. We know it must be true because it can not be otherwise.

Hiram Maxim, *Scientific American* pg 80-81, 1912

G

Tail-Flip

I settled on the Knowles microphones pretty early on. I can no longer clearly recall who or what introduced me to the Knowles FG3329, but I do remember that it did not come to me in a dream. The first "array" consisted of 4 microphones on metal stems about 70cm high (much like the seven microphone version in Fig. G.2). The microphones were obtained in the usual way. I phoned up the company posing as a bat researcher investigating the sonar beams of echolocating bats, wanting to test their microphones for this **giant** array I was building. Its amazing what stories people will

Figure G.1: Initially, there were some technical difficulties...

believe. The array structure was constructed using PVC piping and I ran experiments in a fly-by-night kind of operation: I would go into the room and assemble the array by attaching the PVC piping together. I would take my data and then break down my array and stow it in the lab. I used the four bandpass filter units we have in the laboratory (Kronhite and Stanford Instruments) to condition and amplify the signals. The signals were digitized on the wavebook, which I ran at 200 kHz. This enabled me to test the concept of using arrays just before Cindy left for Germany.

My initial success with four microphones propelled me on to a life full of heady excess. I moved onto seven microphones. This posed several problems. Firstly I had to make new friends. Knowles was getting suspicious of the bat researcher story and

Figure G.2: Seven mike array

I had to gather various people together who made calls from various different phones in various accents asking for microphone samples. I understand that Knowles later launched a full scale market study on the demand for microphones for bat sonar arrays[1]. I also married one of the people who made these calls for me. When I had four microphones I could arrange them to be all in the view of the two cameras - though

[1]For their generosity Knowles is acknowledged in two of the papers dealing directly with the array.

slightly out of the calibrated region. This allowed me to digitize the microphone positions in the same coordinate frame as the bat and target. With seven microphones I could no longer arrange them to be all in the view of both cameras. I measured the array dimensions and then used the digitized positions of the four microphones in the camera views to reconstruct the whole array in camera coordinates. This added additional error since rigidity is not the chief virtue of PVC piping. I also broke the bank as far as filters went. We did not have enough filters to serve seven channels. I built my own.

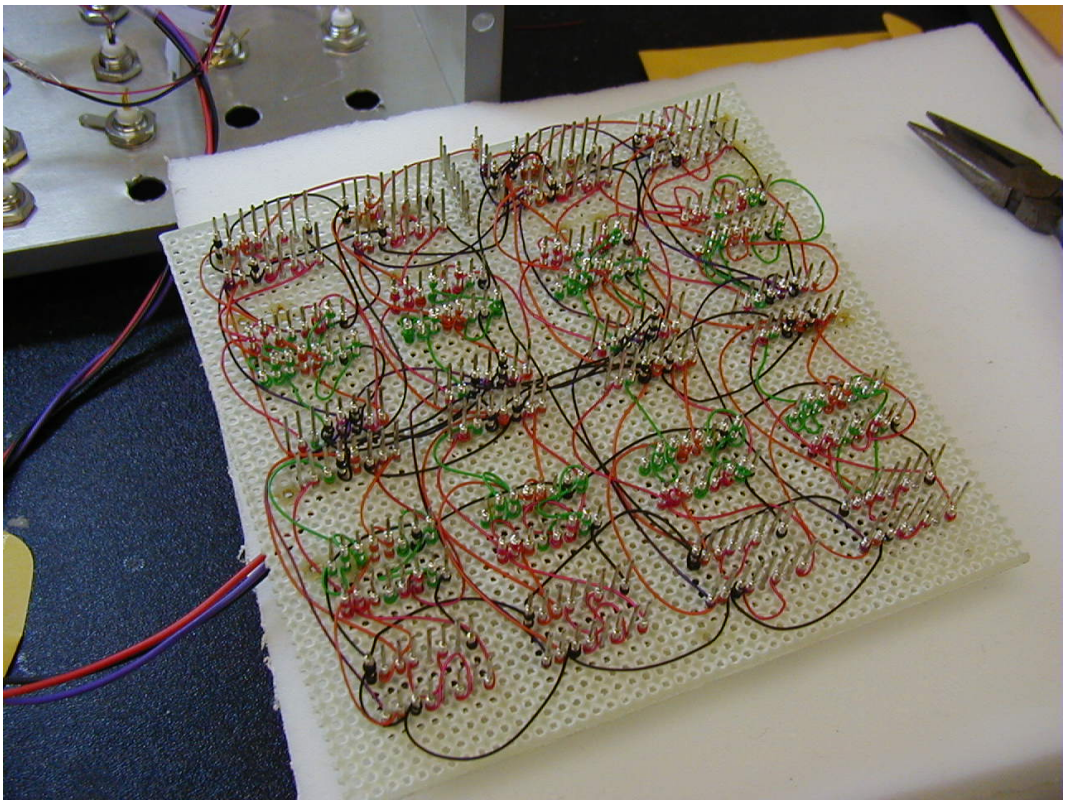

Figure G.3: Wirewrap!

Manjit Sahota introduced me to an odd chip called the AD622 that basically provided an adjustable gain for the input signal depending on the value of one external

resistor. I used an active filter based round the TL084 to filter the signal before passing it to the AD622 for gain. I used wire-wrap (a technique I learnt from Timmer) to create the circuit (Fig. G.3). I will not wire wrap again.

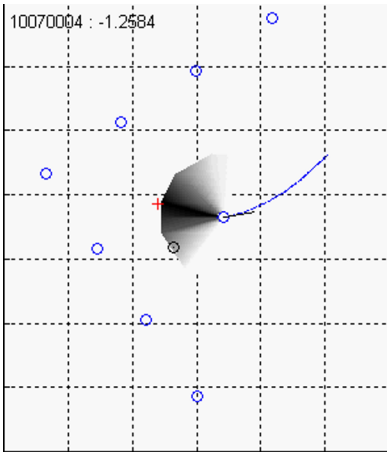

Figure G.4: Example of a sonar beam pattern reconstructed from seven microphones

I used the wavebook to digitize the signals, but now I was down to 140 kHz a channel. It was at this time that I began to be acquainted with a strange problem that has plagued me since. Everything would be going fine, I would be taking data, then I would discover that all my amplifiers had started to oscillate and these oscillations had swamped out my signal. It was hard to detect this "lock-up" condition without an oscilloscope and I learnt to run my experiments with one eye on the bat, one eye on the worm and the remaining eye on the oscilloscope. During the same period I also learnt to make full use of my four hands. The lock-up condition was remedied by switching off and then switching on the filter power supply. I began to think the culprit was the power supply, but I could never prove it.

It was with the seven microphones that I developed my current sonar beam pattern animation representation (Fig. G.4). I remember presenting the data at a lab meeting and at that meeting Jonathan gave me the idea to switch the polarity of my represen-

tation - I was originally using white to represent the loudest intensity which created a distracting region of black around the beam. I also decided from the seven microphone data that a 1m spacing between microphones was adequate to sample the sonar beam.

After a while I got tired of assembling and reassembling the array every day. I also wanted to make a larger one that covered more space, to increase my chances of getting data. I thought that if people saw me carting about so much PVC piping they would take me for a plumber. Everyone knows plumbers get paid better than academics, and I was afraid my lab-mates would start to hit me up for money. The real practical problem was of course that now most of my microphones would be well outside the camera's calibrated space and I was getting worried about positional errors that would surely accrue as my plumbing got more elaborate.

I decided to take the plunge and remodel the flight-room. The fastest board we had at that time was an old National Instruments AT-MIO-16-E. If you want to know how old this card is: it has an ISA bus interface. The AT-MIO-16-E has a 1 MHz throughput and a maximum of 16 analog input channels. This limited me in my initial choice of array channels and led to my choosing the envelope detector solution detailed in Chapter 2 and Appendix D. Murat has since come up with an elegant solution to digitizing full band width signals from multiple channels, involving some elaborate compression and shifting of the signal in the frequency domain.

When I was studying prey capture I would tether the mealworm with a fishing line and hang it from the ceiling as I had been taught by the old timers in the lab. "Remember to put a curl at the end", Hannah would say. The only problem with this process was that the bats would win too easily. If you work with animals, you know that the animals always win – in the end. The game is to give them a good fight before you lose.

I would walk out to the room, pick a random spot on the ceiling and stick the needle in, letting the mealworm dangle from the tether. I would get off the ladder, fold it and start to make my way back to my recording equipment. There would be a flutter of wings. A shadow would cross the room. There would be a faint buzz, then a sound of chewing. When I got to the video monitor a blank room would stare back at me. In the darkness I could swear I heard the bat chuckling. I needed to buy more time. I needed to be able to string up the mealworm and return to the video monitor in time to see the bat swoop down onto it. I tried various tricks involving assistants, out-sourcing and voodoo. The bat always won. I thought really hard. There had to be something a human had that could beat a bat. Then it came to me: modern electronics. The wonders of the integrated circuit had saved mankind from so many disasters, perhaps, just perhaps, modern electronics could go head-to-head with a bat. So I built robo-prey (Fig. G.5).

Robo-prey was a film-cannister[2] cut-away, as shown, to make a worm-dispenser. The mealworm was tethered and concealed in the dispenser. The bat would fly around the room, oblivious to the fact that a packed lunch dangled overhead. A motor, when activated, would flip the cannister over and the mealworm would drop out. I would hunker down next to the video monitor with a remote controller cannibalized from a remote controlled soccer ball ("Yes, Cindy. I really, really need that big yellow remote controlled robot ball for my research."). The remote's receiver was hooked up to the dispenser motor. The plan for world domination was to release the dispenser trap-door as the bat flew into view allowing me to record the whole process of search, detection and interception. It worked, more-or-less. The bat would suddenly notice this dangling mealworm and go through various satisfactory changes in behavior that we wrote up

[2]Yes, I use film. That's how OLD I am.

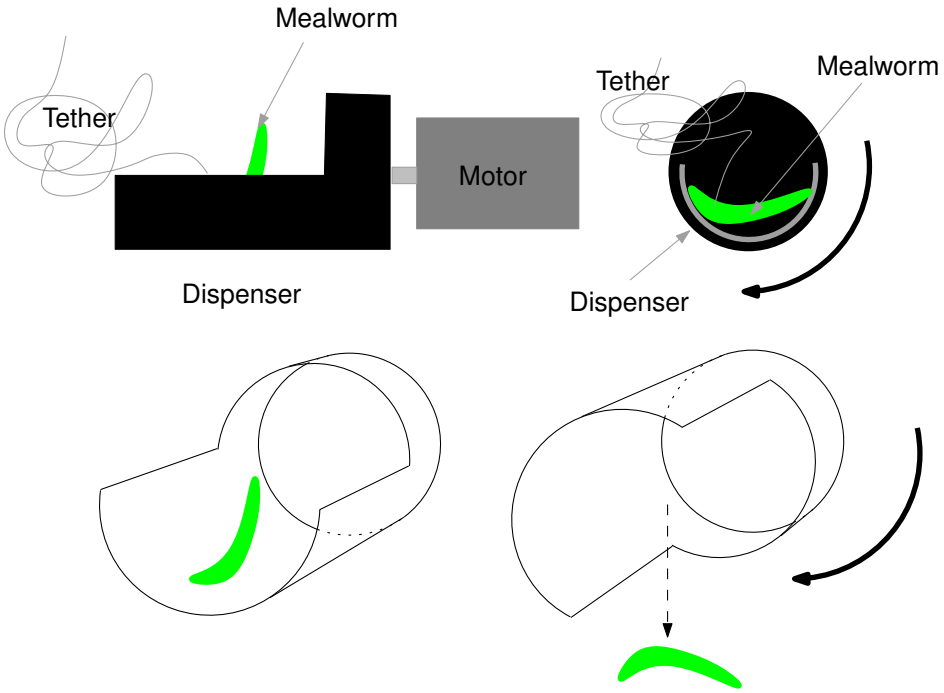

Figure G.5: Robo-prey dispenser

in a paper which, I know for a fact, some one in Canada and some one in Scotland actually read.

I started to get ambitious. I told the lab elders of my plan to build a tunnel the bats would fly through, triggering a light switch that would trip four worm-dispensers. They smiled resignedly. How much harm can one man do in a small room covered with foam padding? they thought. I did not mention anything about the lasers.

I trained the bats to fly through a curtain tunnel and into the "Quad Dropper" (Fig. G.6). Flying through the curtain tunnel the bat would trip two laser beams. The first laser beam triggered a tone circuit that played one of two tones from a speaker ("The Soprano"). Tripping the first laser also armed a controller circuit ("The Brain", Fig. G.7). If the bat flew straight and true it would trip a second laser. This laser would release the controller circuit which would power four dispenser motors ("The muscle").

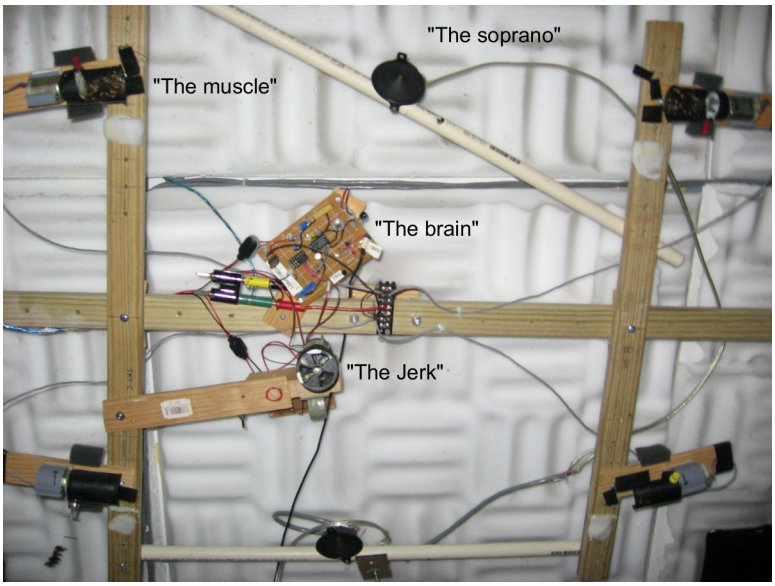

Figure G.6: The Quad Dropper. Laser trip-switch triggered, singing, robotic prey dispenser.

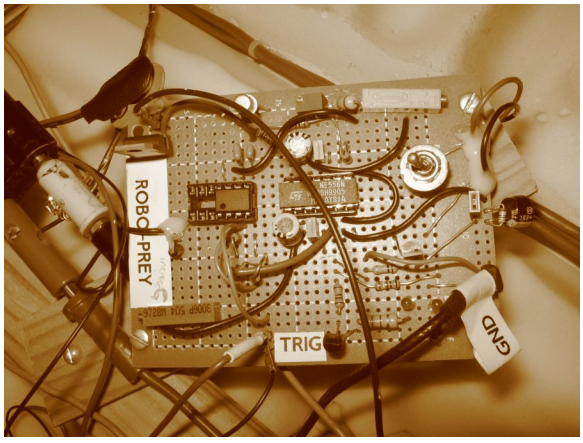

Figure G.7: "The Brain"

Two targets would fall out of two of the four dispensers.

The idea was that the bat would have to choose between the two, and the process of choosing would be instructive and informative. It was. It instructed me in humility and informed me that I was totally out-classed by the bats. The bats played nice the first couple of months. They would come barging out of the tunnel, they would have heard

the tone and would be expecting mealworms to be dropping out of the dispensers, one to the left, one to the right. They would flutter their wings, pause ever-so transiently, and then pounce on one or the other mealworm, most often the closest one.

Then, they "got" it. The mealworm would always be there. No matter what they did *after* coming through the tunnel, the mealworms would just be dangling there. They began to get fancy. One bat would do this artistic "S" shape as it came out of the tunnel hitting the cluster of targets perpendicular to the direction I had intended, ruining the beam pattern recordings. Another bat would just circle round lazily, humming to itself - perhaps relating ethnic jokes about humans - before pouncing on one or the other target. I needed a fix, I needed to save face, or bats would be laughing at humans for the rest of evolution.

I invented "The Jerk". This was a spent bobbin that once held white thread. I mounted it on a motor and threaded the tether through it. I performed brain-surgery on "The Brain" and augmented its powers. Now, after dropping the mealworms "The Brain" would pause for a few hundred milliseconds, before powering up "The Jerk". The bobbin would spin on its axis reeling in the tether, yanking the mealworm out of the way.

It worked.

For a bit.

You must unlearn what you have learned.

Yoda

H

Epilogue

From my friendly contests with the bats, as I tried to wrestle the secrets of their beams from them, I came away with many epiphanies. When I came into Cindy's lab I wasn't an experimentalist. I secretly was, but I didn't know it. When I came to Cindy's lab I was a worshiper of Einstein and Feynman. My conceit was to explain the world with calculations on the back of an envelope.

As I got into experiments I found that I wasn't a failure and, infact, I liked them. I liked the idea that this was not made up knowledge. That this was really happening,

out there, in the world. And I wasn't in control. I was along for the ride. I built circuits that worked, eventually, after a fashion. I pitted myself against small furry creatures that flew in the darkness performing elaborate three dimensional maneuvers that resembled ballet when slowed down by a factor of ten.

And I began to respect an animal's ability to adapt. I had never had a pet, so the epiphany was all the stronger. Bats are adaptable. In colloquial terms one would call them smart. But the true word is adaptable. I would set them a task. They would pay no attention to me. But they would figure out how to get at the food. And you could see them adapting. You could see how they changed their flight path each time until they got it. How they changed their timing, their tactics. A bat, fresh from the hardships of the wild, is a force to reckon with. It is motivated, sharp and innovative. It will try a new thing, and another and another till it gets what it wants.
That was my first and greatest epiphany.

Another was what a hunter would call "first blood". It happened when I discovered my first equation. It does not explain the world, it will not cure cancer or the bird flu. It wasn't even new. But it was new to me. And to bats (not that they cared). And the rush that I got when I saw the data, plotted in the right way, was amazing. It happened again when I discovered my second equation. This was slightly newer but, again, it wasn't going to change the world. But the process of discovery was different. The first I had discovered by plotting different variables against each other until I suddenly saw a pattern. This second discovery was what I had hoped for from a life of science. I was trying to explain bat flight tracks as they chased flying insects. I could see a pattern but I couldn't figure it out. I knew of a previous theory and I tried to fit the data to that theory. It fit. A bit. A little stretch here, a little stretch there. But then, I found an alternative explanation that had a basis on theoretical considerations.

And I can't remember how I got it. I remember what happened afterwards. I told Timmer I had "discovered the secret of the bats" and I debated with Dr. Krishnaprasad about the interpretation. But I don't remember how I found out. And that too is interesting; That I don't remember how I found out. But I remember the rush. The rush of "unlearning" what I had learned. The rush of it suddenly making sense - at least for now. And the rush of communicating and arguing about it with others.

And I know now what I am going to do for the rest of my life.

When in doubt, cite Mark Twain

BIBLIOGRAPHY

Adams, Jack A. (1961). Human tracking behavior. *Psychological Bulletin* 58(55): 55–79.

Altes, R. A and E. L. Titlebaum (1970). Bat signals as optimally doppler tolerant waveforms. *Journal of the Acoustical Society of America* 48(4B): 1014–1020.

Altringham, John D. (1996). *Bats- Biology and Behavior*. Oxford University Press, Oxford.

Au, Whitlow W.L. (1993). *The Sonar of Dolphins*. Springer-Verlag, New York.

Au, Whitlow W.L., Arthur N. Popper, and Richard R. Fay (2000). *Hearing by whales and dolphins*. Hearing. Springer-Verlag, New York.

Aytekin, Murat, Elena Grassi, Manjit Sahota, and Cynthia F Moss (2004). The bat head-related transfer function reveals binaural cues for sound localization in azimuth and elevation. *The Journal of the Acoustical Society of America* 116(6): 3594–605.

Beamish, P (1978). Evidence that a captive humpback whale (*Megaptera novaeangliae*) does not use sonar. *Deep-sea research. Part I, Oceanographic research papers* 25(5): 469–472.

Bellman, Richard and Kenneth L. Cooke (1963). *Differential-difference equations*, Vol. 6 of *Mathematics in science and engineering*. Academic Press, New York.

Bendele, Heinz (1986). Mechanosensory cues control chasing behaviour of whirligig beetles (*coleoptera, gyrinidae*). *Journal of Comparative Physiology A: Sensory, Neural and Behavioral Physiology* 158(3): 405 – 411.

Beranek, Leo L. (1986). *Acoustics*. Amer. Inst. of Physics, New York.

Bernstein, Nikolai (1967). *The Coordination and Regulation of Movements*. Pergamon Press, Oxford.

Bilo, Dietrich and Angela Bilo (1983). Neck flexion related activity of flight control muscles in the flow-stimulated pigeon. *Journal of Comparative Physiology A: Sensory, Neural and Behavioral Physiology* 153: 111–122.

Chapman, Seville (1968). Catching a baseball. *American Journal of Physics* 36(10): 868–870.

Clemens, Samuel Longhorn (1961). *The adventures of Tom Sawyer*. Holt, Rinehart and Winston, New York.

Cohen, Yale E. and Richard A Andersen (2002). A common reference frame for movement plans in the posterior parietal cortex. *Nature Reviews Neuroscience* 3(7): 553–562.

Covey, Ellen and John H. Casseday (1995). *The lower brainstem auditory pathways*, p. 262. Springer-Verlag, New York, A. N. Popper and R. R. Fay.

Cutting, James E, Peter M. Vishton, and Paul A. Braren (1995). How we avoid collisions with stationary and moving obstacles. *Psychological Review* 102(4): 627–651.

Denzinger, Annette, Elizabeth K. V. Kalko, and Gareth Jones (2004). *Ecological and Evolutionary Aspects of Echolocation in Bats*, pp. 311–326. In Thomas et al. (2004), 1st edition.

Drake, Stillman (1957). *Discoveries and Opinions of Galileo*. Doubleday Anchor Books, New York.

Durrell, Gerald (2000). *My Family and Other Animals*. Penguin Books, New York.

Eggers, F (1927). Nähere mitteilungen über das johnstonsche sinnesorgan und über das ausweichvermögen der taumelkäfer. *Zoologischer Anzeiger* 71: 136–156.

Erwin, Harry Richard, Willard W Wilson, and Cynthia F Moss (2001). A computational sensorimotor model of bat echolocation. *Journal of the Acoustical Society of America* 110(2): 1176–1187.

Fajen, Brett R. and William H Warren (2004). Visual guidance of intercepting a moving target on foot. *Perception* 33(6): 689–715.

Fenton, M.B., D Audet, Martin K. Obrist, and J. Rydell (1995). Signal strength, timing, and self-deafening - the evolution of echolocation in bats. *Paleobiology* 21(2): 229–242.

Feynman, Richard Phillips, Ralph Leighton, and Edward Hutchings (1985). *"Surely you're joking, Mr. Feynman!" : adventures of a curious character*. W.W. Norton, New York.

Fischer, B. and E. Ramsperger (1984). Human express saccades: extremely short reaction times of goal directed eye movements. *Experimental Brain Research* 57(1): 191 – 195.

Fuzessery, Zoltan M, Jeffrey J Wenstrup, J C Hall, and S Leroy (2003). Inhibition has little effect on response latencies in the inferior colliculus. *Journal of the Association for Research in Otolaryngology* 4(1): 60–73.

Galambos, Robert (1942). The avoidance of obstacles by flying bats: Spallanzani's ideas (1794) and later theories. *Isis* 34(2): 132–140.

Ghose, Kaushik, Timothy Ken Horiuchi, P. S. Krishnaprasad, and Cynthia F Moss (2006). Echolocating bats use a nearly time-optimal strategy to intercept prey. *Public Library of Science: Biology* .

Ghose, Kaushik and Cynthia F Moss (2003). The sonar beam pattern of a flying bat as it tracks tethered insects. *Journal of the Acoustical Society of America* 114(2): 1120–1131.

Ghose, Kaushik and Cynthia F Moss (2006). Steering by hearing: A bat's acoustic gaze is linked to its flight motor output by a delayed, adaptive linear law. *Journal of Neuroscience* 26(6): 1704–1710.

Gibson, James Jerome (1950). *The perception of the visual world*. Houghton Mifflin, Boston, MA.

Gibson, James Jerome (1966). *The senses considered as perceptual systems*. Houghton Mifflin, Boston, MA.

Gilbert, Cole (1997). Visual control of cursorial prey pursuit by tiger beetles (*cicindelidae*). *Journal of Comparative Physiology A: Sensory, Neural and Behavioral Physiology* 181(3): 217–230.

Grasso, Renato, S. Glasauer, Y. Takei, and Alain Berthoz (1996). The predictive brain: anticipatory control of head direction for the steering of locomotion. *Neuroreport* 7(6): 1170–1174.

Grasso, Renato, Pascal Prevost, and Alain Berthoz (1998). Eye-head coordination for the steering of locomotion in humans: an anticipatory synergy. *Neuroscience Letters* 253(2): 115–118.

Griffin, Donald R (1958). *Listening in the dark*. Yale University Press, CT.

Griffin, Donald R, Frederick Atilla Webster, and Charles R Michael (1960). The echolocation of flying insects by bats. *Animal Behavior* 8(3-4): 141–154.

Grinnell, A. D. and Hans-Ulrich Schnitzler (1977). Directional sensitivity of echolocation in horseshoe bat, *Rhinolophus-ferrumequinum* 2. behavioral directionality of hearing. *Journal of Comparative Physiology A: Sensory, Neural and Behavioral Physiology* 116: 63–76.

Groebbels, Franz (1929). Der vogel als automatisch sich steuerndes flugzeug. *Naturewissenschaften* 17(46): 890–893.

Hartley, David J and Roderick A Suthers (1987). The sound emission pattern and the acoustical role of the noseleaf in the echolocating bat, *Carollia perspicillata*. *Journal of the Acoustical Society of America* 82(6): 1892–1900.

Hartley, David J and Roderick A Suthers (1989). The sound emission pattern of the echolocating bat, *Eptesicus fuscus*. *Journal of the Acoustical Society of America* 85(3): 1348–1351.

Hartridge, H (1920). The avoidance of objects by bats in their flight. *Journal of Physiology* 54: 54–57.

Hayes, N. D. (1950). Roots of the transcendental equation associated with a certain differential-difference equation. *Journal of the London Mathematical Society* 25: 226–232.

Hollands, Mark A, J N Vickers, and Aftab E Patla (2002). "look where you're going!": Gaze behavior associated with maintaining and changing the direction of locomotion. *Experimental Brain research* 143(2): 221–230.

Höller, Patrick and U. Schmidt (1996). The orientation behaviour of the lesser spearnosed bat, phyllostomus discolor (*chiroptera*) in a model roost. concurrence of visual, echoacoustical and endogenous spatial information. *Journal of Comparative Physiology A: Sensory, Neural and Behavioral Physiology* 179(2): 245–254.

Hope, G. M. and K. P. Bhatnagar (1979). Electrical response of bat retina to spectral stimulation: comparison of four microchiropteran species. *Experientia* 35(9): 1189–1191.

Howell, David C. (1997). *Statistical Methods for Psychology*. International Thompson Publishing Inc, Belmont, CA, 4 edition.

Imai, Takao, Steven T. Moore, Theodore Raphan, and Bernard Cohen (2001). Interaction of the body, head, and eyes during walking and turning. *Experimental Brain research* 136(1): 1–18.

Isaacs, Rufus (1965). *Differential games; a mathematical theory with applications to warfare and pursuit, control and optimization*. The SIAM series in applied mathematics. Wiley, New York.

Jensen, Marianne Egebjerg and Lee A. Miller (1999). Echolocation signals of the bat eptesicus serotinus recorded using a vertical microphone array: Effect of flight altitude on searching signals. *Behavioral Ecology and Sociobiology* 47: 60–69.

Jerome, Jerome Klapka (1981). *Three men in a boat*. Time-Life Books, Alexandria, VA.

Johnson, Mark, Peter T Madsen, Walter M X Zimmer, Natacha Aguilar De Soto, and Peter L Tyack (2004). Beaked whales echolocate on prey. *Proceedings of the Royal Society of London B: Biological Sciences* 271 Suppl 6: S383–6.

Justh, Eric W. and P. S. Krishnaprasad (2005). Steering laws for motion camouflage. *arXiv:math.OC/0508023 v1* .

Kalko, Elizabeth K. V. (1995). Insect pursuit, prey capture and echolocation in pipestirelle bats (*microchiroptera*). *Animal Behavior* 50(4): 861–880.

Kick, Shelley A. and James A. Simmons (1984). Automatic gain control in the bat's sonar receiver and the neuroethology of echolocation. *Journal of Neuroscience* 4(11): 2725–2737.

Kinsler, Lawrence E and Austin R Frey (1962). *Fundamentals of Acoustics*. John Wiley, NewYork, 2nd edition.

Kuc, Roman (1994). Sensorimotor model of bat echolocation and prey capture. *Journal of the Acoustical Society of America* 96(4): 1965–1978.

Kurtz, Gary, Leigh Brackett, Lawrence Kasdan, Irvin Kershner, George Lucas, Mark Hamill, Harrison Ford, Carrie Fisher, Billy Dee Williams, and Anthony Daniels (1980). *Star Wars. Episode V, The empire strikes back*. Twentieth Century Fox Home Entertainment, Beverly Hills, CA.

Lanchester, B. S and R. F Mark (1975). Pursuit and prediction in the tracking of moving food by a teleost fish (*Acanthaluteres spilomelanurus*). *Journal of Experimental Biology* 63(3): 627–645.

Land, Michael F (1999). Motion and vision: why animals move their eyes. *Journal of Comparative Physiology A: Sensory, Neural and Behavioral Physiology* 185(4): 341–352.

Land, Michael F and T. S. Collett (1974). Chasing behaviour of houseflies (*fannia canicularis*) a description and analysis. *Journal of Comparative Physiology A: Sensory, Neural and Behavioral Physiology* 89(4): 331–357.

Land, Michael F and R D Fernald (1992). The evolution of eyes. *Annual review of neuroscience* 15: 1–29.

Land, Michael F and D. N. Lee (1994). Where we look when we steer. *Nature* 369(6483): 742 – 744.

Land, Michael F and Benjamin W Tatler (2001). Steering with the head: The visual strategy of a racing driver. *Current Biology* 11: 1215–1220.

Lawrence, Beatrice D. and James A. Simmons (1982). Measurements of atmospheric attenuation at ultrasonic frequencies and the significance for echolocation by bats. *Journal of the Acoustical Society of America* 71(3): 585–590.

Lennon, John and Paul McCartney (1969). *Come together [recorded by The Beatles]*. Apple, Capitol Records, Abbey Road Studios.

Lewis, F. P., J. H. Fullard, and S. B. Morrill (1993). Auditory influences on the flight behaviour of moths in a Nearctic site: II. Flight times, heights, and erraticism. *Canadian Journal of Zoology* 71(8): 1562–1568.

Masters, W.M (1988). *Prey Interception: Predictive and Nonpredictive Strategies*, Vol. 156 of *NATO ASI series. Series A, Life sciences*, pp. 467–470. New York : Plenum Press.

Masters, W.M, A.J.M Moffat, and James A. Simmons (1985). Sonar tracking of horizontally moving targets by the big brown bat, *Eptesicus fuscus*. *Science* 228(4705): 1331–1333.

Maxim, Hiram Hiram (1912). Preventing collisions at sea: A mechanical application of the bat's sixth sense. *Scientific American* pp. 80–81.

McBeath, Michael K., Dennis M. Shaffer, and M. K. Kaiser (1995). How baseball outfielders determine where to run to catch fly balls. *Science* 268(5210): 569–573.

McFadden, Sarah and J. Wallman (2001). *Shifts of Attention*, chapter 2, p. 22. Springer-Verlag, New York.

McManus, Patrick F (2000). *I fish; therefore, I am*. Galahad Books, Edison, NJ.

Mencken, Henry Louis (1956). *Minority report: H.L. Mencken's notebooks*. Knopf, New York, 1 edition.

Miller, Lee A. and Jens Olesen (1979). Avoidance behavior in green lacewings I. Behavior of free flying green lacewings to hunting bats and ultrasound. *Jour-*

nal of Comparative Physiology A: Sensory, Neural and Behavioral Physiology 131(2): 113 – 120.

Miller, Patrick J O, Mark P Johnson, and Peter L Tyack (2004). Sperm whale behaviour indicates the use of echolocation click buzzes ”creaks” in prey capture. *Proceedings of the Royal Society of London B: Biological Sciences* 271(1554): 2239–2247.

Mizutani, A, J. S. Chahl, and M. V. Srinivasan (2003). Motion camouflage in dragonflies. *Nature* 423(6940): 604–604.

Møhl, Bertel, Magnus Wahlberg, Peter T. Madsen, Lee A. Miller, and Annemarie F Surlykke (2000). Sperm whale clicks: Directionality and source level revisited. *Journal of the Acoustical Society of America* 107(1): 638–648.

Morrill, S. B. and J. H. Fullard (1992). Auditory influences on the flight behaviour of moths in a Nearctic site. I. Flight tendency. *Canadian Journal of Zoology* 70(6): 1097–1011.

Moss, Cynthia F, Kari Bohn, Hannah Gilkenson, and Annemarie Surlykke (2006). Active listening for spatial orientation in a complex auditory scene. *Public Library of Science : Biology* (*In press*).

Moss, Cynthia F and Hans-Ulrich Schnitzler (1995). *Behavioral studies of auditory information processing*, chapter 3, pp. 87–145. In Popper and Fay (1995).

Moss, Cynthia F and Shiva Ranjan Sinha (2003). Neurobiology of echolocation in bats. *Current Opinion in Neurobiology* 13(6): 751–758.

Moss, Cynthia F and Annemarie Surlykke (2001). Auditory scene analysis by echolocation in bats. *The Journal of the Acoustical Society of America* 110(4): 2207–26.

Müller, Rolf and Hans-Ulrich Schnitzler (1999). Acoustic flow perception in CF-bats: Properties of the available cues. *Journal of the Acoustical Society of America* 105(5): 2958–2966.

Neuweiler, Gerhard (2000). *The biology of bats*. Oxford University Press, New York.

Neuweiler, Gerhard, V. Bruns, and G Schuller (1980). Ears adapted for the detection of motion, or how echolocating bats have exploited the capacities of the mammalian auditory system. *Journal of the Acoustical Society of America* 68(3): 741–753.

Obrist, Martin K. (1995). Flexible bat echolocation: the influence of individual, habitat and conspecifics on sonar signal design. *Behavioral Ecology and Sociobiology* 36(3): 207–219.

Olberg, R M, A H Worthington, and K R Venator (2000). Prey pursuit and interception in dragonflies. *Journal of Comparative Physiology A: Sensory, Neural and Behavioral Physiology* 186(2): 155–162.

Oommen, Brian S., Ryan M. Smith, and John S. Stahl (2004). The influence of future gaze orientation upon eye-head coupling during saccades. *Experimental Brain Research* 155(1): 9–18.

Popper, Arthur N. and Richard R. Fay (1995). *Hearing by Bats*. Springer Verlag, New York.

Pouget, Alexandre and Lawrence H Snyder (2000). Computational approaches to sensorimotor transformations. *Nature Neuroscience* 3(Supp): 1192–1198.

Renaud, Donna L. and Arthur N. Popper (1975). Sound localization by the bottlenose porpoise tursiops truncatus. *Journal of Experimental Biology* 63(3): 569–585.

Rizzolatti, Giacomo, L Riggio, I. Dascola, and C. Umilta (1987). Reorienting attention across the horizontal and vertical meridians: evidence in favor of a premotor theory of attention. *Neuropsychologia* 25(1A): 31–40.

Roeder, Kenneth David (1967). *Nerve Cells and Insect Behavior*. Harvard College, 2 edition.

Roeder, Kenneth David and Asher Eugene Treat (1961). The detection and evasion of bats by moths. *American Scientist* 49(2): 135–148.

Roscoe, Stanley N. (1968). Airborne displays for flight and navigation. *Human Factors* 10(4): 321.

Salinas, Emilio and Larry F Abbott (1995). Transfer of coded information from sensory to motor networks. *Journal of Neuroscience* 15: 6461–6474.

Savitzky, A. and M. J. E. Golay (1964). Smoothing and differentiation of data by simplified least squares procedures. *Analytical Chemistry* 36: 1627–1639.

Schnitzler, Hans-Ulrich (1968). Ultrasonic sounds of horseshoe bats (*chiroptera-rhinolophidae*) in different orientation situations. *Zeitschrift fur vergleichende physiologie* 57(4): 376–408.

Schnitzler, Hans-Ulrich and A. D. Grinnell (1977). Directional sensitivity of echolocation in horseshoe bat, *Rhinolophus-ferrumequinum* 1. directionality of sound emission. *Journal of Comparative Physiology A: Sensory, Neural and Behavioral Physiology* 116(1): 51–61.

Schnitzler, Hans-Ulrich, Elizabeth K. V. Kalko, and Annemarie F Surlykke (1987). The echolocation and hunting behavior of the bat, *Pipistrellus kuhli*. *Journal of Comparative Physiology A: Sensory, Neural and Behavioral Physiology* 161(2): 267–274.

Shaffer, Dennis M., Scott M. Krauchunas, Marianna Eddy, and Michael K. McBeath (2004). How dogs navigate to catch frisbees. *Psychological Science* 15(7): 437–441.

Simmons, James A (1969). Acoustic radiation patterns for the echolocating bats *Chilonycteris rubiginosa* and *Eptesicus fuscus*. *Journal of the Acoustical Society of America* 46(4B): 1054–1056.

Simmons, James A. (1971). Echolocation in bats: Signal processing of echoes for target range. *Science* 171(3974): 925–928.

Simmons, James A. (1987). *Directional Hearing in Echolocating Animals*, p. 217. Springer-Verlag New York, W. A. Yost and G. Gourevitch.

Simmons, James A., M.B. Fenton, and Michael J. O'Farrell (1979). Echolocation and pursuit of prey by bats. *Science* 203(4375): 16–21.

Simmons, James A., Seth S. Horowitz, Michael J. O'Farrell, and David N. Lee (2001). Versatility of biosonar in the big brown bat, *Eptesicus fuscus*. *Acoustic Research Letters Online* 2(1): 43–48.

Strother, G. K. and M. Mogus (1970). Acoustical beam patterns for bats: Some theoretical considerations. *Journal of the Acoustical Society of America* 48(6 (II)): 1430–1432.

Surlykke, Annemarie F and Cynthia F Moss (2000). Echolocation behavior of big brown bats, *Eptesicus fuscus*, in the field and the laboratory. *Journal of the Acoustical Society of America* 108(5): 2419–2429.

Tagore, Rabindra Nath (1961). *Kanika (Specks)*, Vol. 1. West Bengal Government, Santiniketan, Birth Centenary edition.

Tavolga, William N (1976). *Acoustic obstacle detection in the sea catfish (Arius felis)*, pp. 185–204. Developments in Aquaculture and Fisheries Science, 5. Elsevier, New York.

Thomas, Jeanette A., Cynthia F Moss, and Marianne Vater (2004). *Echolocation in Bats and Dolphins*. The University of Chicago Press, Chicago.

Thurber, James Grover (1999). *My Life and Hard Times*. Perennial Classics, New York.

Tolstoy, Leo (1939). *Anna Karenina*. Random House, New York.

Triblehorn, Jeffrey D. and David D Yager (2005a). *Acoustic interactions between Insects and Bats: A model for the Interplay of Neural and Ecological Specializations*, chapter 5, pp. 77–104. Oxford University Press, New York, New York, 1st edition.

Triblehorn, Jeffrey D. and David D Yager (2005b). Timing of praying mantis evasive responses during simulated bat attack sequences. *Journal of Experimental Biology* 208(10): 1867–1876.

Valentine, Doreen E and Cynthia F Moss (1997). Spatially selective auditory responses in the superior colliculus of the echolocating bat. *Journal of Neuroscience* 17(5): 1720–1733.

Valentine, Doreen E, Shiva Ranjan Sinha, and Cynthia F Moss (2002). Orienting responses and vocalizations produced by microstimulation in the superior colliculus of the echolocating bat, *Eptesicus fuscus*. *Journal of Comparative Physiology A: Sensory, Neural and Behavioral Physiology* 188(2): 89–108.

Wann, John P and David K Swapp (2000). Why you should look where you are going. *Nature Neuroscience* 3(7): 647–648.

Warren, William H, Bruce A Kay, Wendy D Zosh, Andrew P Duchon, and Stephanie Sahue (2001). Optic flow is used to control human walking. *Nature neuroscience* 4(2): 213–216.

Watterson, Bill (2005). *The Complete Calvin and Hobbes*. Andrews McMeel Publishing, Kansas City, Mo.

Webster, Frederick Atilla and Oliver G. Brazier (1965). Experimental studies on target detection, evaluation and interception by echolocating bats. Technical report, Aerospace Medical Research Labs, Wright-Patterson.

Wilkie, R. M. and John P Wann (2003). Eye-movements aid the control of locomotion. *Journal of Vision* 3(11): 677–684.

Wilson, V J, R Boyle, K Fukushima, P K Rose, Y Shinoda, Y Sugiuchi, and Y Uchino (1995). The vestibulocollic reflex. *Journal of Vestibular Research* 5(3): 147–170.

Wilson, Willard W and Cynthia F Moss (2004). *Sensory-Motor Behavior of Free-Flying FM bats during Target Capture*, pp. 22–27. In Thomas et al. (2004).

Wong, Josephine G and Dean A Waters (2001). The synchronization of signal emission with wingbeat during the approach phase in soprano pipisrelles (*Pipistrellus Pygmaeus*). *Journal of Experimental Biology* 204(3): 575–583.

Yager, David D, Michael L. May, and M.B. Fenton (1990). Ultrasound-triggered, flight-gated evasive maneuvers in the praying mantis *Parasphendale agrionina*. I. Free flight. *Journal of Experimental Biology* 152: 17–39.

Yarbus, Alfred Lukjanovitj (1961). Eye movements during the examination of complicated objects. *Biofizika* 6(2): 52–56.

Yarbus, Alfred Lukjanovitj (1965). *Eye movements and vision*. Plenum Press, New York.

Yuan, Luke Chia-Liu (1948). Homing and navigational courses of automatic target-seeking devices. *Journal of Applied Physics* 19(12): 1122–1128.

Zarchan, Paul (1994). *Tactical and Strategic Missile Guidance*, Vol. 157 of *Progress in Astronautics and Aeronautics*. AIAA, 2nd edition.

Index

Kaushik Ghose

kaushik.ghose@gmail.com
http://www.glue.umd.edu/~kghose

Neuroscience and Cognitive Science Program
Dept. Psychology
Univ. Maryland, College Park
College Park, Maryland 20742
USA

Synopsis

I am a Neuroscientist interested in robotic modeling, computational modeling and electrophysiological recording of neural circuits implicated in animal behavior. I have skills in electrical engineering, signal processing, computer programming, animal training and theoretical neuroscience. I am experienced in communicating scientific findings to both specialized and lay audiences. I have received recognition for both my research and course work. I have been interviewed by news agencies interested in bringing my research to a wider audience.

Education

Doctoral	1999-2006	University of Maryland, College Park, MD, USA	**Neuroscience and Cognitive Science** Thesis on the sonar beam pattern of echolocating bats. Course work on systems neuroscience, cognitive neuroscience, hearing, computational neuroscience, neuromorphic engineering.
Masters	1997-1999	Indian Institute of Science, Bangalore, India	**Systems Science and Automation** Thesis on Acoustic Echo Cancellers Course work on pattern recognition, speech recognition, computer vision, computer graphics, digital signal processing, control theory.
Bachelors	1993-1997	Jadavpur University, Calcutta, India	**Electrical Engineering** Course work in control sytems, microprocessors, power engineering and electronics. Practical experience in machining metal parts, welding and metal forging.

Research Interests

Neuroethology: Neural basis of behavior, attentional processing, sensorimotor processing, echolocation and hearing.

Computational Neuroscience: The use of software and hardware modeling of neural systems to address neuroethological questions (neural basis of behaviors).

Biomimetic engineering: Development of robots/robot algorithms based on principles learnt from studies of animal nervous systems.

Scientific Skills

Computational

- MATLAB (numerical simulation, data acquisition and GUI design)
- C++ (numerical simulation, GUI design using QT, MySQL database interfaces)
- Ruby, Javascript and Ajax
- Neuron. (Single cell and network simulations, model creation using C++)
- Linux, Unix and Microsoft Windows systems

Hardware

- Digital signal acquisition using National Instruments boards (using C++ and MATLAB interfaces)
- Circuit design (active amplifiers, filters)
- Printed circuit board design
- Carpentry, design and building of experimental rigs
- I attended the **Neuromorphic Engineering Workshop** at Telluride Colorado in 2001, where I was exposed to analog VLSI and other techniques of modeling neural systems for implementation on robotics platforms.

Neuroscience

- Handling/training bats
- Designing and conducting behavioral experiments
- I attended the **Neural Systems and Behavior course at the Marine Biological Laboratory** (NSnB 2005) where I was exposed to a variety of animal models and neural recording paradigms.

Journal Publications

Kaushik Ghose, Timothy K. Horiuchi, P.S. Krishnaprasad and Cynthia F. Moss (2006) Echolocating bats use a nearly time-optimal stratgey to intercept prey. ***Public Library of Science: Biology***, in press. (pdf)

Kaushik Ghose and Cynthia F. Moss (2006) Steering by Hearing: A Bat's Acoustic Gaze Is Linked to Its Flight Motor Output by a Delayed, Adaptive Linear Law ***Journal of Neuroscience***, 26(6), 1704-1710. (pdf) Supplementary video S1, S2 , Publicity video , Interview on Discovery Channel

Kaushik Ghose and Cynthia F. Moss (2003) The sonar beam pattern of a flying bat as it tracks moving and stationary prey ***Journal of the Acoustical society of America***, 114(2), 1120-1131. (pdf) Beam pattern animations

Ernst Niebur, Mounya Elhilali, Iyad Obeid, Justin Werfel, Mark Blanchard, Mattia Frasca, **Kaushik Ghose,** Constanze Hofstoetter, Giovanni Indiveri, Mark W. Tilden (2001) Research, robots, and reality: A statement on current trends in biorobotics ***Behavioral and Brain Sciences***, 24 (6): 1072 - *This was published as a commentary to the main article, and was the outcome of group discussions at the Neuromorphic Engineering Workshop at Telluride in 2001. In the pdf our commentary appears on page 40. (pdf)*

Kaushik Ghose and V. Umapathi Reddy (2000) A double-talk detector for acoustic echo cancellation applications ***Signal Processing***, 80 (8), 1459-1467. (pdf)

Invited Talks

Kaushik Ghose (2005) Sonar beam direction and flight control in an echolocating bat. ***Baylor College of Medicine, Texas*** (Invited).

Kaushik Ghose and Cynthia F. Moss (2005) The acoustic gaze of echolocating bats. ***Acoustical Society of America annual meeting, Minneapolis, Minnesota*** (invited)

Kaushik Ghose, Timothy K. Horiuchi and Cynthia F. Moss (2004) Spatial attention drives acoustic behavior in echolocating bats. ***7th International Congress in Neuroethology, Nyborg, Denmark*** (invited).

Invited Talks (Not First Author)

Cynthia F. Moss and **Kaushik Ghose** (2006) Steering by Hearing in Echolocating bats. ***COSYNE 2006, Salt Lake City, Utah***

Cynthia F. Moss, **Kaushik Ghose** and Shiva R. Sinha (2004) Action and audition for 3-D spatial orientation by echolocation in bats. ***International Congress in Acoustics, Kyoto, Japan*** (invited).

Cynthia F. Moss, **Kaushik Ghose**, Marianne Jensen and Annemarie Surlykke (2004) Acoustic behavior of echolocating bats in complex environments ***Meeting of the Acoustical Society of America, NYC, Special session in Animal Bioacoustics: Natural Acoustic Behavior of Animals: Session in Memory of Donald R. Griffin III, J. Acoust. Society of America, vol. 115: 2156-2157*** (invited).

Cynthia F. Moss, **Kaushik Ghose**, Marieanne Jensen and Annemarie Surlykke (2003) The bat's sonar cries index its acoustic gaze. ***First Conference on Acoustic Communication by Animals, Acoustical Society of America, College Park, Maryland*** (invited).

Cynthia F. Moss, Shiva R. Sinha and **Kaushik Ghose** (2003) Audiomotor integration for active sensing in the echolocating bat, Eptesicus fuscus. ***Meeting of the Acoustical Society of America, Austin, Texas*** (invited).

Talks

Kaushik Ghose and Cynthia F. Moss (2003) Chirp where you go ***First International Conference on Animal Communication, College Park, Maryland***.

Kaushik Ghose and Cynthia Moss (2001) Active sensing by echolocation: sonar beam width, direction and temporal patterning controlled by free-flying FM- bats ***6th International Congress of Neuroethology, Bonn.***

Conference Abstracts

Kaushik Ghose, Timothy K. Horiuchi, P.S. Krishnaprasad and Cynthia F. Moss (2005) Echolocating bats use a prey intercept stratgey that is time-optimal in a local, piece-wise linear sense ***Program No. 79.1. 2005 Abstract Viewer/Itinerary Planner. Washington, DC: Society for Neuroscience, 2005. Online.*** (*poster pdf*)

Ben Falk, Tameeka Williams, Murat Aytekin, **Kaushik Ghose** and Cynthia F. Moss (2005) Texture discrimination by echolocation: acoustics and behavior ***Program No. 78.20. 2005 Abstract Viewer/Itinerary Planner. Washington, DC: Society for Neuroscience, 2005. Online.***

Kaushik Ghose, Timothy K. Horiuchi and Cynthia F. Moss (2004) Linking spatial attention and sonar beam direction in an echolocating bat ***Program No. 332.7. 2004 Abstract Viewer/Itinerary Planner. Washington, DC: Society for Neuroscience, 2004. Online.*** (*poster pdf*)

Kaushik Ghose and Cynthia F. Moss (2004) Steering by Hearing: The Head Directing Strategy of An Echolocating Bat. ***7th International Congress in Neuroethology, Nyborg, Denmark*** (*poster pdf*)

Kaushik Ghose and Cynthia F. Moss (2004) The bat's head aim governs flight, simplifying computation during interception. ***Computational Neuroscience Meeting, Baltimore, Maryland***

Kaushik Ghose, Cynthia F. Moss, Marianne Egebjerg Jensen, Annemarie Surlykke (2003) The Beam Pattern of Eptesicus fuscus as an Index of Spatial Attention Abstract #1586, ***ARO midwinter meeting, Daytona, Florida*** (*poster pdf*)

Marianne Egebjerg Jensen, Cynthia F. Moss, Annemarie Surlykke, **Kaushik Ghose** (2003) Spatial Orientation and Memory in the Echolocating Bat, *Eptesicus Fuscus* Abstract #1727, ***ARO midwinter meeting, Daytona, Florida***

Kaushik Ghose and Cynthia Moss (2002) The Headaim of Echolocating Bats Tracking Moving and Stationary Prey Abstract #57, ***ARO midwinter meeting, Florida*** (*poster pdf*)

Kaushik Ghose and Cynthia Moss (2001) Direction of the sonar beam pattern in the free-flying echolocating bat, *Eptesicus fuscus* Abstract #20344, ***ARO midwinter meeting, Florida***

Kaushik Ghose, Dmitry Zotkin, Ramani Duraiswami, Cynthia F. Moss (2001) Multimodal localization of a flying bat ***ICASSP, Salt Lake City, Utah*** pdf

Student Presentations

Kaushik Ghose and Cynthia F. Moss (2004) The Head Directing Strategy Of An Echolocating Bat ***Poster at GRID 2004.*** (Won joint first prize there)

Kaushik Ghose, Cynthia F. Moss, Timothy Horiuchi (2003) Selective Information Processing in the Sonar System of a Bat ***Poster at the research review day 2003 at ISR***.

Kaushik Ghose, Cynthia F. Moss (2002) What the sonar beam patterns of flying echolocating bats can tell us. ***Talk at ISR***

Rock Z. Shi, **Kaushik Ghose**, Timothy Horiuchi (2002) Neuromorphic VLSI-Based Bat Echolocation Using Interaural Level Differences ***Demonstration and poster , Research Review Day 2002 at ISR***

Kaushik Ghose and Cynthia F. Moss (2002) The Beamaim of Echolocating Bats Tracking Stationary and Moving Prey ***Poster at research review day 2002 at ISR***

Media Coverage

- Interviewed by ***Discovery Channel Canada*** for their Daily Planet show. The interview focused on the work presented in The Journal of Neuroscience 2006. This work was also covered by ***WTOP*** (Capitol News, Washington DC) and ***Stern Magazine***, Germany among others.
- The visualization technique I developed during my doctoral thesis work was featured in ***Science Magazine*** as part of the ***National Science Foundation*** and ***Science Magazine*** sponsored ***Scientific Visualization Challenge 2004.***

Recognition and Awards

Graduate work: University of Maryland

- George Harhalakis Outstanding Systems Engineering Graduate Student Award (2004)
  - (Awarded to one graduate student each year for outstanding interdisciplinary work)
- 2 year Jack Bartlett Fellowship
  - (Awarded to one student in the department of psychology, covers tuition and living expenses)
- The Journal of Neuroscience 2006 article was recommended to the ***Faculty of 1000*** list by Prof. Leonard Mahler, Univ. Ottowa, Canada.
- The visualization technique I developed during my doctoral thesis work was awarded frist prize in the ***National Science Foundation and Science Magazine Scientific Visualization Challenge 2004.***
- A poster I presented at the Univ. Maryland Graduate Research Interaction Day (2004) won joint first prize.

Undergraduate work

- University medal (For overall first position in the Bachelor's in Electrical Engineering exam)
- Barindra Memorial Bronze medal (For securing highest scores in the papers "Electric power Distribution" and "Power System Performance")
- B.N. Paul Memorial Gold-Centred Silver Medal (For securing the highest score in the paper "Electric Drives")
- Ashoke Memorial Bronze Medal (For standing first in Electrical Engineering at the B.E. Examination 1997)
- Subodh Kumar Basu Memorial (Bronze) Medal (For securing the highest score in Electrical Engineering Laboratory in 1997

Teaching Experience

- Statistics for Graduates in Psychology (University of Maryland)
- Statistics for Undergraduates in Psychology (University of Maryland)

Academic Service

- Reviewer for the Journal of the Acoustical Society of America
- Reviewer for the American Journal of Physics

Society Memberships

- Society for Neuroscience (2003-)
- Association for research in Otolaryngology (ARO) (1999 – 2004)
- Institute for Electronics and Electrical Engineers (IEEE) (1997 – 2005)